LABORATORY STUDY OF PARTICLE RESUSPENSION, OXIDATION AND METAL RELEASE IN FLOODED MINE TAILINGS

MEND Project 2.15.3

This work was done on behalf of MEND and sponsored by
Battle Mountain Canada Limited, Falconbridge Limited, INCO Limited,
Noranda Mineral and Exploration Limited; Teck Corporation
as well as the
Ontario Ministry of Northern Development and Mines and
Canada Centre for Mineral and Energy Technology (CANMET)
Through the Canada/Northern Ontario Development Agreement (NODA)

November 1998

FINAL REPORT

on the

LABORATORY STUDY OF PARTICLE RESUSPENSION, OXIDATION AND METAL RELEASE IN FLOODED MINE TAILINGS

submitted to

Canada Centre for Mineral and Energy Technology (CANMET),
Noranda, Falconbridge, Inco, Battle Mountain and Teck Corporation

by

Ernest K. Yanful and Ajay Verma

Geotechnical Research Centre
Department of Civil and Environmental Engineering
The University of Western Ontario, London, Ontario, Canada N6A 5B9

PWGSC Contract No. 23440-6-1030/001/SQ

MEND Report 2.153

November 1998

EXECUTIVE SUMMARY

The use of shallow water cover (up to 2 m) to flood reactive sulphide mine tailings is a popular method of acid drainage prevention used by the mining industry. In flooded tailings, wind-induced turbulence can increase the oxygen flux from air into water by creating turbulence at the air-water interface, thus promoting mechanical mixing of oxygen from air into the water and thus keeping the dissolved oxygen concentrations at saturation levels. Turbulence can also resuspend tailings particles in the oxygen-saturated water cover and expose tailings to greater contact with oxygen, possibly leading to increased oxidation and metal release.

In late 1996, the Geotechnical Research Centre at The University of Western Ontario initiated a study to investigate the contribution of resuspension to tailings oxidation and acid generation under laboratory conditions. The study was undertaken on behalf of MEND and sponsored by Battle Mountain Canada Limited, Falconbridge Limited, INCO Limited, Noranda Mineral and Exploration Limited, Teck Corporation, Ontario Ministry of Northern Development and Mines and Canada Centre for Mineral and Energy Technology (CANMET) through the CANADA/Northern Ontario Development Agreement (NODA). This report presents the results of the study.

The study involved a series of laboratory experiments performed in Plexiglas columns packed with unoxidized pyrrhotite tailings, which were then flooded with 45, 60 and 80 cm deep water covers. The tailings were obtained directly from the mill discharge pipelines at the Falconbridge Strathcona Mines, near Sudbury, Ontario. The water cover was stirred at 140, 170 and 200 revolutions per minute to suspend the underlying tailings. Control experiments involving water-covered tailings without stirring were also conducted for comparison. To facilitate the analysis of the results, the stirrer speed and the depth of water cover were used to define a mixing index, a dimensionless parameter that measures the degree of mixing in the water cover. Oxygen mass transfer from air to the water cover was measured for each mixing index. The water cover was also monitored for dissolved oxygen (DO), pH, conductivity, sulphate and metals. At the end of the experiments (126 days), suspended tailings, surficial tailings and undisturbed solid tailings and pore water were sampled for chemical analysis. The bulk and surface

mineralogy of the tailings were also examined.

Key findings and conclusions arising from the study are as follow:

1. Resuspension increases sulphide tailings oxidation, acid generation and metal release. This is based on sulphide (pyrrhotite) depletion, oxygen consumption, pH, sulphate and metal loadings.
2. Oxidation products are lighter than the original tailings (specific gravity of 2.7 versus 3.9-4.4 for the original tailings).
3. Oxidation products include iron oxyhydroxides (possibly goethite) and gypsum.
4. Suspended tailings are finer than tailings at rest: 80% of the suspended tailings are finer than 0.018 mm, compared to only 30% of the original tailings.
5. Unoxidized suspended tailings contain sulphide mineral (pyrrhotite) as well as gangue minerals.
6. The rate at which oxygen is transferred into the water cover is independent of mixing index.
7. The release of nickel, zinc, aluminium, and manganese increases with mixing index.
8. Significant bed erosion occurs at a threshold (critical) mixing index. This threshold value would occur in shallow water covers (possibly 60 cm or shallower).

The results of the study suggest that when tailings are resuspended, whether by mechanical stirring or by intense wind and wave activity, sulphide oxidation is accelerated with consequent precipitation of secondary iron oxyhydroxide minerals. These minerals tend to have a large surface area when freshly precipitated and can adsorb or scavenge trace metals released during the primary oxidation reactions. Further research is recommended to assess the long-term stability of the oxyhydroxides, especially as conditions in the water become reducing, under which iron hydroxides tend to dissolve and are likely to release scavenged metals. Metals released in the water cover, as a result of increased oxidation due to resuspension, do not infiltrate deep into the underlying tailings. The impact of this resuspension-induced oxidation and metal release on the overall water quality in the field should be assessed. Various factors including dilution and contributions from groundwater and precipitation will have an influence on the overall water quality in the field. These factors are not evaluated in the present laboratory study.

SOMMAIRE

L'utilisation de couvertures aqueuses peu profondes (jusqu'a 2 m) pour submerger les residus miniers sulfurés est une méthode populaire utilisée par l'industrie minière pour prévenir le drainage minier acide. La turbulence que produit le vent dans les parcs à residus submerges peut accélérer le transfert d'oxygene, de l'air vers l'eau, en créant de laturbulence à l'interface air-eau, provoquant ainsi le melange mécanique de l'oxygene dans l'eau et maintenant les concentrations d'oxygene dissous à des niveaux de saturation. La turbulence peut Cgalement resuspendre les particules de residus dans la couverture aqueuse saturée d'oxygene et exposer les residus à un contact plus étroit avec l'oxygene, augmentant ainsi les possibilités d'oxydation et de degagement de métaux.

Vers la fin de l'année *1996,* le *Geotechnical Research Centre (University of Western Ontario)* a mené une etude en laboratoire portant sur les effets de la resuspension des residus sur l'oxydation et la production d'acide. L'étude, entreprise pour le compte du Programme de neutralisation des eaux de drainage dans l'environnement minier (NEDEM), a été commanditée par *Battle Mountain Canada Limited,* Falconbridge Limitée, INCO Limitée, Mines et Exploration Noranda Inc., *Teck Corporation,* le Minister-e du developpement du Nord et des mines de l'ontario, et le Centre canadien de la technologie des mines et des mineraux (CANMET) dans le cadre de 1'Entente (Canada-Ontario) de developpement du nord de 1'Ontario (EDNO). Le present rapport fait &at des resultats des travaux.

L'etude en laboratoire a consist&e dans une serie d'essais dans des colonnes de Plexiglas remplies de residus de pyrrhotine inoxydes qui ont ete submerges par des couvertures aqueuses de 45, 60 et 80 cm de profondeur. Les residus provenaient directement des pipelines de la decharge de residus du concentrateur de *Strathcona Mines* de Falconbridge, situees a proximite de Sudbury, en Ontario. La couverture aqueuse a ettc agitee a 140, 170 et 200 revolutions par minute afin de suspendre les residus sous-jacents. Les residus submerges ont ete soumis a des essais de contrcile sans agitation a des fins de comparaison. Pour faciliter l'analyse des resultats, on a utilise la vitesse de l'agitateur et la profondeur de la couverture aqueuse en vue de deftir 1' indice de melange, un parametre saris dimension qui mesure le degre de mixage de la couverture aqueuse. On a mesure le transfert

de la masse d'oxygène, de l'air dans la couverture aqueuse, pour chaque indice de melange et surveillé la couverture aqueuse afin de déterminer son contenu d'oxygène dissous, son pH, sa conductivité et sa teneur en sulfates et en métaux. Au terme des essais (126 jours), on a échantillonné les résidus en suspension, les résidus de surface et les rksidus solides non déplacés ainsi que l'eau interstitielle aux fins de l'analyse chimique. L'ensemble des résidus ainsi que leur minéralogie superficielle ont également fait l'objet d'un examen.

Les constatations et conclusions principales de l'étude sont les suivantes :

1. La resuspension accélère l'oxydation des rksidus sulfurés, la production d'acide et le dégagement de métaux. Ce phénomène est basé sur l'épuisement des sulfures (pyrrhotine), la consommation d'oxygène, le pH, le sulfate et la charge de métaux.
2. Les produits d'oxydation dont la gravité spécifique est de 2,7 sont plus légers que les résidus originaux dont la gravité spécifique est de 3,9 - 4,4.
3. Les produits d'oxydationincluent les oxyhydroxydes ferriques (possiblement la goéthite) et le gypse.
4. Les résidus en suspension sont plus fins que les résidus au repos : 80 % des résidus en suspension comparativement à 30 % des résidus originaux ont une dimension de moins de 0,018 mm.
5. Les rksidus en suspension inoxydés contiennent un minéral sulfuré, soit la pyrrhotine, ainsi que des minéraux de gangue.
6. La vitesse du transfert de l'oxygène à la couverture aqueuse est indépendante de l'indice de melange.
7. Le dégagement de nickel, de zinc, d'aluminium et de manganèse augmente en fonction de l'indice de melange.
8. Une érosion importante du lit se produit quand l'indice de melange atteint le seuil critique. Dans les couvertures aqueuses peu profondes (possiblement 60 cm ou moins) le mélange pourrait atteindre le seuil critique.

Les résultats de l'étude laissent croire que laresuspension des rksidus, soit par agitation mécanique ou par de grands vents et de fortes vagues, accélère l'oxydation des sulfures et la précipitation subséquente des oxyhydroxydes ferriques. Dès leur précipitation, ces

minéraux ont habituellement une large aire de surface et peuvent adsorber ou entrainer des metaux traces libérés par les reactions que provoque l'oxydation initiale. On recommande de mener des recherches plus poussées afin d'évaluer la stabilité à long terme des oxyhydroxydes, en particulier quand les conditions de l'eau deviennent réductrices, ce qui peut causer la dissolution des hydroxydes ferriques et possiblement entrainer le degagement de metaux. Les metaux qui sont libérés dans la couverture aqueuse en raison de l'oxydation accélérée causée par la resuspension ne s'infiltrent pas profondement dans les résidus sous-jacents. L'impact de cette oxydation induite par la resuspension et le degagement de metaux sur la qualite globale de l'eau qui se trouve sur le terrain devrait être évaluée. Divers elements, y compris la dilution et les effets de l'eau souterraine et des precipitations affecteront la qualité globale de l'eau. Dans la présente etude en laboratoire, ces elements n'ont pas été évalués.

TABLE OF CONTENTS

Page

EXECUTIVE SUMMARY ii

TABLE OF CONTENTS iv

LIST OF FIGURES vi

1. INTRODUCTION 1

2. MATERIALS AND METHODS 3

2.1 Mine Tailings 3

2.2 Column Design and Fabrication 4

2.3 Packing of Tailings 6

2.4 Resuspension Experiments 6

2.5 Decommissioning of Columns 7

2.6 Sample Preservation 8

2.7 Unoxidized Resuspended Tailings 8

2.8 Oxygen Flux Measurements 8

Figures 2.1 to 2.5 10

3. RESULTS 15

3.1 Initial Chemistry of Water Cover 15

3.2 Electrical Conductivity 15

3.3 Dissolved Oxygen (DO) 15

3.4 pH and SO_4^{2-} 17

3.5 Depth of Unoxidized Tailings at End of Experiments 18

3.6 Suspended Tailings at End of Experiments 19

Page

3.7 Particle Size and Mineralogy of Unoxidized Resuspended Tailings 22

3.8 Influence of Resupension on Undisturbed Tailings 22

3.9 Pore Water Chemistry of Undisturbed Tailings 23

3.10 Cumulative Metal Release in the Water Cover 26

Figures 3.1 to 3.88 29

4. ANALYSIS AND DISCUSSION 117

4.1 Resuspension 117

4.2 Oxidation of Suspended Tailings 118

4.3 Influence of Mixing 119

4.4 Secondary Mineral Precipitation 122

4.5 Shear Stress Generated in Stirred Columns 123

Figures 4.1 to 4.7 125

5. CONCLUSIONS 132

ACKNOWLEDGEMENTS 133

REFERENCES 134

LIST OF FIGURES

Figure 2.1 X-ray diffkactogram of original unoxidized tailings

Figure 2.2 Optical photograph of original unoxidized tailings

Figure 2.3 Scanning electron photomicrograph and energy dispersion analysis of unoxidized original tailings showing pyrrhotite

Figure 2.4 Scanning electron photomicrograph of unoxidized original tailings showing silicates

Figure 2.5 Schematic view of column assembly

Figure 3.1 Variation of electrical conductivity with time in 80 cm water cover

Figure 3.2 Variation of electrical conductivity with time in 60 cm water cover

Figure 3.3 Variation of electrical conductivity with time in 45 cm water cover

Figure 3.4 Variation of DO concentration versus time in 80 cm water cover

Figure 3.5 Variation of DO concentration versus time in 60 cm water cover

Figure 3.6 Variation of DO concentration versus time in 45 cm water cover

Figure 3.7 DO versus time for Column C/40/200 during oxygen flux measurements

Figure 3.8 A typical variation of mass transfer velocity with time, Column C/45/200

Figure 3.9 Dissolved oxygen consumption versus time

Figure 3.10 pH versus time for 80 cm water cover stirred at 200 rpm

Figure 3.11 pH versus time for 60 cm water cover stirred at 170 rpm

Figure 3.12 pH versus time for 45 cm water cover stirred at 140 rpm

Figure 3.13 Sulphate versus time for 80 cm water cover stirred at 200, 170 and 140 rpm

Figure 3.14 Sulphate versus time for 60 cm water cover stirred at 200, 170 and 140 rpm

Figure 3.15 Sulphate versus time for 45 cm water cover stirred at 200, 170 and 140 rpm

Figure 3.16 Variation of thickness of oxidized tailings with mixing index

Figure 3.17 Photograph of suspended tailings particles in 80, 60 and 45 cm water covers stirred at 200 rpm

Figure 3.18 Photograph of suspended tailings particles in 80, 60 and 45 cm water covers stirred at 170 rpm

Figure 3.19 Photograph of suspended tailings particles in 80, 60 and 45 cm water covers stirred at 140 rpm

Figure 3.20 Photograph of ripples observed in 80 cm water cover stirred at 200 rpm

Figure 3.21 Photograph of ripples observed in 80 cm water cover stirred at 170 rpm

Figure 3.22 X-ray diffractogram of resuspended tailings in 80 cm water cover stirred at 200 rpm

Figure 3.23 X-ray diffractogram of resuspended tailings in 80 cm water cover stirred at 170 rpm

Figure 3.24 X-ray diffractogram of resuspended tailings in 80 cm water cover stirred at 140rpm

Figure 3.25 X-ray diffractogram of resuspended tailings in 60 cm water cover stirred at 200 rpm

Figure 3.26 X-ray diffractogram of resuspended tailings in 60 cm water cover stirred at 170rpm

Figure 3.27 X-ray diffractogram of resuspended tailings in 60 cm water cover stirred at 140 rpm

Figure 3.28 X-ray diffiactogram of resuspended tailings in 45 cm water cover stirred at 200 rpm

Figure 3.29 X-ray diffractogram of resuspended tailings in 45 cm water cover stirred at 170rpm

Figure 3.30 X-ray diffiactogram of resuspended tailings in 45 cm water cover stirred at 140rpm

Figure 3.3 1 Optical photograph of resuspended particles in 80 cm water cover stirred at 140 rpm (20 cm above tailings surface)

Figure 3.32 Optical photograph of resuspended particles in 80 cm water cover stirred at 140 rpm (40 cm above tailings surface)

Figure 3.33 Optical photograph of resuspended particles in 60 cm water cover stirred at 200 rpm (20 cm above tailings surface)

Figure 3.34 Optical photograph of resuspended particles in 60 cm water cover stirred at 200 rpm (40 cm above tailings surface)

Figure 3.35 Optical photograph of resuspended particles in 60 cm water cover stirred at 140 rpm (20 cm above tailings surface)

Figure 3.36 Optical photograph of resuspended particles in 60 cm water cover stirred at 140 rpm (40 cm above taings surface)

Figure 3.37 Optical photograph of resuspended particles in 45 cm water cover stirred at 200 rpm (20 cm above tailings surface)

Figure 3.38 Optical photograph of resuspended particles in 45 cm water cover stirred at 200 rpm (40 cm above tailings surface)

Figure 3.39 Optical photograph of resuspended particles in 45 cm water cover stirred at 140 rpm (20 cm above tailings surface)

Figure 3.40 Optical photograph of resuspended particles in 45 cm water cover stirred at 140 rpm (40 cm above tailings surface)

Figure 3.4 1 Scanning electron photomicrograph of resuspended particles in 80 cm water cover stirred at 140 rpm

Figure 3.42 Scanning electron photomicrograph of resuspended particles in 60 cm water cover stirred at 170 rpm

Figure 3.43 Scanning electron photomicrograph of resuspended particles in 45 cm water cover stirred at 170 rpm

Figure 3.44 Particle size distributions of oxidized resuspended tailings

Figure 3.45 Particle size distributions of oxidized and unoxidized resuspended tailings

Figure 3.46 Variation of resuspended tailings concentration with mixing index

Figure 3.47 X-ray diffractogram of unoxidized resuspended tailings in 45 cm water cover stirred at 200 rpm (20 cm above tailings surface)

Figure 3.48 X-ray diffkactogram of unoxidized resuspended tailings in 60 cm water cover stirred at 200 rpm (20 cm above tailings surface)

Figure 3.49 X-ray diffkactogram of unoxidized resuspended tailings in 45 cm water cover stirred at 140 rpm (20 cm above tailings surface)

Figure 3.50 X-ray diffractogram of unoxidized resuspended tailings in 80 cm water cover stirred at 140 rpm (20 cm above tailings surface)

Figure 3.51 X-ray diffractogram of unoxidized resuspended tailings in 45 cm water cover stirred at 200 rpm (40 cm above tailings surface)

Figure 3.52 X-ray diffiactogram of unoxidized resuspended tailings in 60 cm water cover stirred at 200 rpm (40 cm above tailings surface)

Figure 3.53 X-ray diffractogram of unoxidized resuspended tailings in 45 cm water cover stirred at 140 rpm (40 cm above tailings surface)

Figure 3.54 X-ray diffractogram of unoxidized resuspended tailings in 60 cm water cover stirred at 140 rpm (40 cm above tailings surface)

Figure 3.55 Ratio of pyrrhotite to amphibole peak intensities versus mixing index

Figure 3.56 Optical photograph of surface of tailings in 80 cm water cover stirred at 140 rpm

Figure 3.57 Optical photograph of surface of tailings in static 80 cm water cover

Figure 3.58 X-ray diffractogram of surface of undisturbed tailings underlying 80 cm water cover stirred at 170 rpm

Figure 3.59 X-ray diffkactogram of surface of undisturbed tailings underlying 80 cm water cover stirred at 140 rpm

Figure 3.60 X-ray diffiactogram of surface of undisturbed tailings underlying 60 cm water cover stirred at 170 rpm

Figure 3.61 X-ray diffractogram of surface of undisturbed tailings underlying 45 cm water cover stirred at 170 rpm

Figure 3.62 X-ray diffkactogram of surface of undisturbed tailings underlying static 80 cm water cover

Figure 3.63 X-ray diffractogram of surface of undisturbed tailings underlying static 45 cm water cover

Figure 3.64 Total Fe and S profiles in undisturbed tailings below static 80 cm water cover and cover stirred at 140 rpm

Figure 3.65 Total Cu, Ni, Al, Mg and Ca profiles in undisturbed tailings below static 80 cm water cover and cover stirred at 140 rpm

Figure 3.66 pH profile for tailings pore water

Figure 3.67 Mg, K, Aℓ and Si concentration profiles for tailings pore water below 80 cm water cover stirred at 140 rpm

Figure 3.68 Ca, Ni, Na and Fe^{3+} concentration profiles for tailings pore water below 80 cm water cover stirred at 140 rpm

Figure 3.69 Cu, Zn and Mn concentration profiles for tailings pore water below 80 cm water cover stirred at 140 rpm

Figure 3.70 Aℓ, Zn, Ni, Mn and Cu concentration profiles for tailings pore water below static 80 cm water cover

Figure 3.71 Fe^{3+}, Na, Mg and K concentration profiles for tailings pore water below static 80 cm water cover

Figure 3.72 Photograph of Plexiglas columns showing yellowish brown film of suspended particle coating on side walls

Figure 3.73 Scanning electron photomicrograph of precipitate in 60 cm water cover stirred at 200 rpm indicating the presence of iron oxyhydrode

Figure 3.74 Scanning electron photomicrograph of precipitate in 60 cm water cover stirred at 200 rpm indicating the presence of gypsum

Figure 3.75 Variation of ferric iron concentration in 80 cm water cover

Figure 3.76 Variation of ferric iron concentration in 60 cm water cover

Figure 3.77 Variation of ferric iron concentration in 45 cm water cover

Figure 3.78 Variation of ferric iron release with time and mixing index

Figure 3.79 Variation of zinc release with time and mixing index

Figure 3.80 Variation of copper release with time and mixing index

Figure 3.81 Variation of nickel release with time and mixing index

Figure 3.82 Variation of manganese release with time and mixing index

Figure 3.83 Variation of magnesium release with time and mixing index

Figure 3.84 Variation of calcium release with time and mixing index

Figure 3.85 Variation of potassium release with time and mixing index

Figure 3.86 Variation of sodium release with time and mixing index

Figure 3.87 Variation of aluminium release with time and mixing index

Figure 3.88 Variation of silicon release with time and mixing index

Figure 4.1 Variation of ferric iron release with mixing index

Figure 4.2 Variation of ferrous to ferric iron ratio with time in stirred columns

Figure 4.3 Variation of actual versus expected nickel release with mixing index

Figure 4.4 Variation of actual versus expected ferric iron release with mixing index

Figure 4.5 Variation of actual versus expected zinc release with mixing index

Figure 4.6 Variation of actual versus expected calcium release with mixing index

Figure 4.7 Flow of fluid particles in 80 cm water covers stirred at 200, 170 and 140 rpm

1. INTRODUCTION

Many base metal and uranium mine tailings contain reactive sulphide minerals such as pyrite and pyrrhotite. When these minerals are exposed to oxygen and moisture, they oxidize and may produce acidic drainage, if there are insufficient quantities of buffering minerals to neutralize the oxidation products. To curtail this problem the supply of oxygen, the primary oxidant, must be eliminated or significantly reduced. Hence mine tailings are normally disposed of by submerging them under a water cover. The submergence reduces the amount of oxygen available to the sulphide minerals as the oxygen dissolved in water is only 8.6 g/m^3 at $25^{O}C$, compared to 285 g/m^3 available in air. In addition, oxygen diffusivity in water is $\sim 2 \times 10^{-9}$ m^2/s compared to 1.78×10^{-5} m^2/s in air, which suggests that oxygen transfer to submerged tailings by molecular diffusion alone is about 10,000 times slower than to uncovered tailings.

Shallow water covers (0.5-2 m) over reactive tailings have been researched in Canada in a number of laboratory studies (Dave and Vivyurka, 1994; Aubé et al, 1995). These studies examined oxidation rates in fresh tailings and flushing of oxidation products in previously oxidized tailings covered with a varying depth of water. The role of a surface protection barrier in reducing oxidation and upward flux of metals into the water cover has also been studied. The results of these laboratory studies indicate that while a water cover significantly reduces downward metal flux in tailings (by as much as 3000 times), some amount of oxidation may still occur. For example, the study by Dave et al (1994) found that drainage water from flooded tailings had an average pH of $\sim$ 5.0 and an iron concentration of 20 mg/L. It was inferred from laboratory oxidation rate studies that this oxidation was temporary and that only the top few centimetres (up to 10 cm) of the tailings would oxidize to form a crust consisting of a mixture of iron oxyhydroxides and organic substrate. This crust would tend to serve as a barrier to oxygen, thereby minimizing further oxidation.

In flooded or submerged tailings wind is one of the major factors contributing to the formation of acidic drainage. It increases the oxygen flux from air to water by creating turbulence at the air-water interface, thus promoting mechanical mixing of oxygen from

air to water and thus keeping the dissolved oxygen concentrations at saturation levels. Wind driven turbulence can also resuspend fine tailings particles.

Previous resuspension studies on water covers have all focused on tailings stability. No study has yet addressed the possibility of increased sulphide mineral oxidation and acid generation due to resuspension (Yanful and Simms, 1997). In decommissioned tailings and where recycling of pond water is not critical, turbidity of the water cover is not the only consideration. An important question that needs to be addressed is whether resuspended tailings particles include sulphide minerals which, because of their increased contact with oxygen, tend to oxidize more rapidly.

The principal objective of the present study is to describe laboratory experiments performed to examine the influence of resuspension on the oxidation of reactive sulphide tailings. The experiments generated water quality versus time data, which are used to interpret trends and discuss secondary mineral precipitation and overall effectiveness of a water cover above mine tailings.

2. MATERIALS AND METHODS

2.1 Mine Tailings

Fresh unoxidized pyrrhotite tailings were obtained from the Falconbridge Strathcona Mine, near Sudbury, Ontario. The tailings were collected directly from the end of a mill discharge pipeline into plastic bags and sealed. The bags were packed in a 45-gallon drum and filled with water to prevent tailings oxidation. The drums were sealed and sent to The University of Western Ontario.

These tailings are discharged from the mill at 5-10 % solids. The mineralogical composition of the solids (by weight) is 20% gangue (mainly silicates), 75% pyrrhotite, and 0.14% chalcopyrite. The elemental composition is 48% iron, 34% sulphur, 0.05% copper and 0.76% nickel. The specific gravity obtained in the mill is 4.4 and the pH is 9-l 0. The unoxidized solid tailings are dark grey, have a sandy texture and have no odour.

The tailings were analyzed at The University of Western Ontario and their specific gravity was found to average 3.87. The particle size distribution of the original tailings was determined using a Malvern particle size analyzer (Model 2600 SB.09). The mineralogy was determined by X-ray diffraction analysis conducted on a Rigaku diffractometer using CoKα radiation. Diffractograms were corrected to the quartz 101 peak (3.342 A°). The minerals identified were quartz, pyrrhotite, feldspar, kaolinite, amphibole and mica (Figure 2.1). Polished sections were prepared of the samples and photographs taken using an optical microscope. The image was magnified 200 times (Figure 2.2). The photograph indicates the presence of pyrrhotite (light or white) and silicates (dark or black background). Scanning electron microscopy (SEM) was also used to examine the elemental composition of the tailings surface. An IS1 DS-130 scanning electron microscope was used to collect images using a beam potential of 15kV. Figures 2.3 and 2.4 show photomicrographs of the unoxidized original tailings when focused on pyrrhotite and silicates respectively. The percent by weight of iron (56%) and sulphur (44%) shown is typical of pyrrhotite ($Fe_{1-x}S$). In the formula for pyrrhotite, x can vary between 0 and 0.2 (Hurlbut and Klein, 1977), but is typically about 0.125 (Janzen et al.,

1997). A value of 0.125 gives a composition by weight of 58% iron and 42% sulphur, which is close to the values shown in Figure 2.3. The elemental composition of silicates present in the tailings, illustrated in Figure 2.4, includes Na, Mg, Al, Si, S, K, Ca, Fe and Ni. Tailings samples were also digested in an acidic solution (nitric and hydrofluoric acids), and the resulting liquid sample was analyzed using inductively coupled plasma spectrometry (ICP). The results are presented in Table 1.

Table 1 : Elemental Composition of Strathcona Mine Tailings

Element	Al	Ca	Cu	Fe	K	Mg	Mn	Na	Ni	Zn
Weight %	2.53	1.52	0.236	30.9	0.31	1.13	0.07	0.84	0.93	0.05

The results of the elemental and mineralogical analyses show that the tailings consist mainly of pyrrhotite and alumino-silicates (clay minerals and feldspars).

2.2 Column Design and Fabrication

The key objective of the resuspension experiments was to generate different entrainment rates of mine tailings particles suspended in water and compare the metal release rates at various mixing speeds to the base case where there was no resuspension.

To achieve this objective, 12 Plexiglas columns, each with an internal diameter of 30 cm, were fabricated. Four of the columns had a height of 1.2 m to ensure that a water depth of 80 cm could be achieved. Teflon stirrers were attached to 120-V AC motors to stir the water column and resuspend the tailings. Each of the four columns was stirred at 200, 170, 140 and zero rpm (revolutions per minute). A maximum stirrer speed of 200 rpm was chosen to avoid the formation of whirlpools on the water surface, while a stirrer speed of 140 rpm for the 80 cm water cover was found to be the minimum required for resuspension. Figure 2.5 shows a schematic diagram of the column assembly. The next four columns had a height of 1 m to ensure that a water depth of 60 cm could be achieved. The selected stirring speeds were again 200, 170, 140, and zero rpm. The last four columns also had a height of 1 m to achieve a water depth of 45 cm. The length of

the stirrer was adjusted and stirring speeds were as before. All stirrers were immersed 5 cm to minimize splashing of the water surface.

The power source was connected to a voltage stabilizer and the voltage was maintained at 115 V. Each motor was controlled by a voltage regulator. An optical tachometer was used to set the stirrers to the desired rpm. The rpm delivered by the motors was monitored over a 24-hour period and found to fluctuate within (+/-) 2%. The rpm was constantly monitored during the entire duration of the experiments (126 days). In the event the fluctuations exceeded 2%, the rpm of the stirrers was adjusted using the voltage regulators.

Each column had ports at suitable intervals to collect water samples. A perforated, circular Plexiglas separator covered with a geotextile, was fitted with an "O" ring around its periphery to maintain a leak proof joint (Figure 2.5). The separator was placed 15 cm above the bottom of the column, and tailings were packed on top of the separator. This arrangement facilitated sampling of the water below the tailings and ensured that the tailings remained above the separator.

The designation for identifying the columns is as follows:
The column (C) with a water depth of 80 cm and a stirrer speed of 200 rpm is represented by C/80/200, while C/60/170 refers to the column with a water cover of 60 cm and a stirrer speed of 170 rpm, and so on.

The degree of mixing in the column will be directly proportional to the stirrer speed and inversely proportional to the depth of water cover. In this report, a non-dimensional, mixing index is used to designate the degree of mixing. If the degree of mixing achieved in column C/80/200 is given a non-dimensional mixing index of one, then for column C/80/170, the mixing index will be (170/200)*(80/80) = 0.85. Thus column C/40/140 will have a corresponding mixing index of (140/200)*(80/40) = 1.4. The higher the numerical value of the mixing index, the higher the degree of mixing in the column. The calculated mixing indices are presented in Table 2.

Table 2 Mixing indices in stirred and static columns

Column number	Depth of water (cm)	Motor (RPM)	Mixing index
C/80/0	80	0	0
C/80/140	80	140	0.7
C/80/200	80	200	1.0
C/60/0	60	0	0
C/60/140	60	140	0.93
C/60/170	60	170	1.13
C/60/200	60	200	1.33
C/45/0	45	0	0
c/45/1 40	45	140	1.24
c/45/1 70	45	170	1.51
C/45/200	45	200	1.78

2.3 Packing of Tailings

The columns were first filled with tap water and then drained from the bottom port until only the lower 15 cm of the column below the geotextile separator was tilled with water. This ensured that no air bubbles were trapped in the lower 15 cm of the column. Twenty kilograms of tailings were then placed on top of the separator, and tamped with a Teflon rod to achieve a uniform depth of 10 cm. This procedure was followed for all 12 columns. To prevent resuspension during fill-up, a plastic cover was first placed on top of the tailings and then tap water was used to fill the columns to the required depth. The plastic cover was then removed to begin the experiments.

2.4 Resuspension Experiments

Motors were run to generate the desired stirrer speeds for resuspension. The motors were turned off at predetermined times to collect water samples above and below the

tailings in each column. The motors were turned off for about eight hours to allow most of the larger size particles to settle and 125 mL water samples were collected and filtered through 0.45 μm membrane filters. The samples were tested for pH, electrical conductivity, sulphate and metals. Samples for metal determination were acidified to pH 2 with 0.5 mL ultrapure nitric acid per 30 mL sample. Sulphate was determined by ion chromatography, metals by inductively coupled plasma (ICP) spectrometry, pH by a combination electrode using appropriate buffers, and conductivity by electrode and conductivity meter. Dissolved oxygen (DO) was measured in-place using a YSI Model 55 portable dissolved oxygen meter. Initially samples were collected from all the ports and checked for electrical conductivity and pH. Electrical conductivity and pH did not vary much with water cover depth, which suggested that the water cover was well mixed. Consequently, water samples were only collected from a port located 20 cm above the tailings. DO was measured in-place at 5 cm intervals and found to be essentially the same at all depths, confirming that the water cover was well mixed; all subsequent measurements were, therefore, taken at a depth of 20 cm above the tailings. Water samples in the static columns were collected through ports located 5 cm above the tailings.

2.5 Decommissioning of Columns

At the end of the experiments water samples were collected from all the columns while the water cover was being stirred. These water samples were collected without using filters, and were centrifuged to separate suspended tailings particles.

The columns were built to facilitate tailings removal. This was achieved by designing the base of the columns to be easily removed to access the remaining tailings with minimum disturbance. The precipitate that had settled on top of the tailings was removed, and the depth of dark grey, unoxidized tailings remaining was measured. The top layer of the tailings was removed with a spatula, after carefully removing all precipitates. The next 0.5 cm layer of tailings was then removed and the remaining tailings were sliced at 2 cm intervals. All tailings samples collected were subjected to mineralogical and geochemical analyses.

2.6 Sample Preservation

Water samples were preserved as discussed in Section 2.4. Upon sampling, tailings were immediately wrapped in a plastic cover, coated with microcrystalline wax, and then stored at 22^0C. When tailings were required in the dry state for subsequent analysis, the wax cover was removed in a sealed glove box tilled with argon gas, and the tailings were left to dry in the glove box. Tailings samples were then transported for analysis in a dessicator. This procedure ensured that minimal oxidation of tailings took place after their collection.

2.7 Unoxidized Resuspended Tailings

To determine the variation of particle size distribution of unoxidized, resuspended tailings with water cover depth, the columns were re-assembled and filled with unoxidized tailings from the top of the Plexiglas separator to a height of 10 cm. The same water depths and mixing speeds were established as before, and the tailings were sent into suspension. Suspended tailings were sampled at depths of 20 cm and 40 cm above the tailings surface for the analysis of mineralogy and particle size distribution. These samples were collected 10 mins after resuspension had been initiated to allow time for the flow in the columns to stabilize.

2.8 Oxygen Flux Measurements

The same columns were cleaned and filled with fresh tap water and stirred as before. The water was chemically deoxygenated using technical grade sodium sulphite and cobaltous chloride as catalyst. Section 208A of Standard Methods (1980) suggests adding 8.05 g/m^3 of cobaltous chloride and 117 g/m^3 of sodium sulphite to water containing an initial DO concentration of 10 mg/L. The DO concentration in the water was measured and the amounts of reagents needed for complete deoxygenation was calculated. In all cases 10 % additional quantity of reagents was added to ensure complete deoxygenation. These reagents were dissolved in warm distilled water and added to the columns while stirring was in progress. The DO concentrations were continuously monitored and in all cases 100% deoxygenation was achieved. The

measurements showed that the DO concentration was essentially the same at various depths in the water cover, indicating that the water cover was well mixed. Hence all measurements were taken at half the depth of the water cover. DO readings were taken at prescribed times, when concentrations in the water cover started to increase because of oxygen influx caused by the disturbance of the water surface.

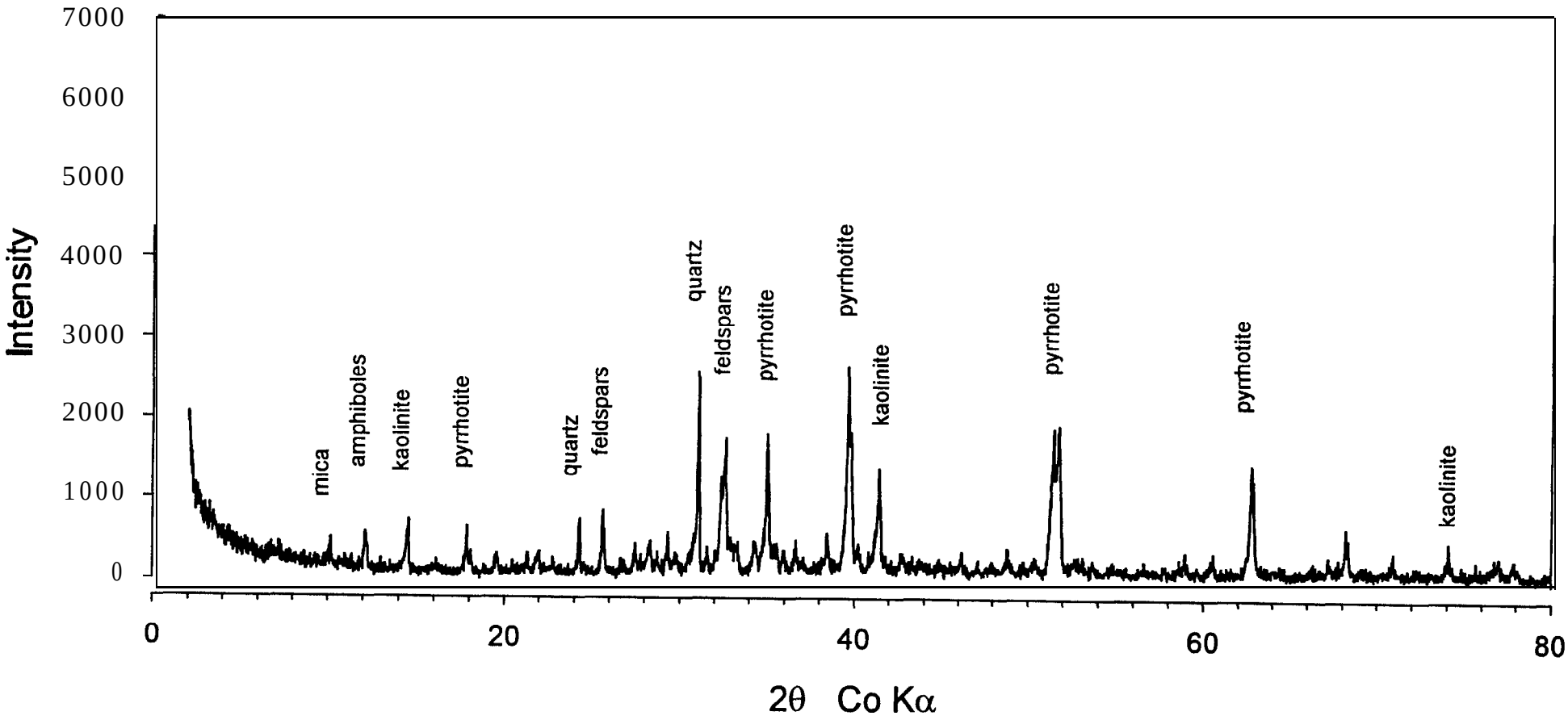

Figure 2.1 X-ray diffractogram of original unoxidized tailings

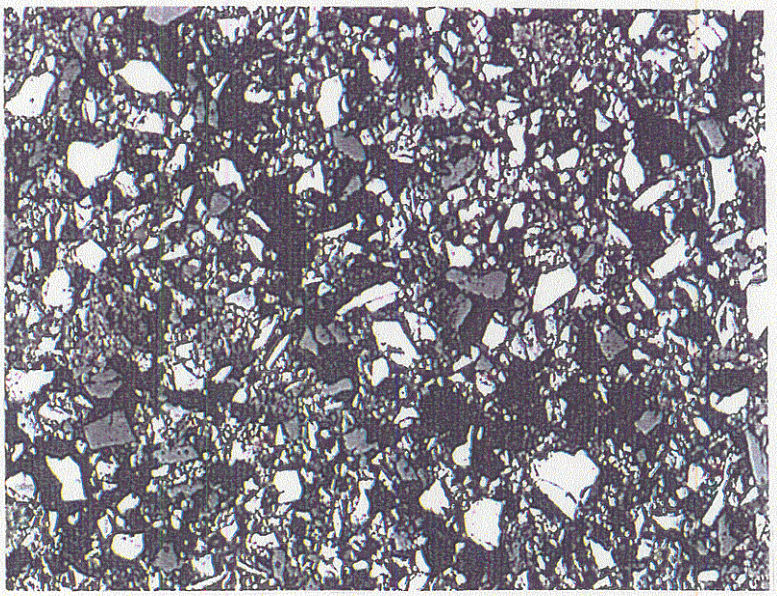

Figure 2.2 Optical photograph of original unoxidized tailings
[Light or white patches show pyrrhotite; dark background indicates silicate]

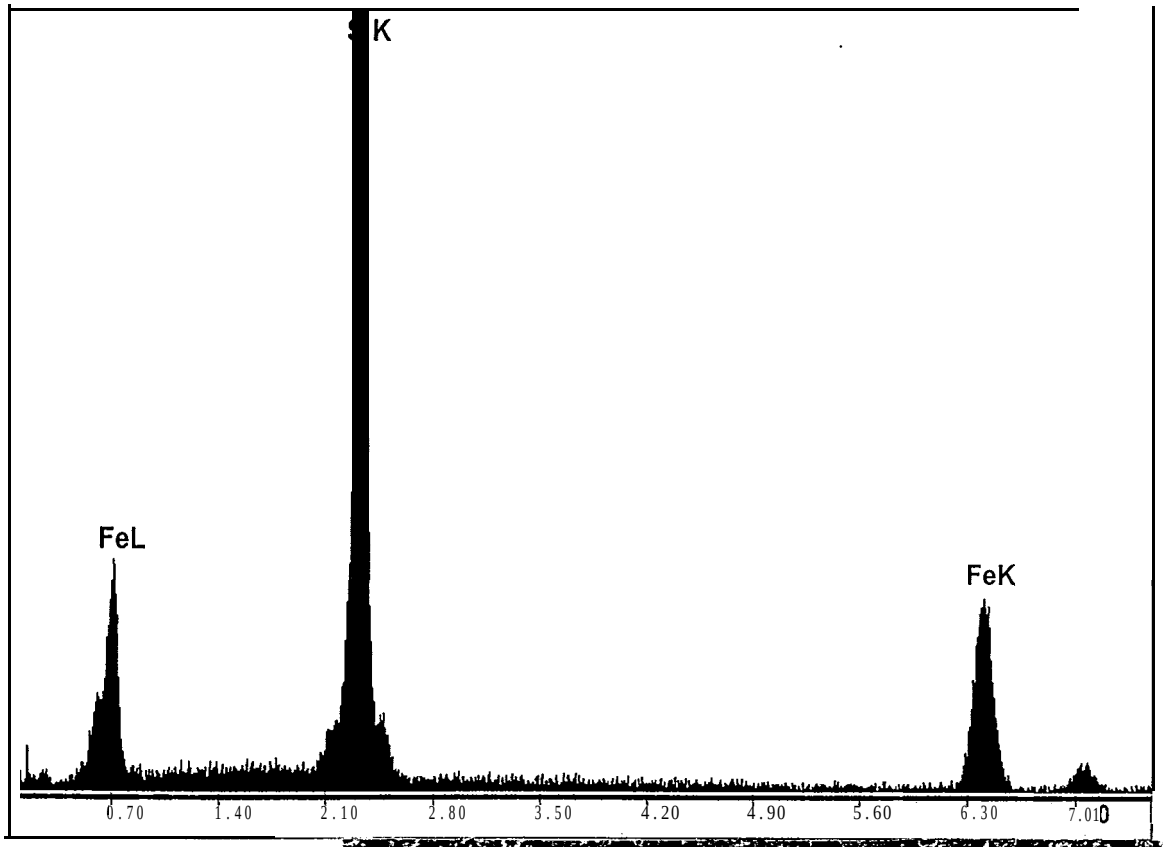

Element	Wt %	At %
SK	55.85	68.78
FeK	44.15	31.22
Total	100.00	100.00

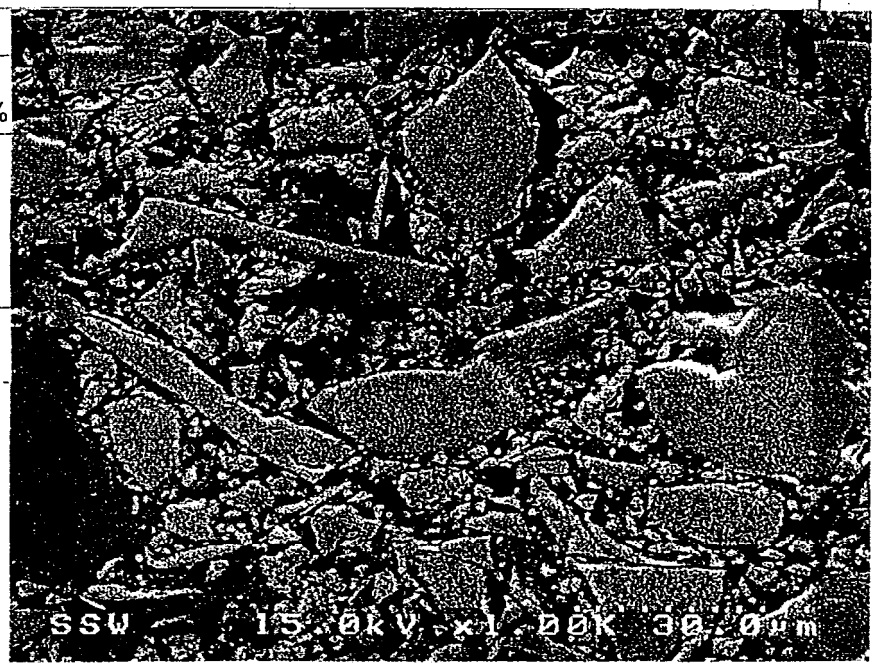

Figure 2.3 Scanning electron photomicrograph and energy dispersion analysis of unoxidized original tailings showing pyrrhotite

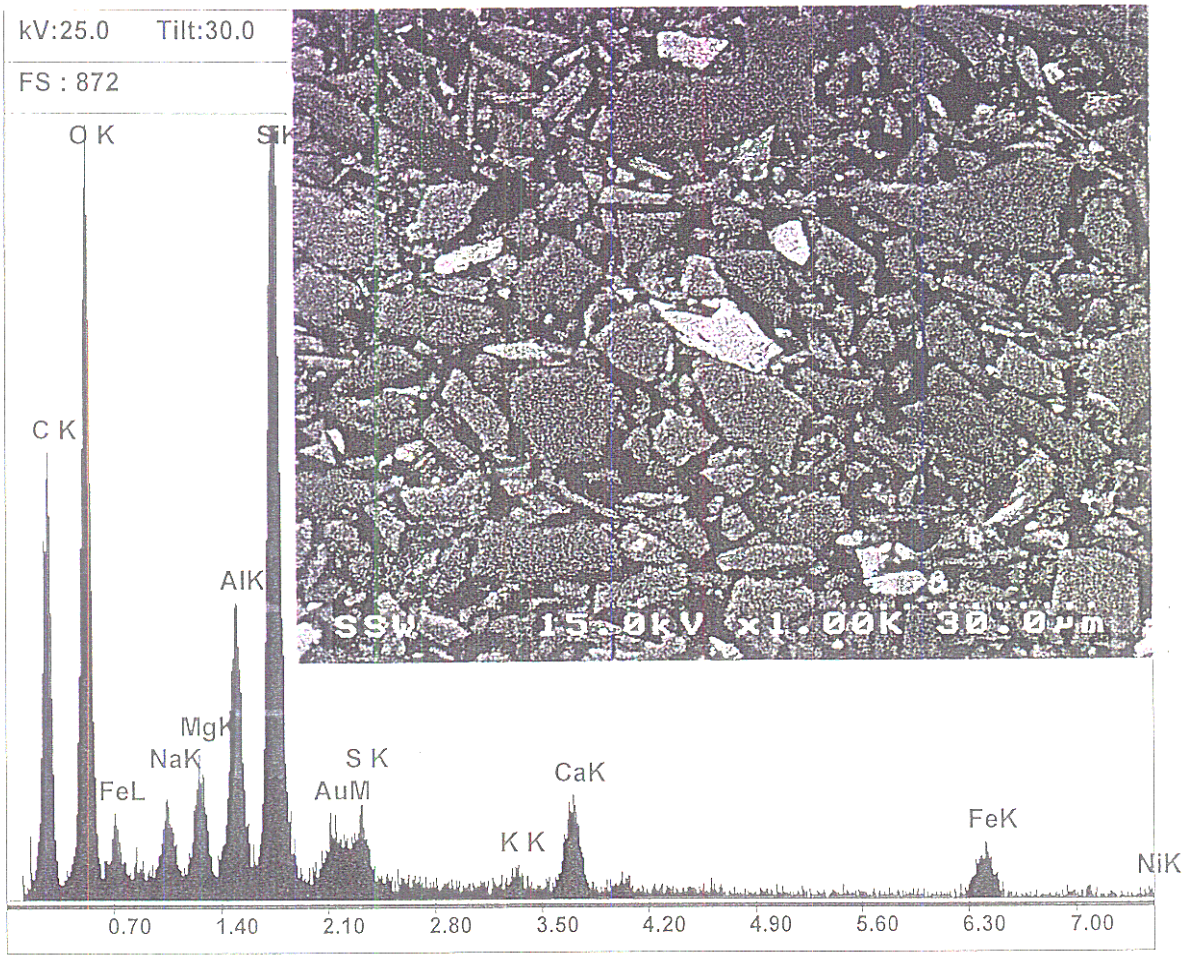

Figure 2.4 Scanning electron photomicrograph of unoxidized original tailings showing silicates

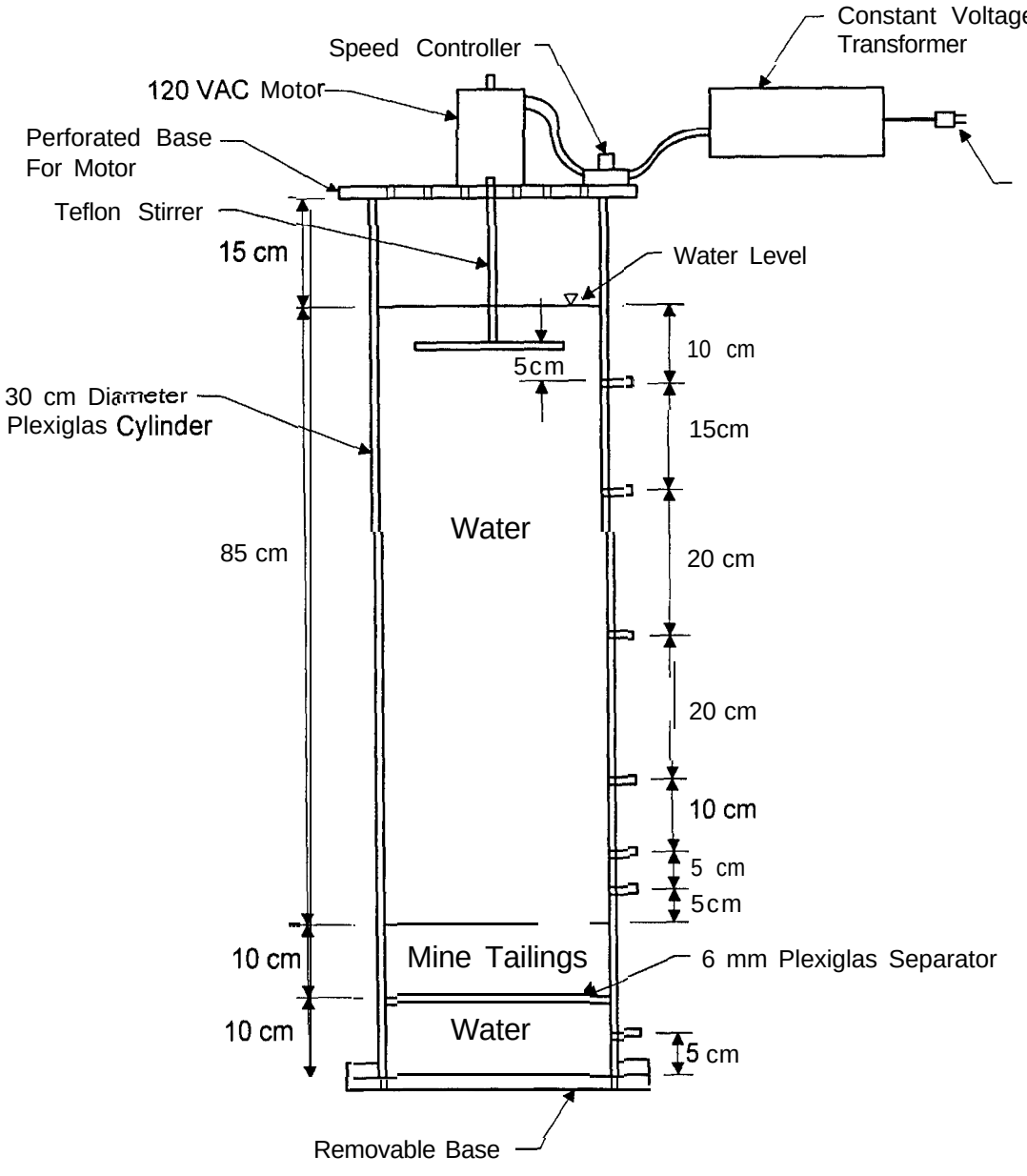

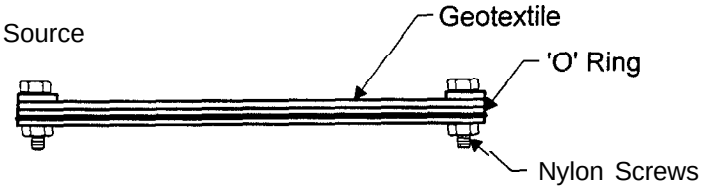

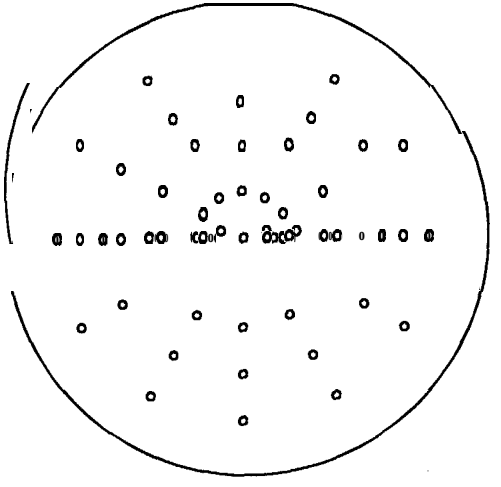

Perforated Plexiglas Disc
30 cm Diameter x 6 mm Thick

Figure 2.5 Schematic view of column assembly

3. RESULTS

3.1 Initial Chemistry of Water Cover

The tap water used in the experiments had dissolved oxygen content of 8.33 mg/L at a temperature of 22^0C. Laboratory temperature remained fairly constant at 22^0C during the experiments. The pH of the water was 7.8 and the electrical conductivity was 210 μS/cm.

3.2 Electrical Conductivity

An indication of dissolved solids concentration in the water cover was obtained by monitoring the change in the electrical conductivity of the water cover with time. Figures 3.1 to 3.3 present measured data for columns with water depths of 80, 60 and 45 cm, respectively. The results show that when tailings are resuspended the electrical conductivity is considerably greater than the case when the particles are at rest. For a given depth of water cover, it is seen that the electrical conductivity increases with an increase in the stirrer speed. The electrical conductivity of the 45 and 60 cm water covers is higher than that of the 80 cm cover. The increase in electrical conductivity is, likely, a result of the increased oxidation that occurs in the resuspended tailings under shallower water covers.

3.3 Dissolved Oxygen (DO)

Figures 3.4 to 3.6 show how the DO concentrations in the 80, 60 and 45 water covers vary with time. For the 80 cm water cover, it is seen that the DO concentration decreases gradually in the static column (C/SO/O), but is much higher than the concentration in the stirred columns (C/80/200, C/80/170 and C/80/140), where tailings are suspended. DO decreases continuously from 8.33 mg/L to less than 0.5 mg/L, and then stabilizes at this value during 80-100 days. For the same water cover depth, DO decreases with increase in stirrer speed. A similar trend is observed for columns with a water depth of 60 cm. For columns with a water depth of 45 cm the decrease in DO concentrations is the same at all stirrer speeds. The measured initial DO concentrations

are close to the reported saturation value of 8.4 mg/L in water at 22°C (Truesdale et al., 1955).

To calculate the DO consumption in the columns, the mass transfer velocity of oxygen from air to water is estimated for each column. From the oxygen flux measurements, readings of DO concentration with time are obtained. Figure 3.7 shows a typical variation of DO concentration with time for column C/40/200. From these readings the mass transfer velocity may be calculated using the following equation:

$$K_L = \frac{h}{t} \ell n \frac{C_s - C(0)}{C_s - C(t)} \qquad [1]$$

The dissolved oxygen consumed (mg/day) may be calculated as follows:

$$\text{Oxygen Consumption} = K_L A\,(C, \text{ - } C(t)) \qquad [2]$$

where,

K_L = mass transfer velocity (m/s)

h = depth of water cover (m)

ℓn = natural logarithm

C_s = dissolved oxygen concentration at saturation limit (mg/L)

C(0)= initial dissolved oxygen concentration (mg/L)

C(t) = dissolved oxygen concentration at time t (s)

A = area of column (m^2)

A typical variation of mass transfer velocity with time is shown in Figure 3.8 for column C/45/200. The mass transfer velocity initially fluctuates with time, but then later stabilizes to a unique value. The stabilized value is used to calculate DO consumption. Table 3 presents measured mass transfer velocities for the stirred columns.

Table 3 Mass transfer velocity of oxygen in various columns

Column number	Mass transfer velocity at 22° C (m/s) x 10^{-5}
C/80/140	2.37
C/80/170	2.02
C/80/200	8.33
C/60/ 140	1.4
C/60/170	2.2
C/60/200	1.58
c/45/1 40	1.49
c/45/1 70	1.69
C/45/200	2.18

For example, using a value of 2.18 x 10^{-5} m/s for column C/45/200 (Table 3), a column area of 0.071 m^2 and DO concentrations C(s) = 8.33 mg/L and C(t) = 0.5 mg/L, an oxygen consumption of 1.03 g/day is calculated for 80-100 days.

DO consumption is presented in Figure 3.9. It is clear that, except for column C/80/200, the DO consumed by resuspended tailings in all columns is very similar. The DO consumption in column C/80/200 at the end of the experiments is four times greater than the consumption in all the other columns. This is because the mass transfer velocity in column C/80/200 is considerably enhanced due to the amount of splashing that occurred on the water surface. In all other columns the transfer velocities are very similar (Table 3).

3.4 pH and SO_4^{-2}

Figures 3.10 to 3.12 show the variation of pH in the water cover with time for columns with water depths of 80, 60, and 45 cm. For columns C/80/200, C/80/170, and C/80/140 the pH decreases rapidly in the first twenty days and then gradually decreases and stabilizes to a value around 2.6. The rate of decrease in pH increases with stirrer speed (rpm). The pH-time data show similar trend in all other stirred columns. The pH of

the static water cover was much higher than that of the stirred water covers and it remained essentially stable at about 7.6 throughout the experiments.

The variation in sulphate concentration for the stirred columns is presented in Figures 3.13 to 3.15. The data show that sulphate production increased significantly when the tailings particles were resuspended. For a particular water cover depth, sulphate production increases as the stirrer speed is increased. In the absence of precipitation of secondary minerals such as gypsum and jarosite, sulphate production would directly indicate pyrrhotite oxidation.

3.5 Depth of Unoxidized Tailings at End of Experiments

Following the dismantling of the columns, the depth of unoxidized tailings was measured after carefully removing the oxidized tailings particles that had settled on top of the undisturbed tailings. Unoxidized tailings were clearly distinguished by their dark grey colour, whereas the oxidized tailings particles were yellowish brown in colour, hence the separation of the oxidized and unoxidized tailings was done visually. The results are presented in Table 4. For a given water cover depth, it can be seen that the thickness of tailings oxidized during the experiments generally increases as the stirrer speed is increased. The data are also presented in terms of mixing index in Figure 3.16.

Table 4 Thickness of tailings oxidized during experiments

Column number	Tailings Oxidized (cm)
C/80/140	1.5
C/80/170	2.0
C/80/200	1.5
C/60/140	4.0
C/60/170	5.0
C/60/200	7.0
C/45/140	7.5
c/45/1 70	8.0
C/45/200	10.0

3.6 Suspended Tailings at End of Experiments

The suspended, oxidized tailings collected at the end of the experiments are yellowish brown in colour (Figures 3.17 to 3.19). The various colour shades of the particles are all indicative of the fact that the pyrrhotite in the tailings oxidize and that iron oxyhydroxides are one of the oxidation products. Figures 3.20 and 3.2 1 show ripples observed on the tailings surface in columns C/80/200 and C/80/170. The ripples are very similar to bed forms developed on the surface of the tailings in flooded tailings pond by the action of wind. In this study the number and height of ripples formed are found to be greater at higher stirrer speeds.

The resuspended tailings collected at the end of the experiment have specific gravities (2.66 to 2.89) that are lower than that of pyrrhotite, suggesting significant alteration of pyrrhotite present in the tailings. The higher stirrer speeds gave values of specific gravity in the lower range, i.e., 2.66 to 2.70. This range of specific gravity is typical of minerals containing silica.

X-ray diffractograms of samples of resuspended tailings collected at 20 cm above the tailings in the stirred the columns are presented in Figures 3.22 to 3.30. The pyrrhotite peak at a diffraction angle 28 of 39.6” has maximum intensity in the original, unoxidized tailings and would, therefore, be used as basis for comparison. A comparison of the ratio of pyrrhotite peak (28 = 39.6”) intensity to that of amphibole (28 = 12°) in suspended and original tailings indicates a reduction in the peak intensity ratio for the suspended tailings and is a reflection of pyrrhotite depletion due to oxidation. Amphiboles (for example, hornblende) and pyrrhotite have similar specific gravities (Deer et al., 1966) and should resuspend to the same extent in the columns. Table 5 presents the calculated peak ratios. They range from 0.169 to 0.825 compared to 4.0 for the original unoxidized tailings. These findings indicate that the rate of oxidation of pyrrhotite present in flooded tailings is increased considerably when the tailings are resuspended in the overlying water cover.

Table 5 Ratio of pyrrhotite to amphibole peak intensities for resuspended tailings and original unoxidized tailings

Column number	Ratio of pyrrhotite to amphibole peak intensities
C/80/200	0.825
C/80/170	0.436
C/80/140	0.357
C/60/200	0.138
C/60/170	0.466
C/60/140	0.380
C/45/200	0.169
c/45/1 70	0.199
c/45/1 40	0.252
Original Unoxidized Tailings	4.0

Polished sections were prepared of the resuspended tailings samples collected at 20 cm depth in the stirred columns and of samples of original tailings. Photographs were taken using an optical microscope at a magnification of 200 times. Figures 3.31 to 3.40 show photographs of the resuspended tailings particles. A few patches of pyrrhotite grains can be seen only for the columns with the lowest degree of mixing, i.e., column C/80/140. The pyrrhotite grains are relatively larger and can be distinguished by their irregular shape and bright white colour. For all other cases, however, negligible pyrrhotite grains are observed, while silicate grains are markedly identifiable by their grey and dull colour.

Scanning electron photomicrographs of the resuspended tailings are presented in Figures 3.4 1, 3.42 and 3.43. The photographs and the accompanying EDX compositional data confirm the absence of pyrrhotite grains, suggesting that most of the pyrrhotite oxidize.

Elemental composition (weight percent) of resuspended tailings samples at 20 cm and of original, unoxidized tailings is presented in Table 6. Total elemental analysis was performed on these particles by acid digestion followed by ICP analysis. The elemental

composition of the original tailings is also given. Comparing the percent iron and sulphur in the resuspended particles and the original tailings, it can be seen that there is an appreciable decrease in the amounts of iron and sulphur present in the resuspended tailings. This again shows that pyrrhotite particles present in resuspended tailings oxidize more than the case when the tailings are at rest.

Figure 3.44 presents particle size distributions of oxidized, resuspended tailings and original, unoxidized tailings. The data are presented only for particle sizes of 0.018 mm or finer, since 90% of the resuspended tailings have particle diameter of less than 0.018mm. The complete particle size distribution of the original tailings is presented the next section. Figure 3.44 suggests that resuspended tailings particles become finer as they oxidize, and that increased stirrer speeds result in finer particle size distribution. The particle size distribution of the oxidized, resuspended particles does not vary significantly with water cover depth.

Table 6 Total elemental composition of original and resuspended tailings at 20 cm depth (weight percent)

Tailings	Original	C/80/140	C/60/200	C/45/200	C/45/1 40
Aluminium	2.53	4.48	6.1	5.89	5.76
Calcium	1.52	2.69	2.06	3.11	2.97
Copper	0.24	0.29	0.08	0.047	0.15
Iron	30.9	17.9	14.3	1.27	11.5
Potassium	0.31	0.47	0.78	0.81	0.63
Magnesium	1.13	1.87	2.37	2.38	2.14
Manganese	0.07	0.11	0.12	0.82	0.13
Sodium	0.84	1.41	1.75	1.82	1.64
Nickel	0.79	0.77	0.20	0.22	0.50
Sulphur	17.0	7.53	2.04	1.72	2.52
Silicon	6.36	11.2	13.2	14.2	13.2
Zinc	0.045	0.0632	0.015	0.015	0.028

3.7 Particle Size and Mineralogy of Unoxidized Resuspended Tailings

Particle size distributions of unoxidized, resuspended tailings particles collected from the different water covers are presented in Figure 3.45. The unoxidized, resuspended tailings are finer at 40 cm above the tailings surface than at 20 cm (see data for column C/80/200). At the same stirrer speed (200 rpm), particle size does not seem to change with water cover depth (from 45 cm to 80 cm). The concentration of resuspended tailings measured in the stirred columns is plotted against mixing index in Figure 3.46. It is evident that columns with higher mixing index resuspend more tailings particles probably because of higher shear stresses generated at the bottom of the water cover. More importantly, it appears that, for a particular depth of water cover, there exists a unique mixing index (and hence shear stress) above which the concentration of resuspended tailings remains the same. This would suggest that the overlying water cover can only accommodate a fixed concentration of resuspended tailings.

The unoxidized, resuspended tailings particles collected from the columns at the 20 and 40 cm depths were subjected to x-ray diffraction analysis and a few of the results are presented in Figures 3.47 to 3.54. The pyrrhotite to amphibole peak ratio for unoxidized, resuspended tailings at 20 cm is plotted against mixing index in Figure 3.55. The ratio appears to increase with mixing index, and might suggest that the amount of pyrrhotite particles resuspended increases with mixing index. Pyrrhotite particles have a higher specific gravity than most non-sulphide particles present in the tailings and would, therefore, require a higher shear stress for erosion and resuspension.

3.8 Influence of Resuspension on Undisturbed Tailings

Figures 3.56 and 3.57 show optical photographs of the tailings surface in columns C/80/140 and C/80/0. Both photographs show similar proportion of pyrrhotite grains (bright white), and thus seem to indicate that tailings in the two columns were oxidized to the same degree. Figures 3.58 to 3.63 present x-ray diffractograms of samples collected from the surface of the tailings in seven of the stirred columns. The pyrrhotite peak intensities at a diffraction angle of 39.6' of samples from the stirred columns range from 1719 to 2435 CPS (counts per second), compared to 1282 to 1838 CPS for the unstirred

columns and 2420 CPS for the original tailings. These data suggest that the amount of pyrrhotite present in the tailings below the static water cover (no stirring) is reduced, as a result of oxidation. The rate of oxidation is greater than that of undisturbed tailings in the stirred columns. Although the DO concentration in the stirred columns is below 0.5 mg/L, oxidation still takes place. The surface of the undisturbed tailings below the stirred water cover is probably in dynamic equilibrium with the suspended tailings so that resuspension and settling rates are equal. Thus, some mixing would occur at the surface of the undisturbed tailings in the stirred columns; the degree of mixing would, however, be much less than that which occurs in tailings suspended in the stirred water cover. Oxygen consumption would, therefore, occur mainly in the stirred water cover. Although oxidation of the surface of the undisturbed tailings in the stirred columns does occur (DO ~ 0.5 mg/L), it is much smaller than the oxidation of tailings in the static columns where the DO concentration is higher (6.5 mg/L).

Undisturbed tailings remaining in the columns at the end of the experiments were extruded and sliced at 2-cm intervals and subjected to ICP analysis. Figures 3.64 and 3.65 show the elemental composition (percent by weight) versus depth for tailings in columns C/80/0 and C/80/140. The figures indicate that metal concentrations are very similar. This suggests that only the eroded surface of the tailings in the stirred columns oxidized extensively and that the oxidation of the remaining tailings was minimal and comparable to that of the tailings in the static columns.

3.9 Pore Water Chemistry of Undisturbed Tailings

Pore water squeezed from the tailings slices was analyzed for pH and metal content. Figure 3.66 shows the variation of pH with depth. The pH of the original unoxidized tailings pore water is 8.0. The data in Figure 3.66 suggest infiltration of oxidation products from the surface to the deeper tailings, resulting in a decrease in the pH of the pore water from its initial value of 8.0. The pH of the tailings pore water is much higher than that of the water cover. The water cover in the stirred columns have an average pH of 2.7 at the end of the experiments. The relatively high pH of the tailings pore water may be explained by buffering provided by aluminosilicate minerals and lime added to the tailings in the mill, prior to their discharge. The pH of tailings pore water in the static

columns is much higher than that of the stirred columns. At greater depths, the pH of the tailings pore water in the static columns is similar to that of the original tailings pore water (Figure 3.66).

Figures 3.67 to 3.69 present profiles of metal concentrations in the tailings pore water for a typical, stirred column C/80/140. Concentration of metals such as aluminium, nickel, copper and zinc in the pore water are much lower than in the overlying water cover. These pore water concentrations are essentially the same at all depths, and are similar to the concentrations in the original tailings pore water. It may be inferred from these data that trace metals released in the water cover, as a result of resuspension-induced oxidation, do not infiltrate the underlying tailings and that tailings remaining at rest in stirred columns undergo negligible oxidation. These metals could either precipitate as secondary minerals or be adsorbed by iron oxyhydroxides at the surface of the tailings. The other metals (magnesium, calcium, manganese and potassium) show a continuous increase in concentration with depth, and the concentrations are much higher than those of the original tailings pore water. This increase in concentration could be attributed to the dissolution of aluminosilicate minerals (clay minerals) and feldspars, as previously noted.

To confirm the above observation, pore water was extracted from the uppermost slices of the tailings from four other columns and analyzed for metals. The results, presented in Table 7, indicate that metal concentrations have a similar order of magnitude in all columns, except in column C/45/200. In column C/45/200 the mixing index was the highest and metal concentrations in the tailings pore water were, generally, of the same order of magnitude as those in the water cover, with the exception of calcium and potassium. This suggests that the upper portion of the tailings was severely disturbed by the surface stresses caused by the stirring of water, which possibly led to the mixing of the water cover with tailings pore water. Thus, at greater tailings depth where disturbance is minimal, one would expect uniform pore water metal profiles with lower concentrations.

Table 7 Pore water metal concentrations in top 2-cm of tailings (mg/L)

Column No.	C/60/140	C/60/0	C/45/140	C/45/200
Aluminum	0.14	0.4	1.9	646.8
Calcium	906	370	880	908
Copper	0.7	0.38	0.7	160.5
Total iron	2280	2.18	4520	5851
Magnesium	238	45	266	699.7
Manganese	27	1.16	36.8	54.1
Nickel	26.6	0.7	97	993.7
Potassium	100	67	127.6	30.87
Silicon	18.86	3.3	27.8	159.4
Sodium	23.4	23.6	31.2	30.87
Zinc	3.18	0.08	11.6	129.95

Figures 3.70 and 3.71 present metal concentrations versus depth plots for tailings pore water in the static or unstirred column C/80/0. A continuous increase in concentration with depth is observed for all metals except aluminium and ferric iron. The tailings pore water metal concentrations are higher than those of the water cover and the original tailings pore water. This suggests that metals released as a result of surface oxidation in the static column infiltrates the deeper tailings and are, likely, not removed from solution by precipitation and/or adsorption in the static columns.

X-ray analysis of the precipitate collected from column C/80/170 at the end of the experiments did not show the presence of iron oxyhydroxides, quite possibly because of their small quantity or their amorphous nature. The sides of the Plexiglas columns were coated with a thin yellowish film, as shown in Figure 3.75. X-ray analysis of this film shows the presence of iron oxyhydroxide, possibly goethite, at nearly the same diffraction angle as the quartz peak. The reason iron oxyhydroxides is detected in these samples could possibly be because they are concentrated in the resuspended tailings. Scanning

electron photomicrographs of the precipitate collected from the columns (Figures 3.73 and 3.74) show the presence of iron oxyhydroxide and gypsum, respectively. ICP analysis of the precipitate showed the presence of copper, nickel and zinc, indicating these metals are scavenged by or coprecipitating with iron oxyhydroxides.

3.10 Cumulative Metal Release in the Water Cover

Iron

Figures 3.75 to 3.77 show the variation of ferric iron concentration with time in columns with water cover depths of 80, 60 and 45 cm. For all columns, the ferric iron concentration increases between the 20^{th} and 60^{th} day. The pH in the stirred columns ranges from 3.0 to 3.5 between the 20^{th} and 60^{th} day. Ferric iron becomes soluble at pH less than 3.5; thus its concentration in solution increases drastically, which would account for the increase in ferric iron concentration between the 20^{th} and 60^{th} day in all the columns.

Figure 3.78 shows the variation of ferric iron release (concentration x volume of water cover) into the water cover for all columns. Although columns with high mixing indices oxidize greater quantities of tailings, they apparently do not necessarily release the highest amount of ferric iron. This indicates that at high mixing index ferric iron is removed from the water cover. Ferric iron release in the stirred column with the least mixing index is 3 122 times greater than the release in static columns.

Zinc, copper, and nickel

The total amounts of zinc, copper, and nickel released in the water cover are highest for columns with the highest mixing index and lowest for the column with the lowest mixing index as shown in Figures 3.79 to 3.81. The rate of release of these metals increases when the pH in the columns is less than 3.5. At this pH the ferric iron concentration in solution is high, resulting in the leaching of metals from their respective sulphides. Thus the ferric iron concentration decreases at high mixing indices. The least release of zinc is 1020 times greater than the release in static columns. The respective copper and nickel releases in stirred columns are 3 18 and 138 times greater than their release in static columns.

Magnesium, manganese, calcium, potassium and sodium

Manganese and magnesium releases (Figures 3.82 and 3.83) are the maximum in the column with the highest mixing index and minimum in the column with the lowest mixing index. Manganese release in the column with the least mixing index is about 10 times the release in the static columns, while the corresponding value for magnesium is 3.5 times. A different trend is observed for calcium, sodium or potassium as shown in Figures 3.84 to 3.86. In fact for potassium, the column with the highest mixing index (C/45/200) gives the least cumulative metal release, suggesting potassium removal from the water cover. Potassium, sodium and calcium release is the maximum, initially, when the pH of the water cover was higher than 3.5, but decreases with time. This suggests that the release of these metals is not influenced by the pH of the water cover or by ferric iron release. These elements are probably released mainly as a result of tailings resuspension and, with time, appear to be precipitating out of solution. The release rate does not vary significantly with mixing index, unlike the previously mentioned metals whose release is associated with pyrrhotite oxidation. The maximum release of sodium in the stirred columns is only 1.4 times the value in the static columns. For calcium it is 2.0. Potassium release is slightly higher in the static columns than in the stirred columns.

Aluminium and silicon

Aluminium release is the maximum in the column with the highest mixing index (C45/200) and minimum in the column with the lowest mixing index (C/80/140) as shown in Figure 3.87. Aluminium release at the lowest mixing index is 623 times the release in the static columns (no mixing), while silicon release is 29 times (Figure 3.88).

The metal cumulative release at the end of the experiments for all mixing indices is presented in Table 8. Metal release in the stirred columns (mixing index > 0) is considerably greater than the release in the static columns (zero mixing index), indicating that resuspended tailings oxidize more than the tailings at rest. In general, an increase in mixing index leads to greater metal release, suggesting an increase in the rate of oxidation of resuspended tailings.

Table 8 Cumulative metal and sulphate releases at end of the experiments (mg/L)

Mixing Index	Al	Ca	Cu	Fe^{+3}	Ni	Zn	SO_4^{-2}
1.78	458	525	242	4280	1130	83.8	25700
1.51	311	479	197	3620	715	60.5	15570
1.33	221	367	138	4430	593	47.2	11824
1.24	189	421	84.9	3490	349	40.5	10600
1.13	143	308	14	3210	283	26.6	7717
1.0	135	290	65.2	3690	266	24	3611
0.93	96.6	245	25.7	681	189	12.4	6477
0.85	75.2	234	14.9	501	164	10.2	2461
0.7	49.9	201	6.24	1280	122	9.05	2080
0	0.08	99.8	0.02	0.16	0.93	0.01	80
0	0.05	110	0.02	0.02	0.72	0.01	280
0	0.05	179	0.02	0.02	8.2	0.02	400

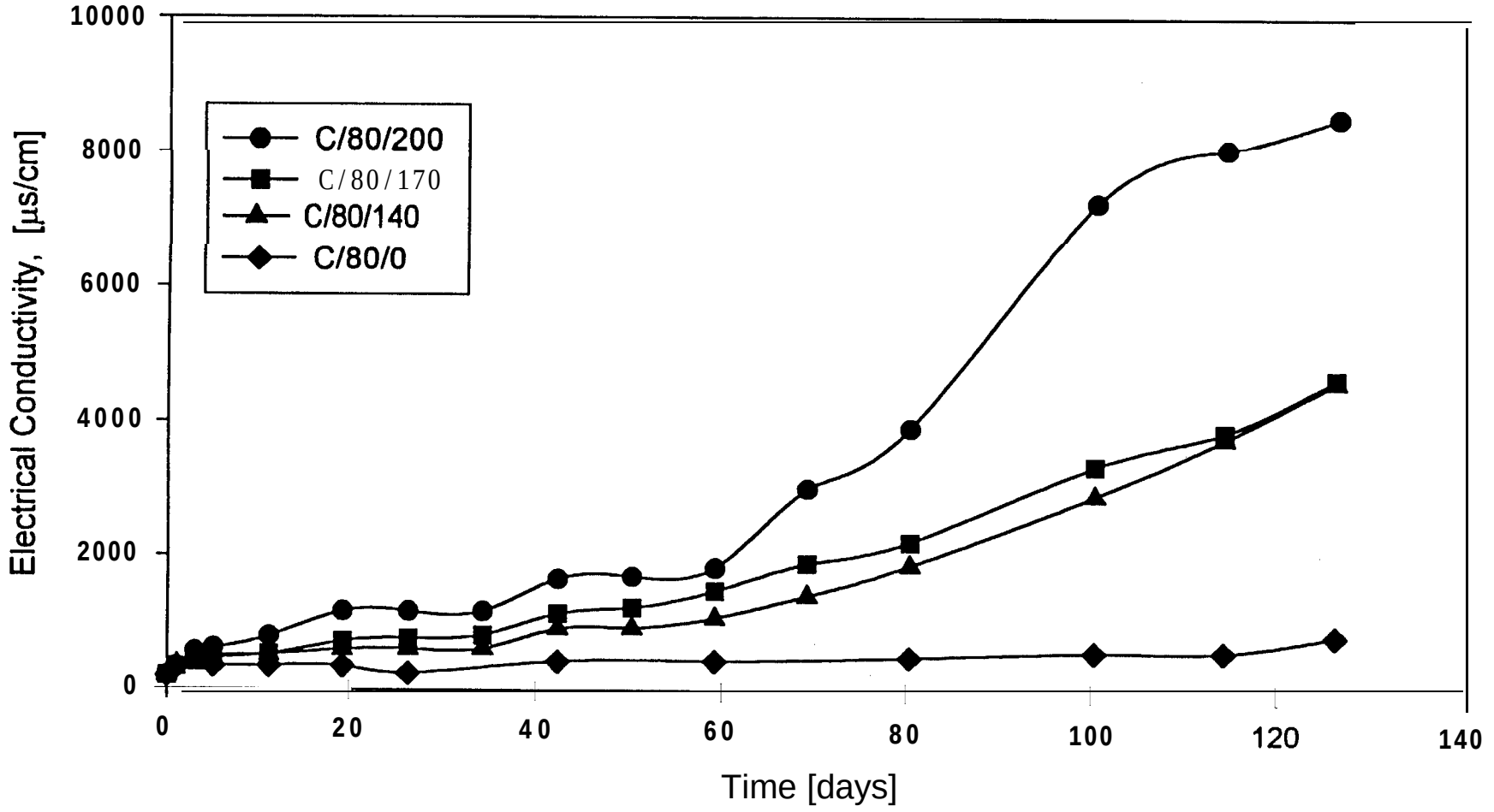

Figure 3.1 Variation of electrical conductivity with time in 80 cm water cover

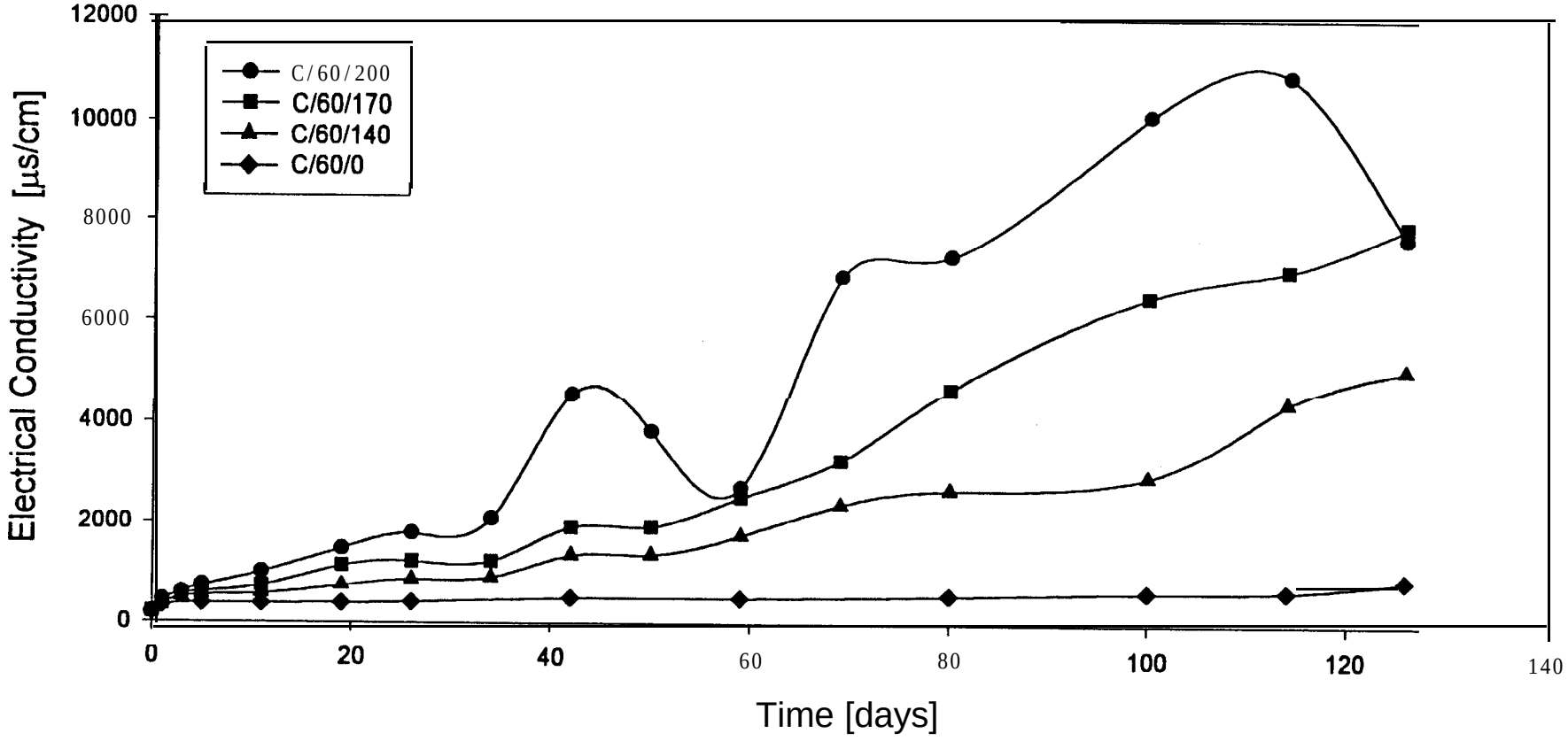

Figure 3.2 Variation of electrical conductivity with time in 60 cm water cover

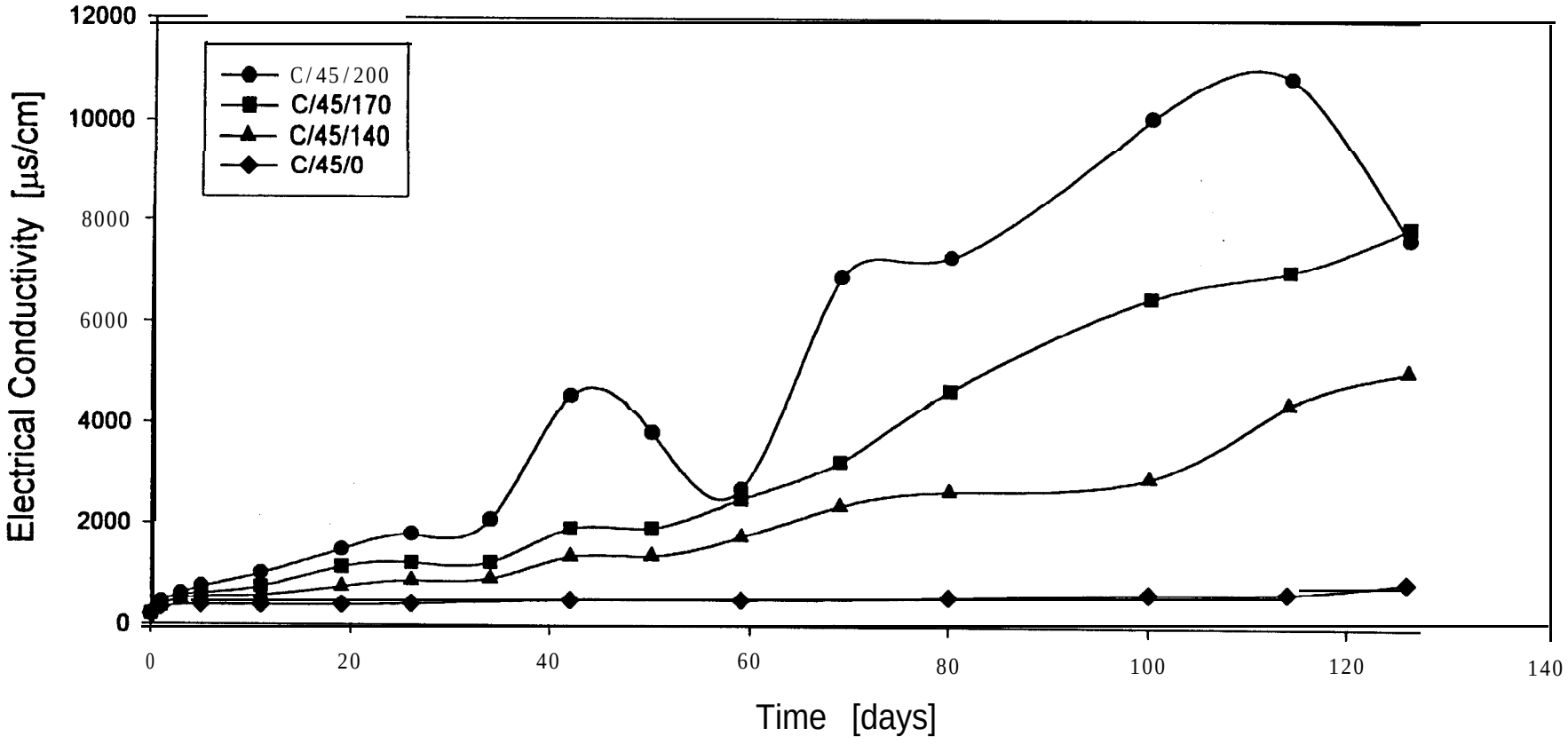

Figure 3.3 Variation of electrical conductivity with time in 45 cm water cover

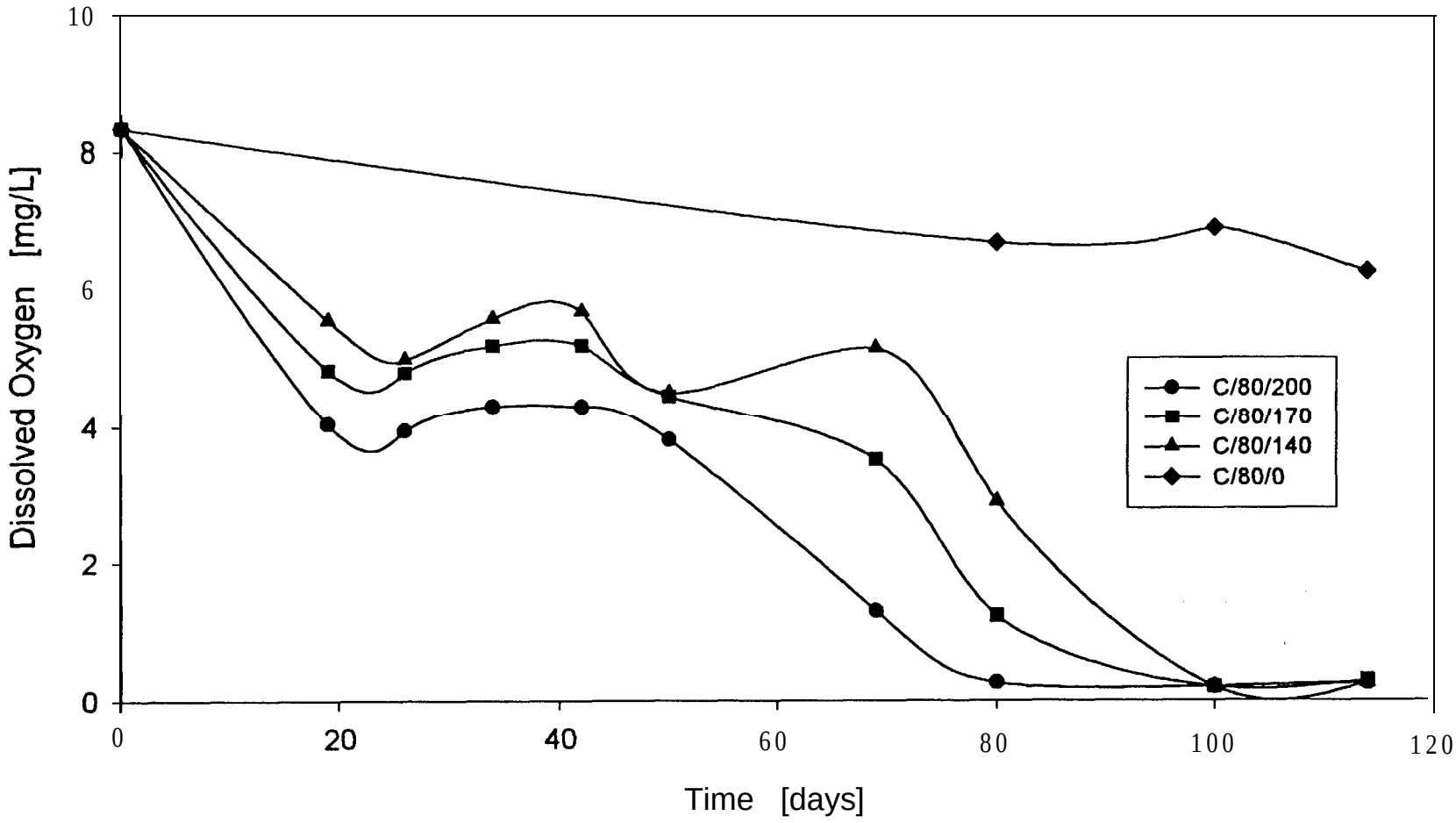

Figure 3.4 Variation of DO concentration versus time in 80 cm water cover

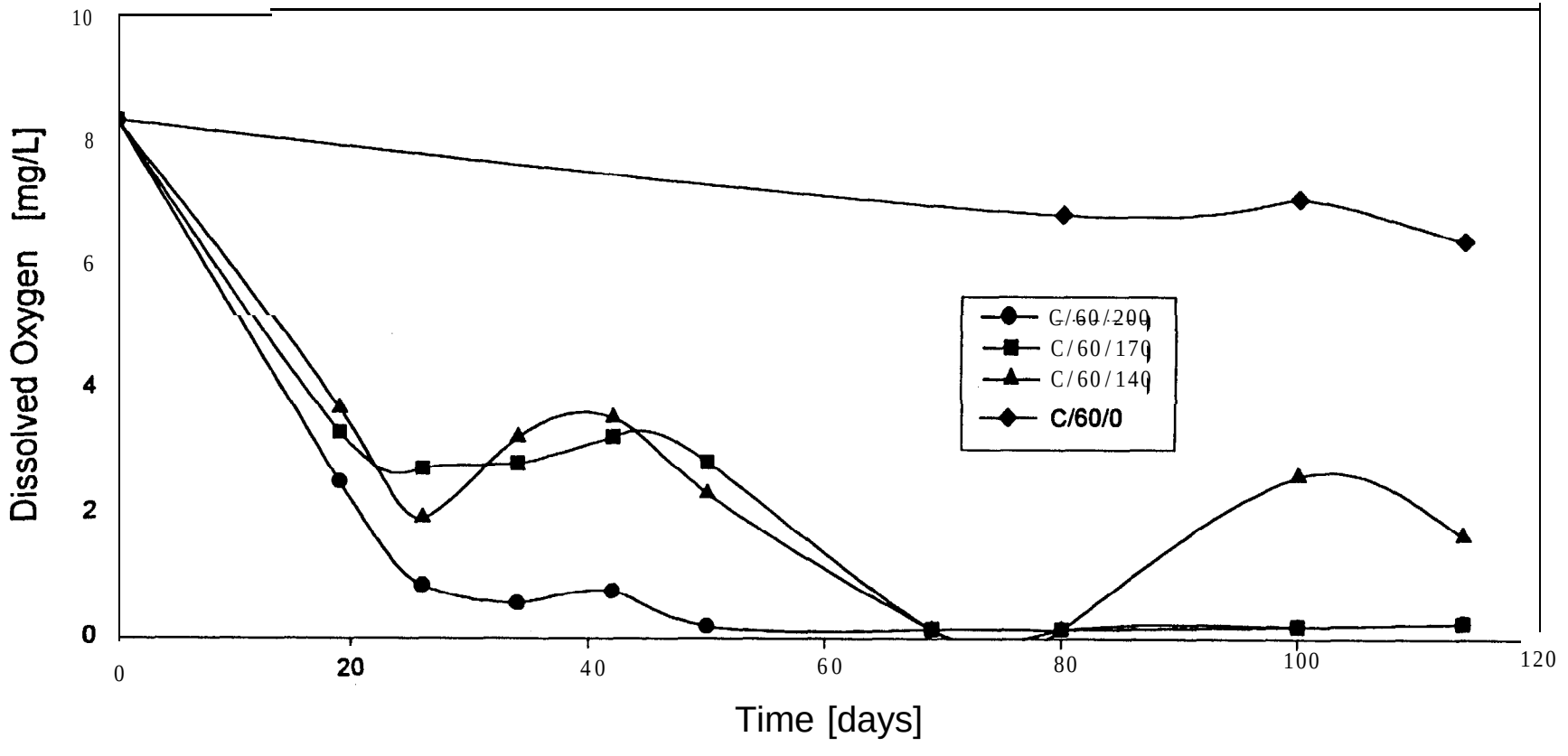

Figure 3.5 Variation of DO concentration versus time in 60 cm water cover

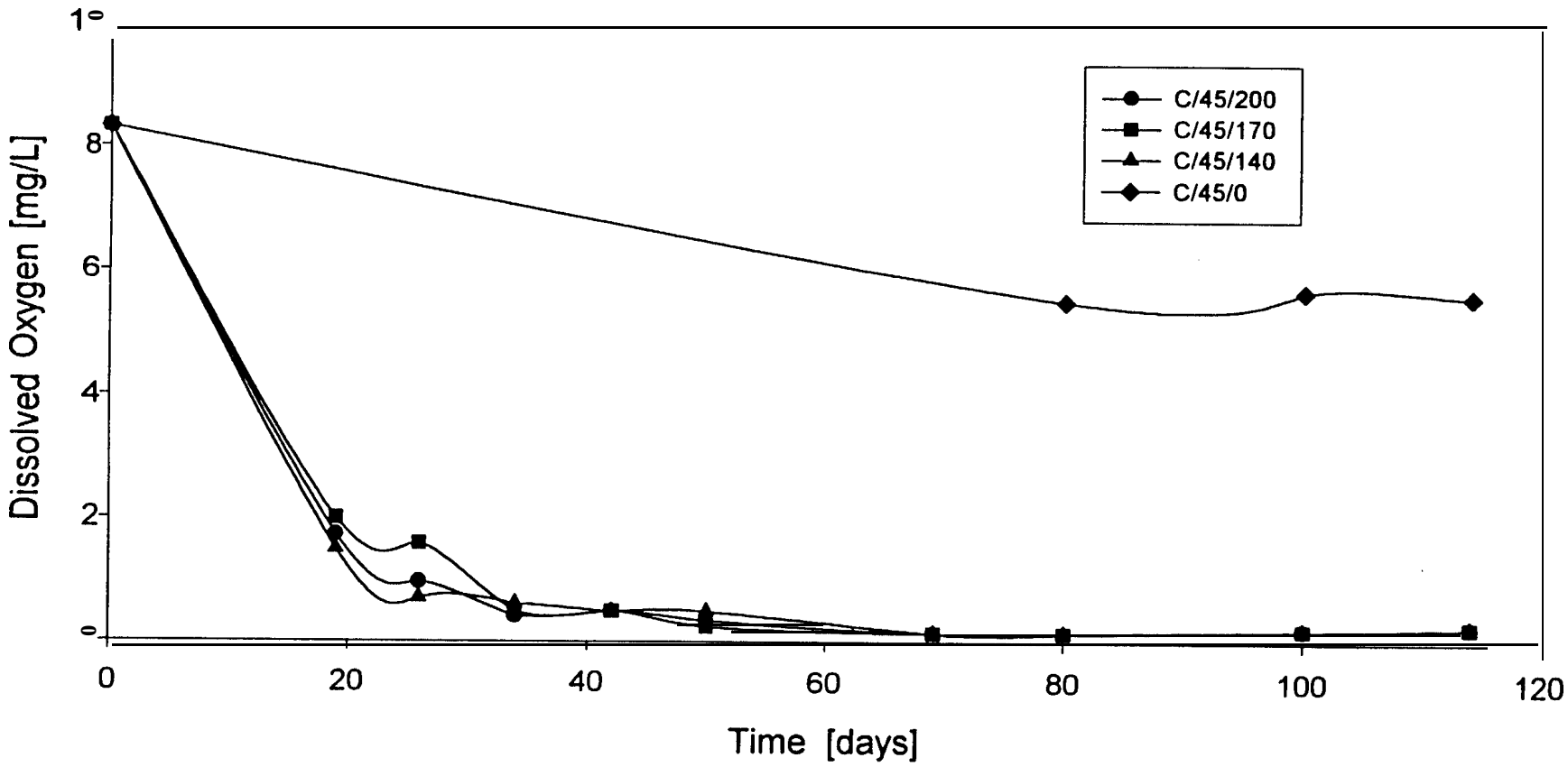

Figure 3.6 Variation of DO concentration versus time in 45 cm water cover

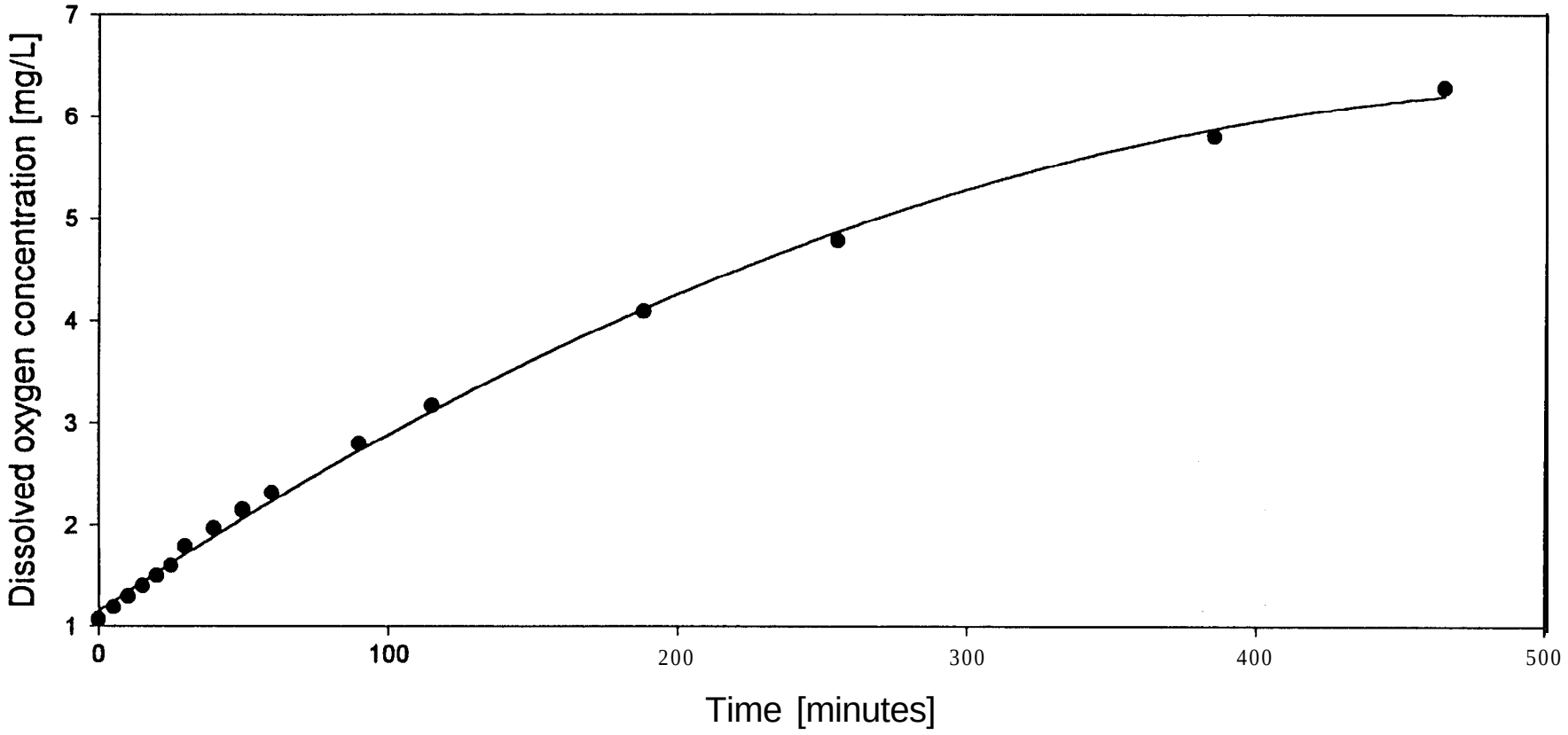

Figure 3.7 DO versus time for Column C/40/200 during oxygen flux measurements

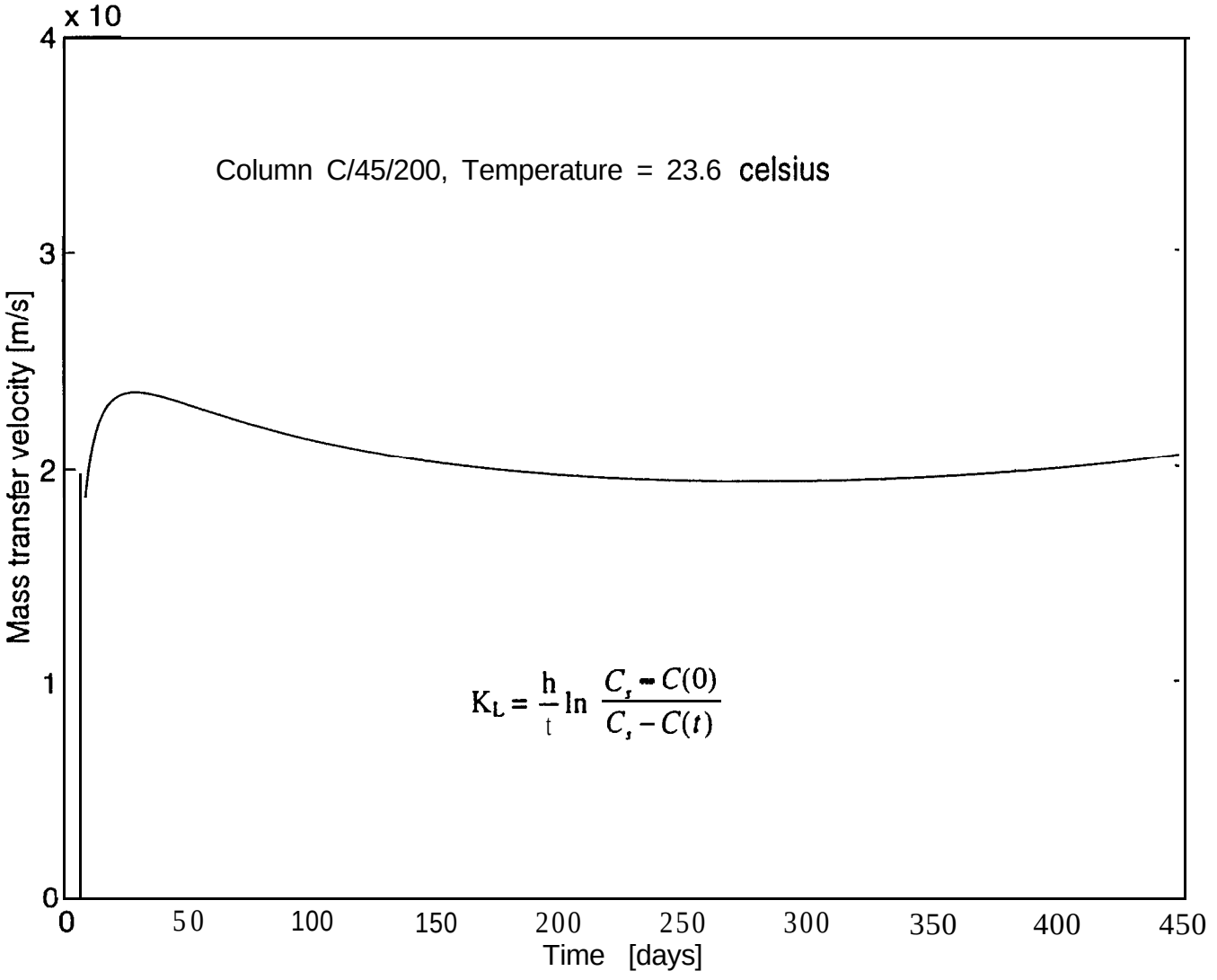

Figure 3.8 A typical variation of mass transfer velocity with time, Column C/45/200

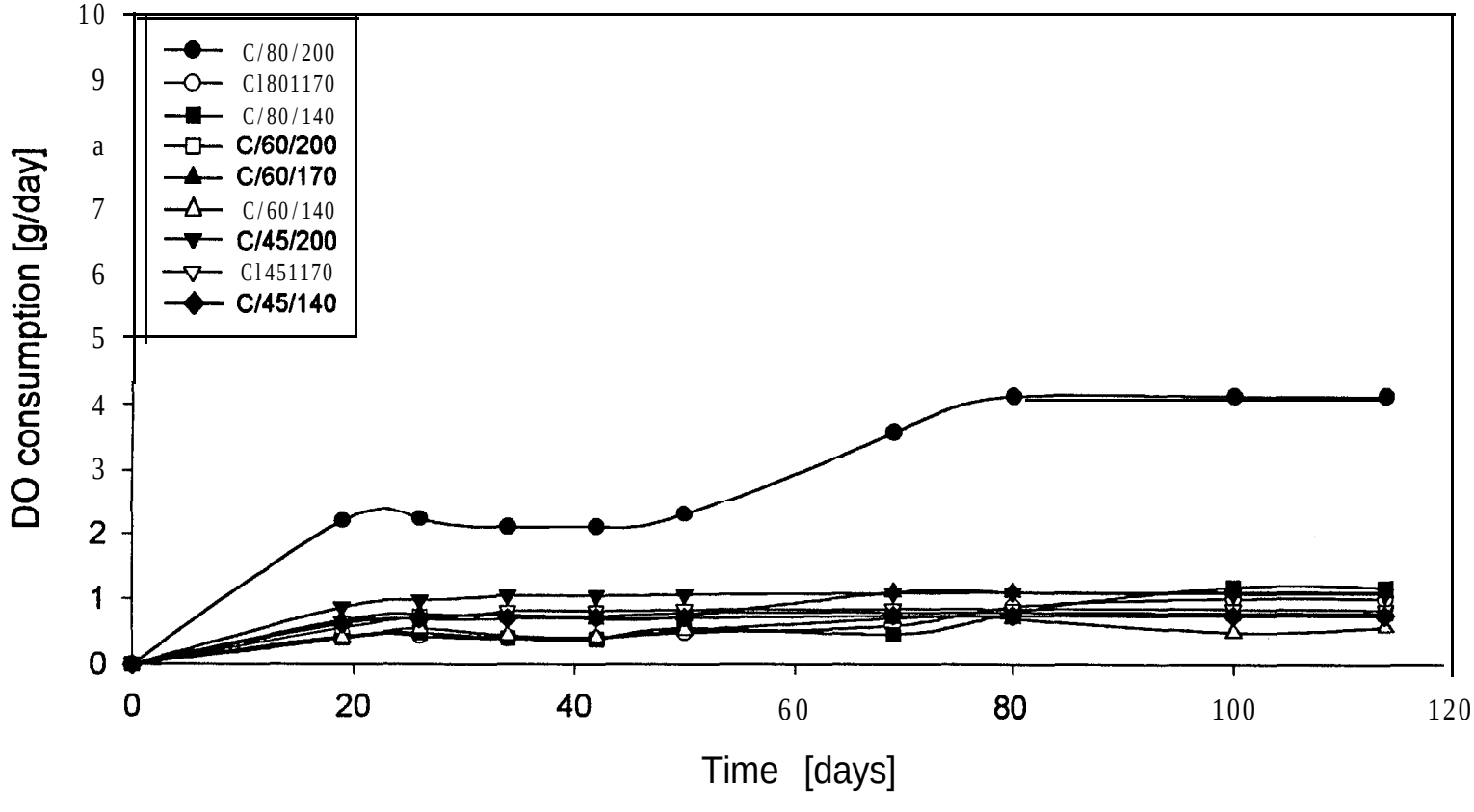

Figure 3.9 Dissolved oxygen consumption versus time

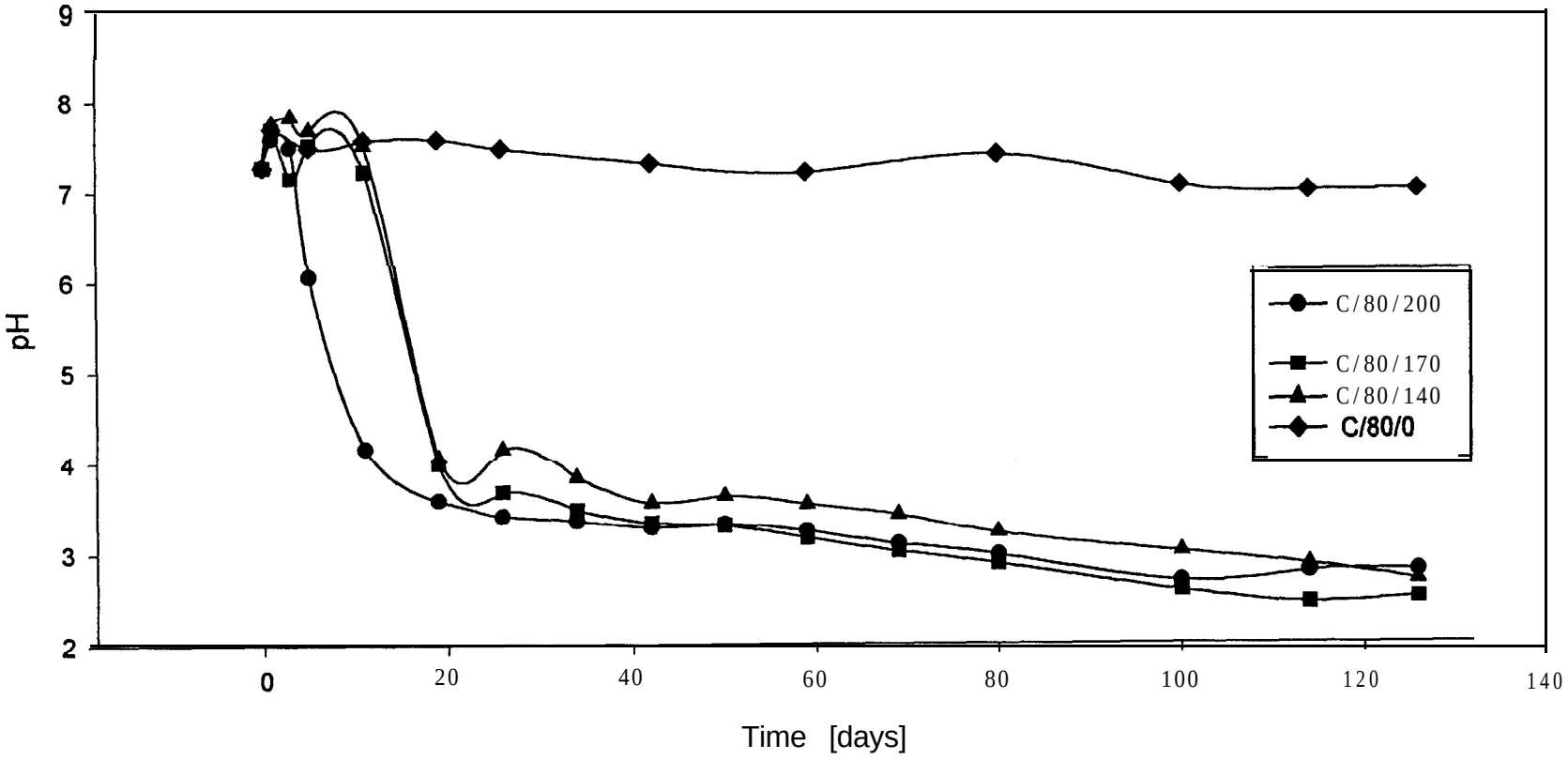

Figure 3. 10 pH versus time for 80 cm water cover stirred at 200 rpm

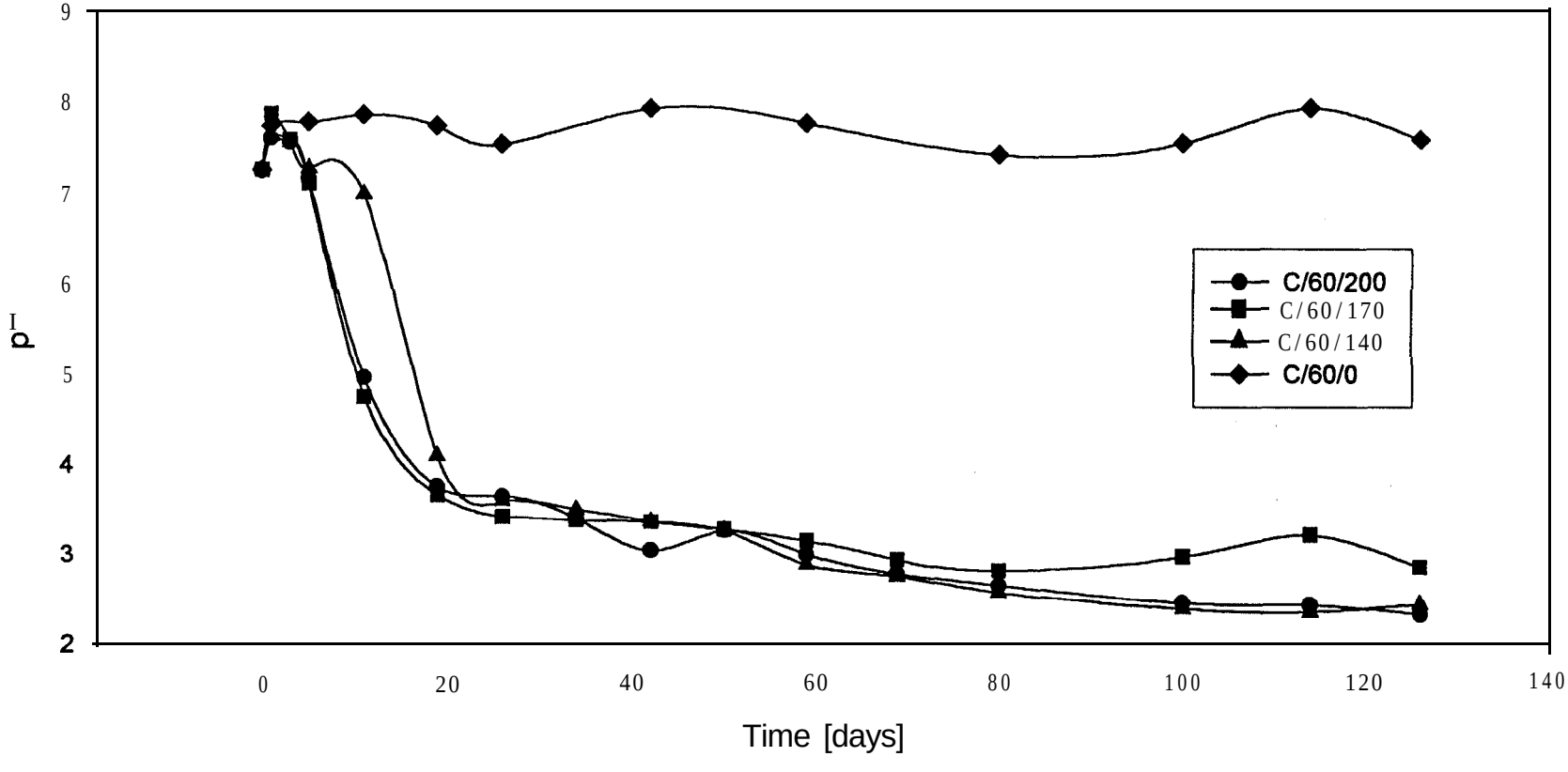

Figure 3.11 pH versus time for 60 cm water cover stirred at 170 rpm

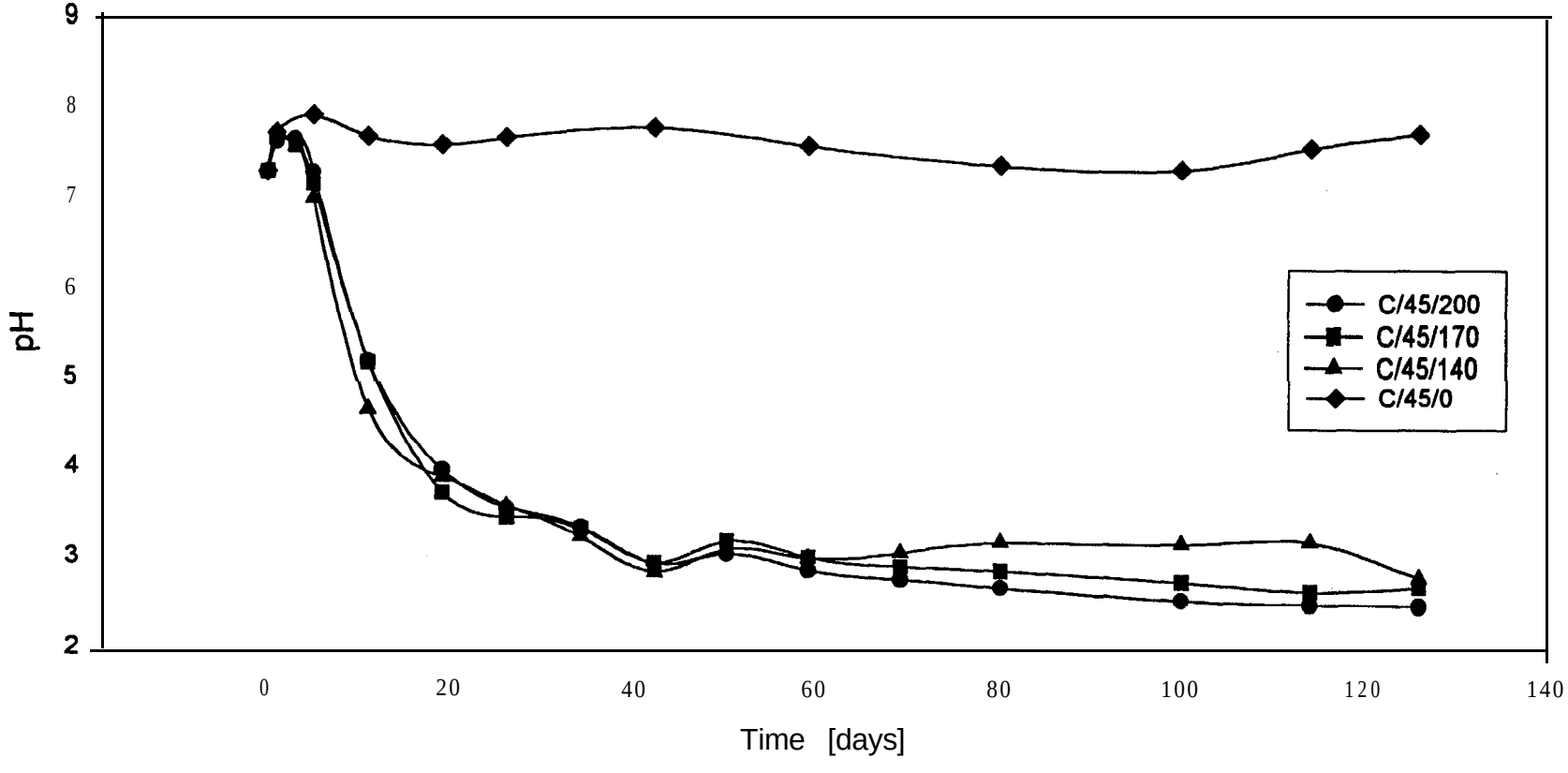

Figure 3.12 pH versus time for 45 cm water cover stirred at 140 rpm

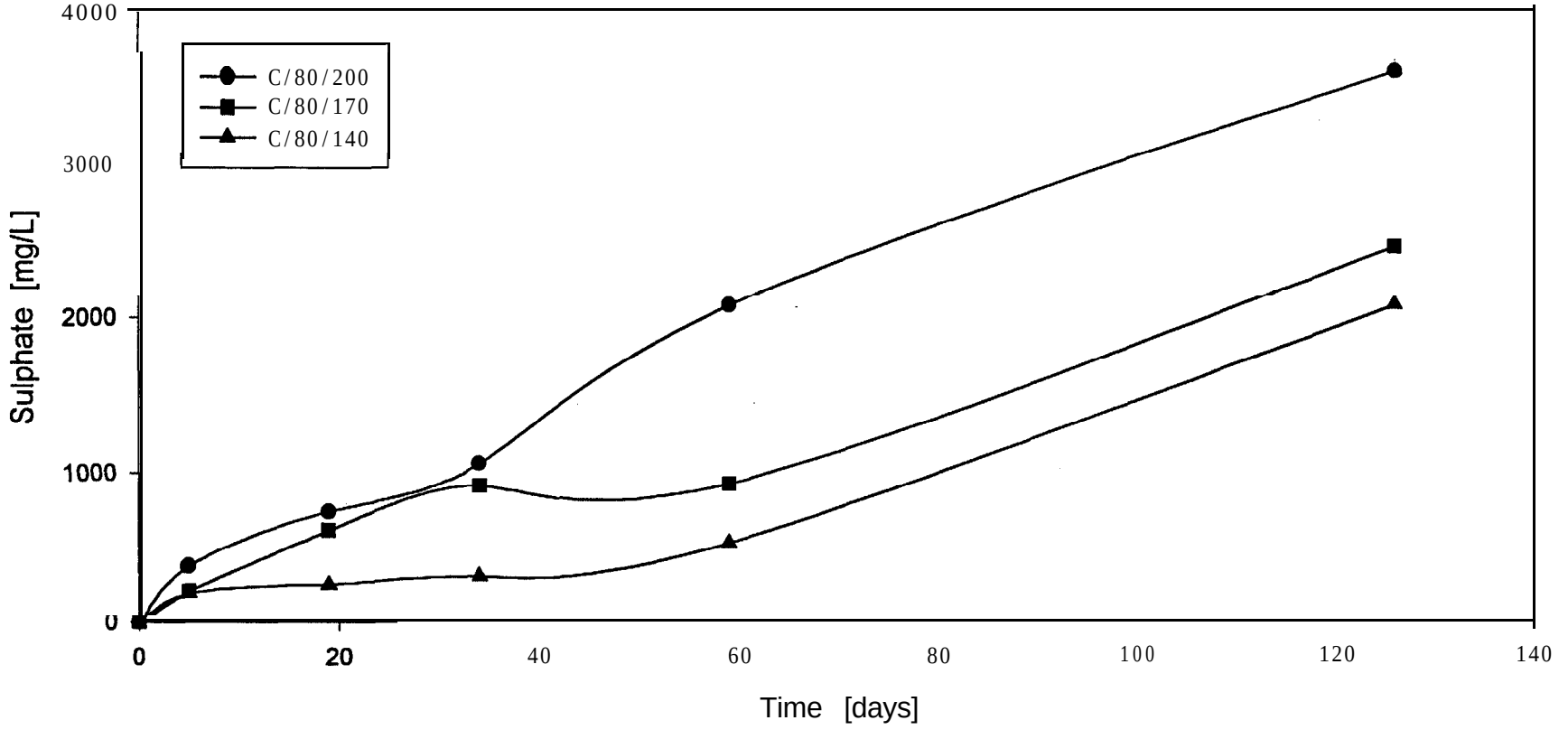

Figure 3.13 Sulphate versus time for 80 cm water cover stirred at 200, 170 and 140 rpm

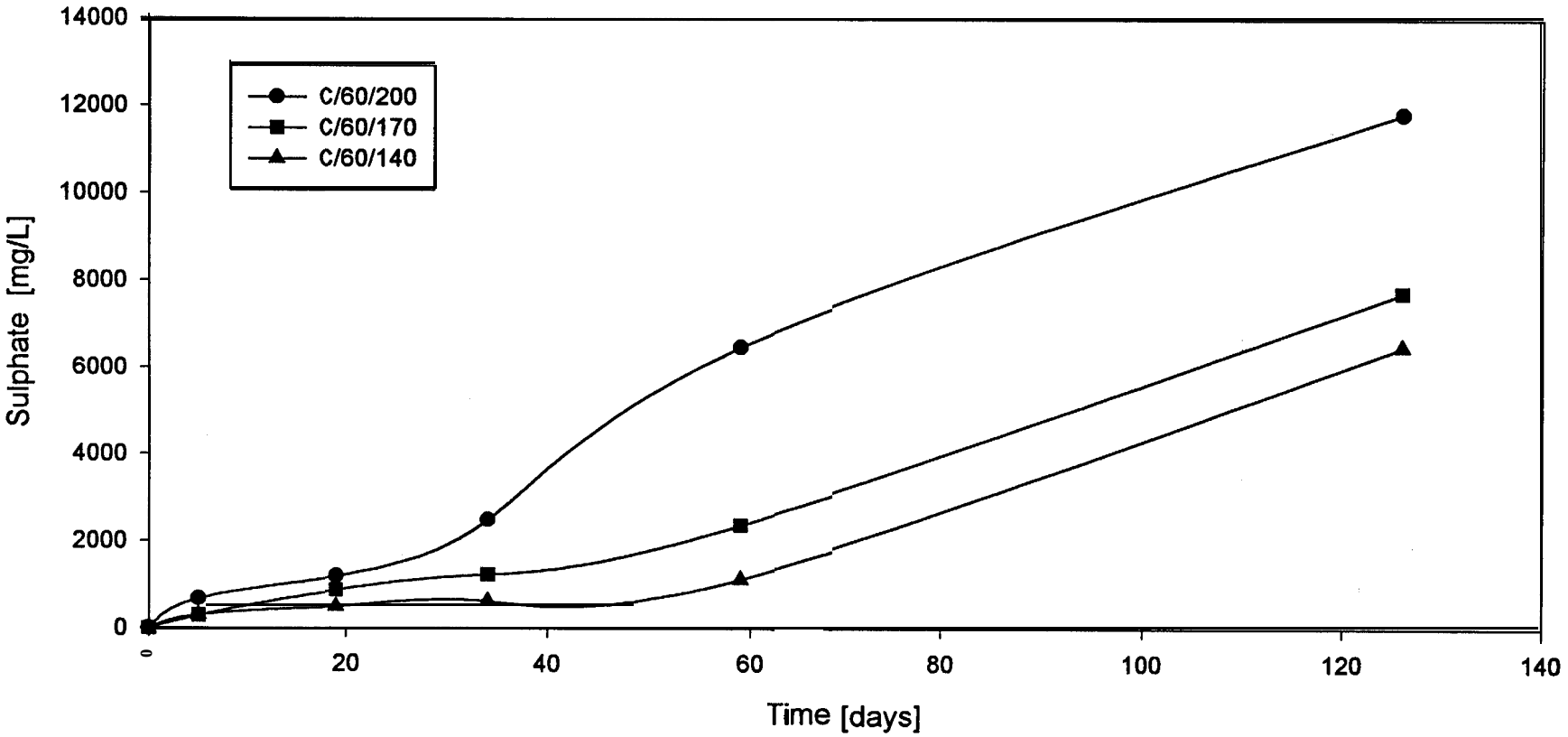

Figure 3.14 Sulphate versus time for 60 cn water cover stirred at 200, 170 and 140 rpm

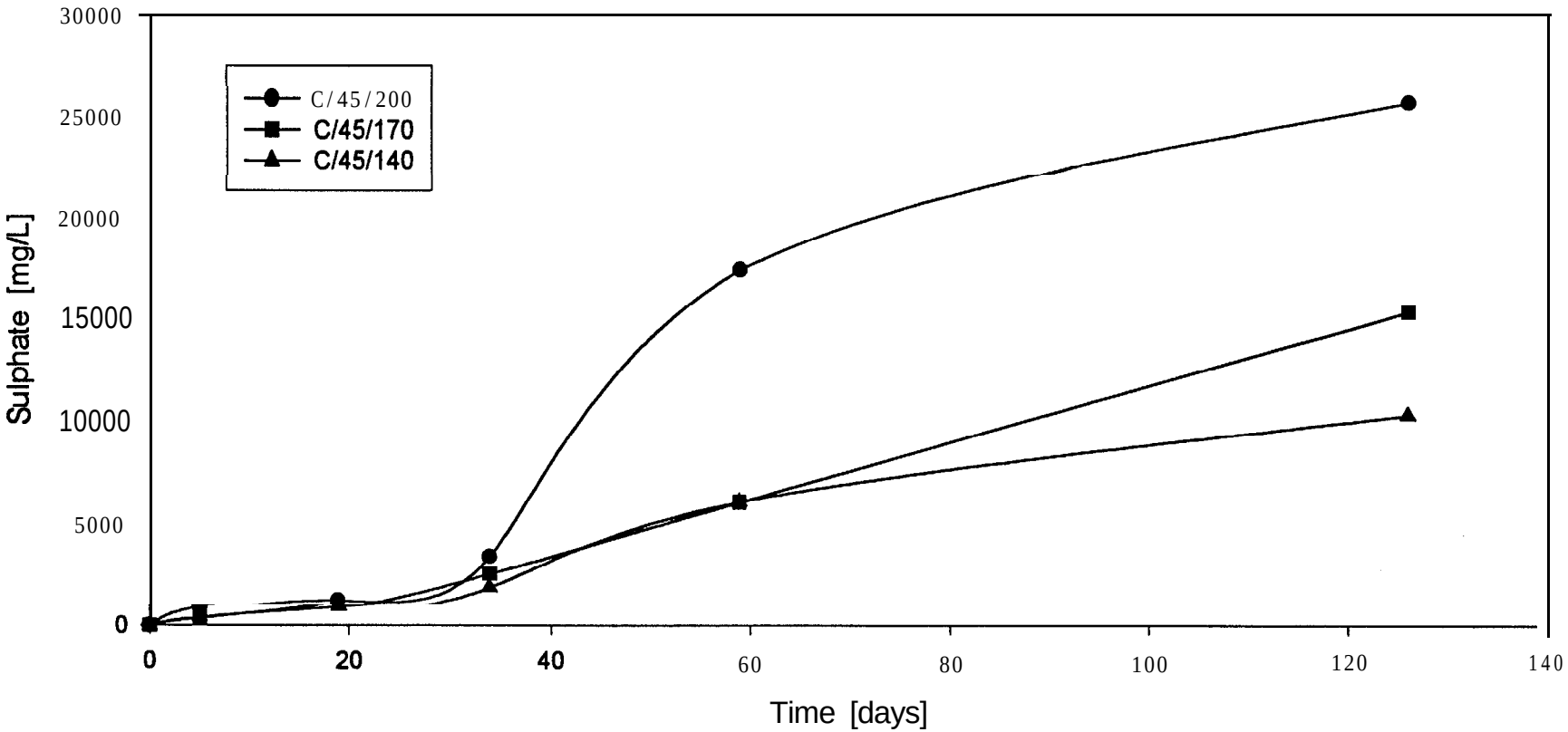

Figure 3.15 Sulphate versus time for 45 cm water cover stirred at 200, 170 and 140 rpm

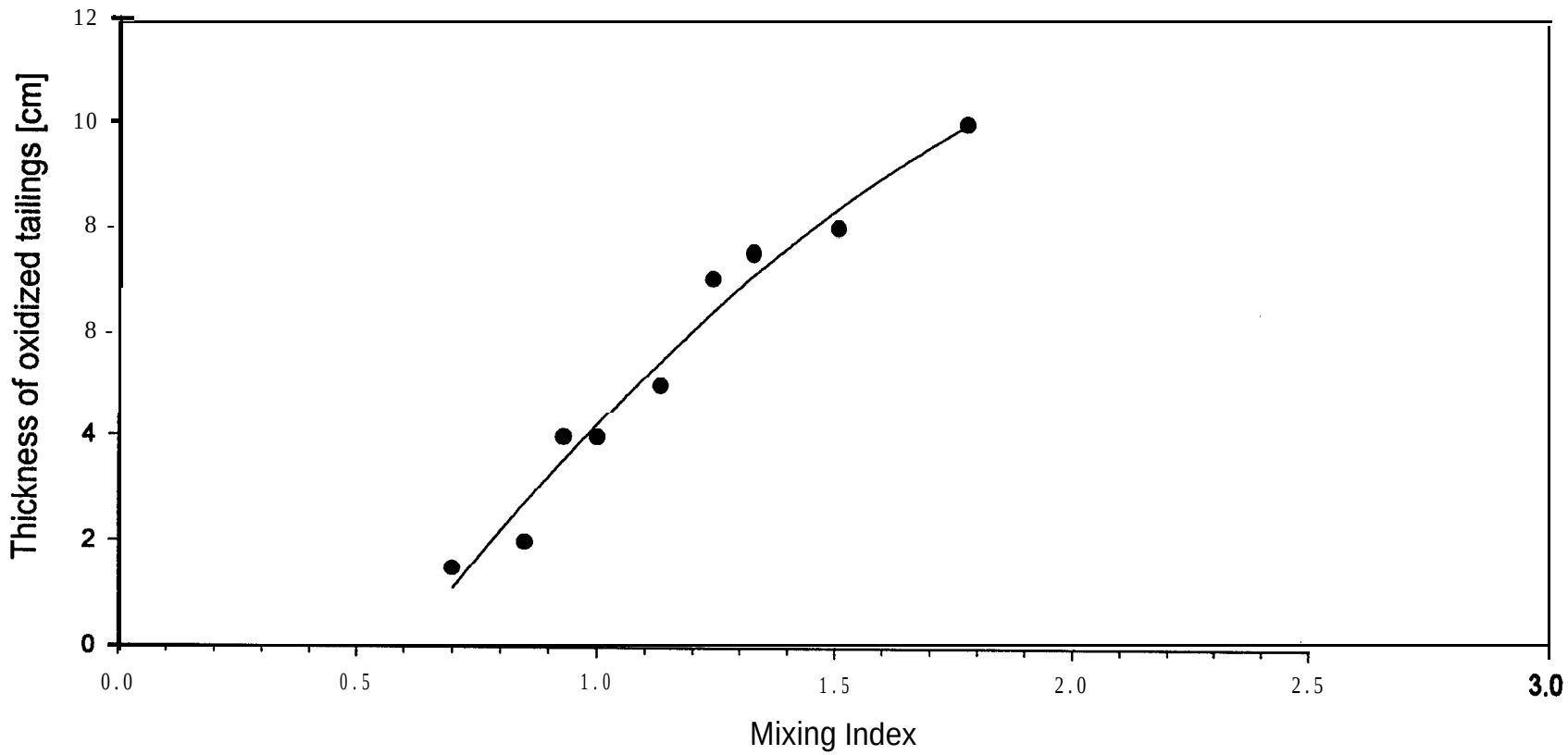

Figure 3.16 Variation of thickness of oxidized tailings with mixing index

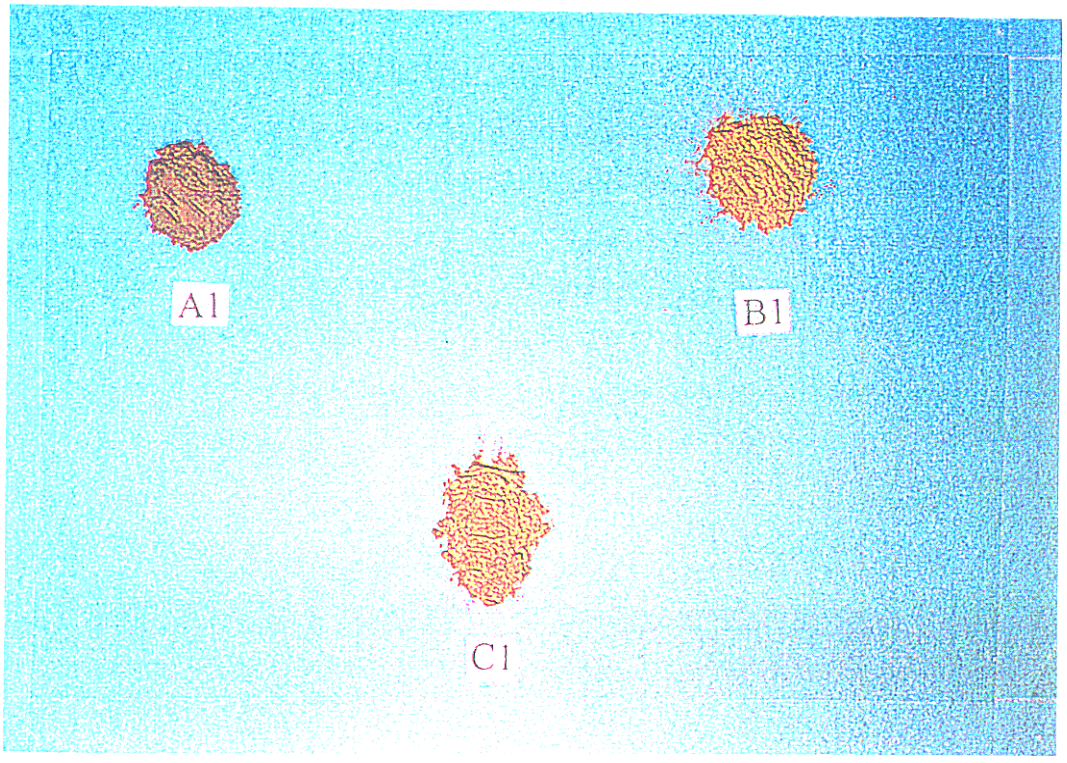

Figure 3.17 Photograph of suspended tailings particles in 80, 60 and 45 cm water covers stirred at 200 rpm

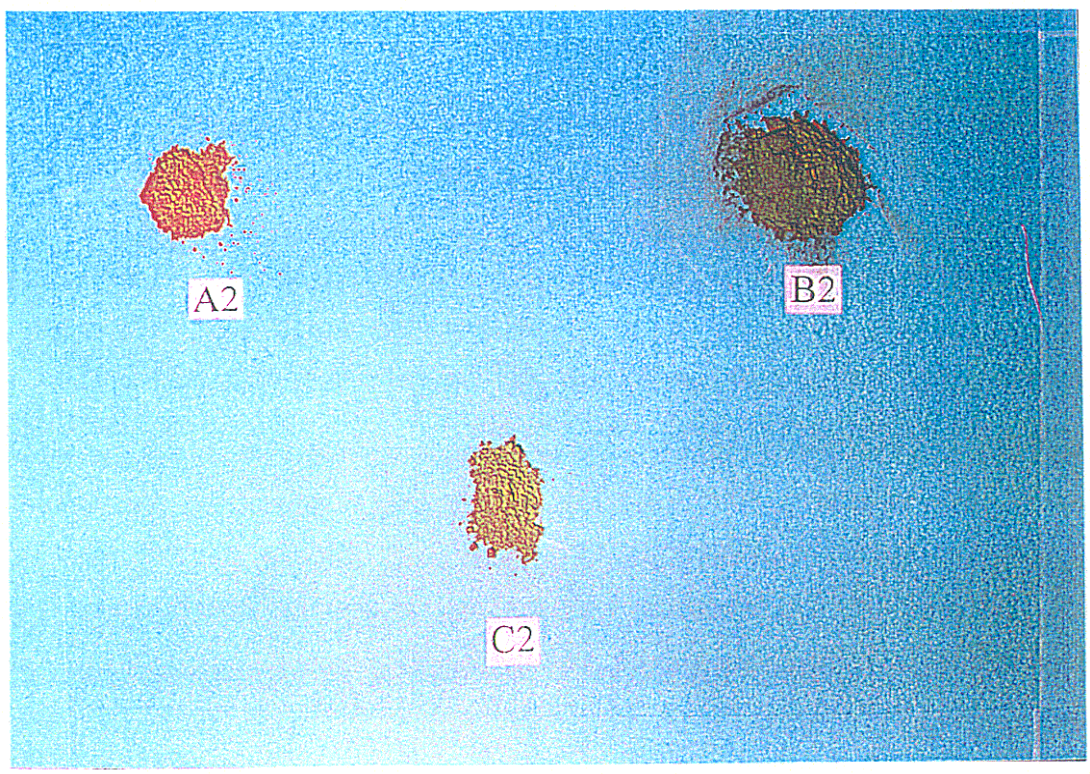

Figure 3.18 Photograph of suspended tailings particles in 80, 60 and 45 cm water covers stirred at 170 rpm

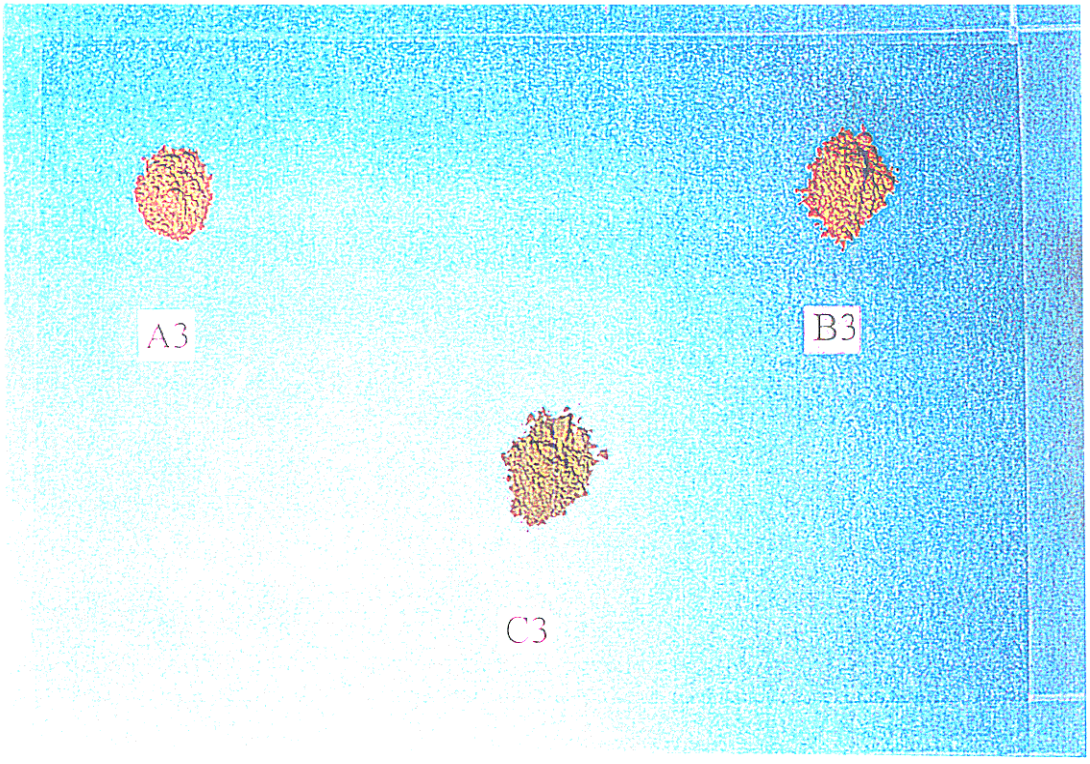

Figure 3.19 Photograph of suspended tailings particles in 80 60 and 45 cm water covers stirred at 140 rpm

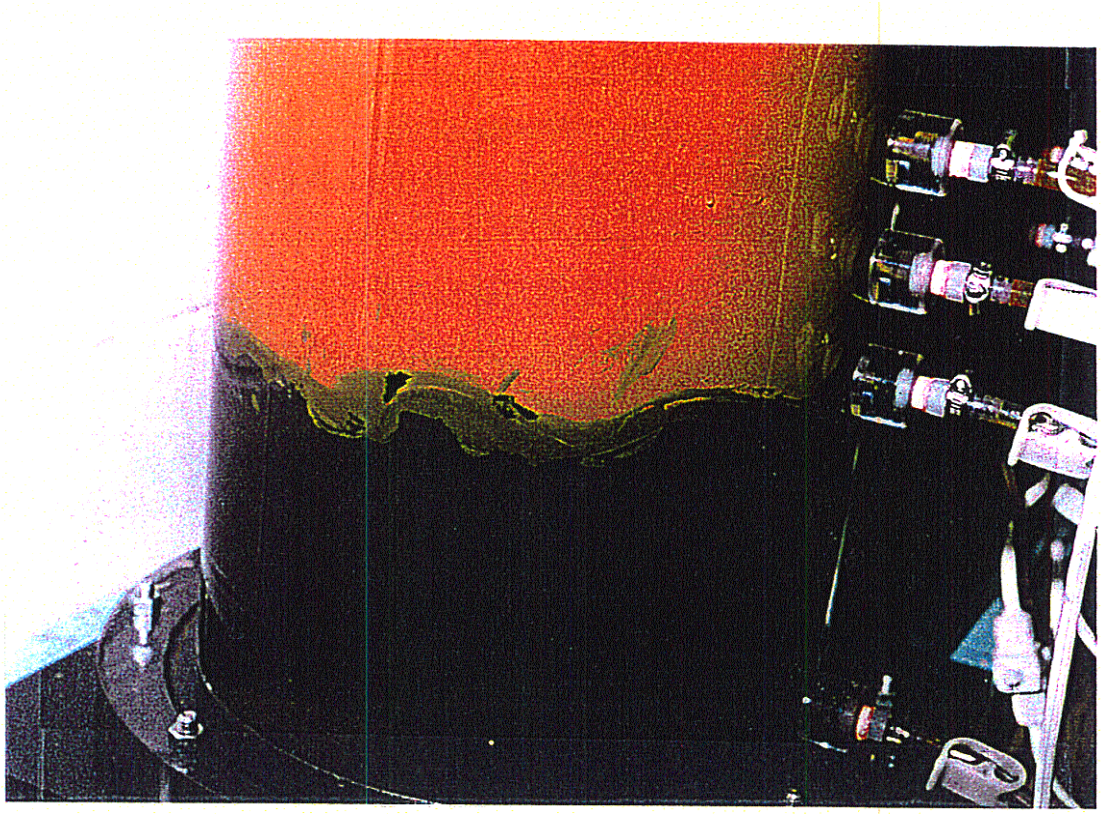

Figure 3.20 Photograph of ripples observed in 80 cm water cover stirred at 200 rpm

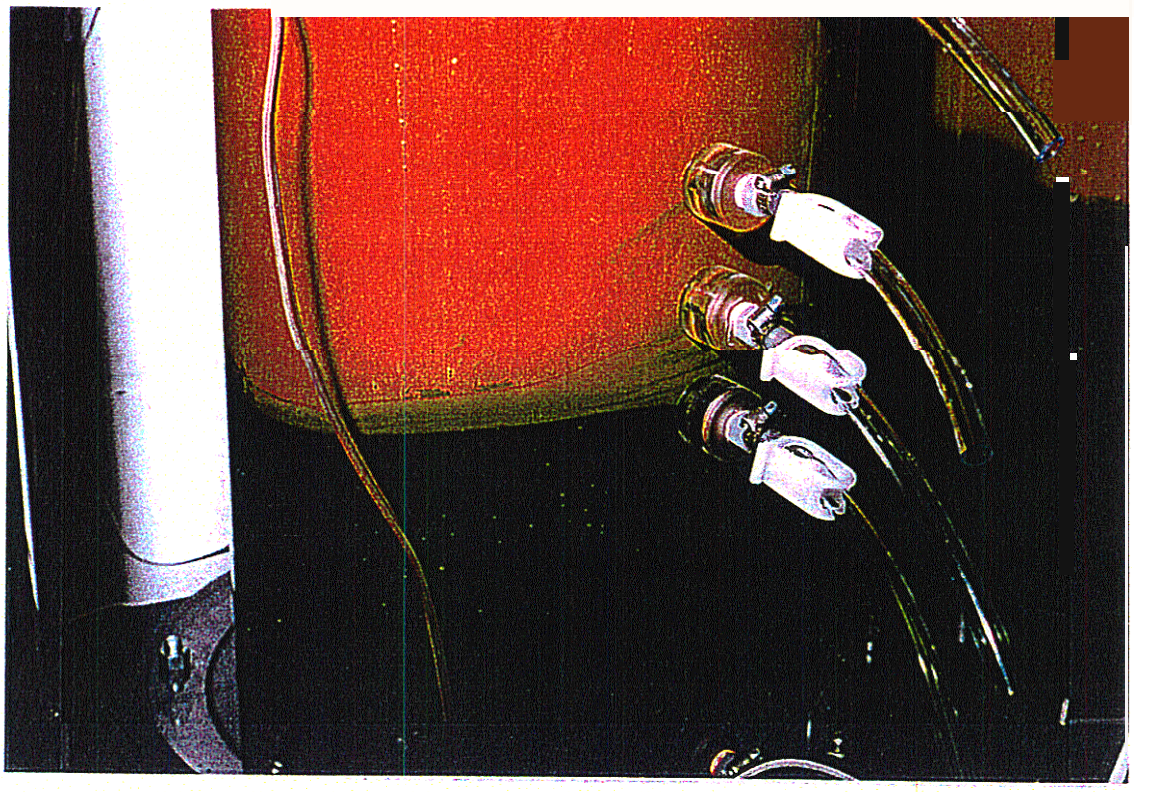

Figure 3.21 Photograph of ripples observed in 80 cm water cover stirred at 170 rpm

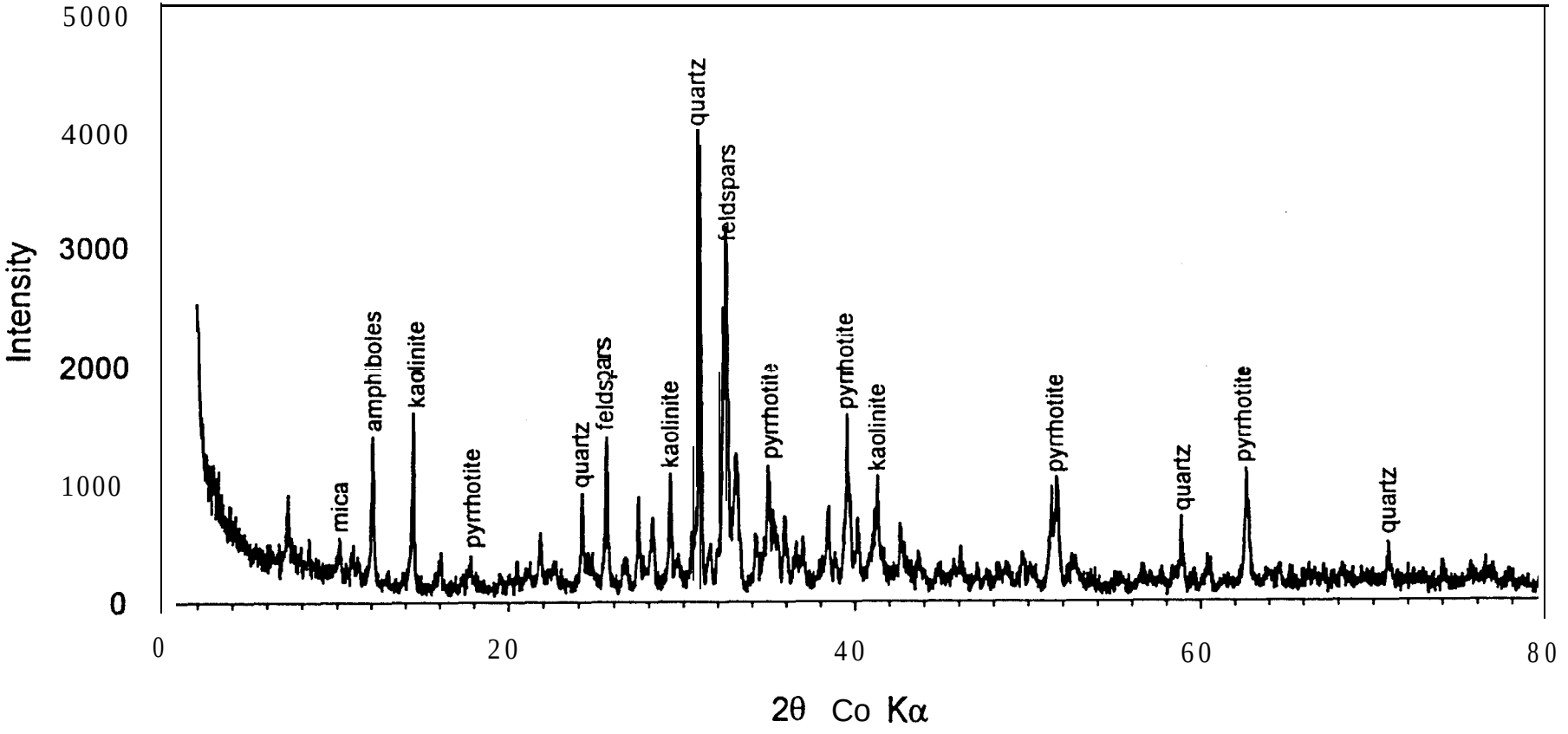

Figure 3.22 X-ray diffractogram of resuspended tailings in 80 cm water cover stirred at 200 rpm

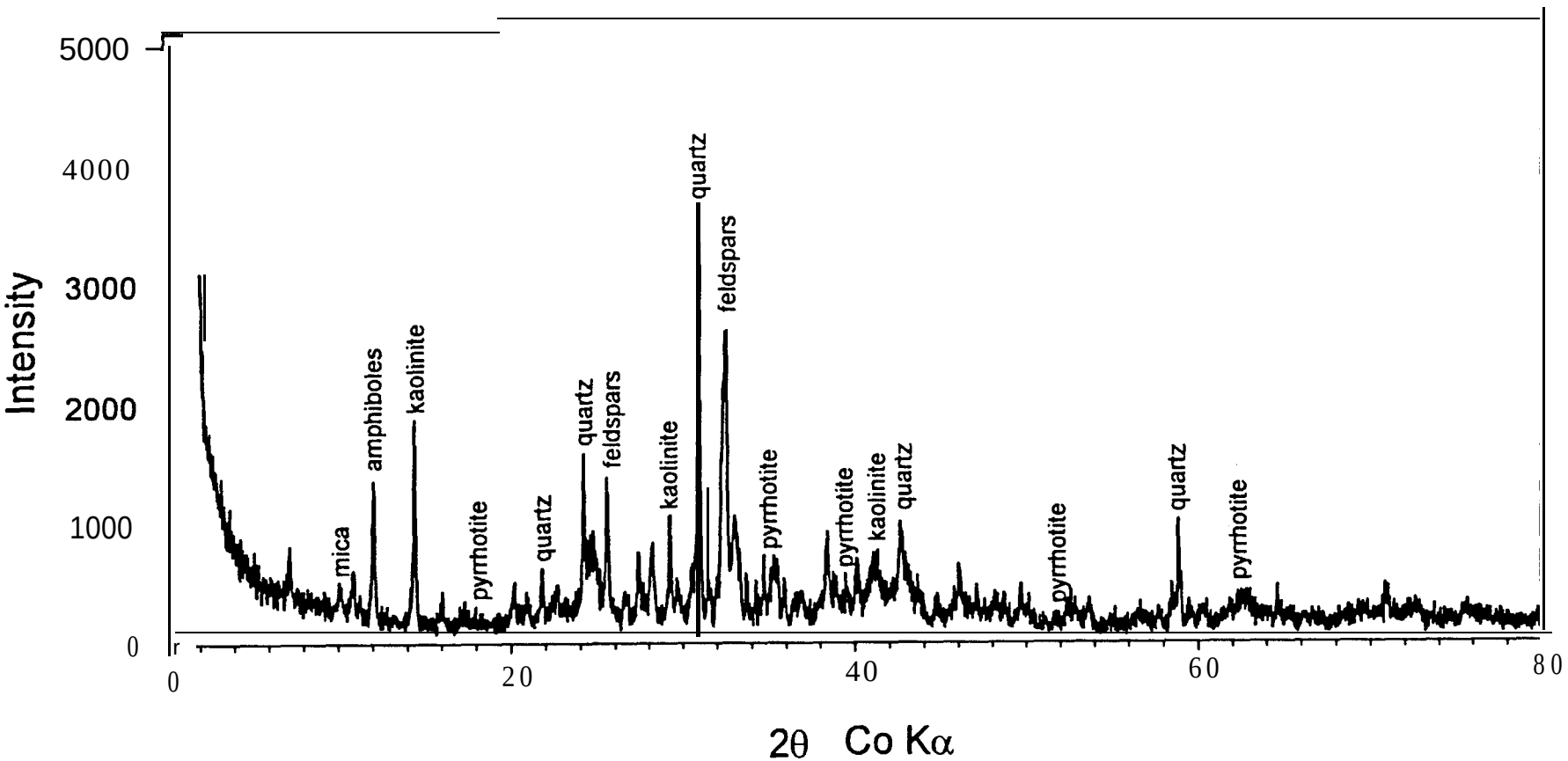

Figure 3.23 X-ray diffractogram of resuspended tailings in 80 cm water cover stirred at 170 rpm

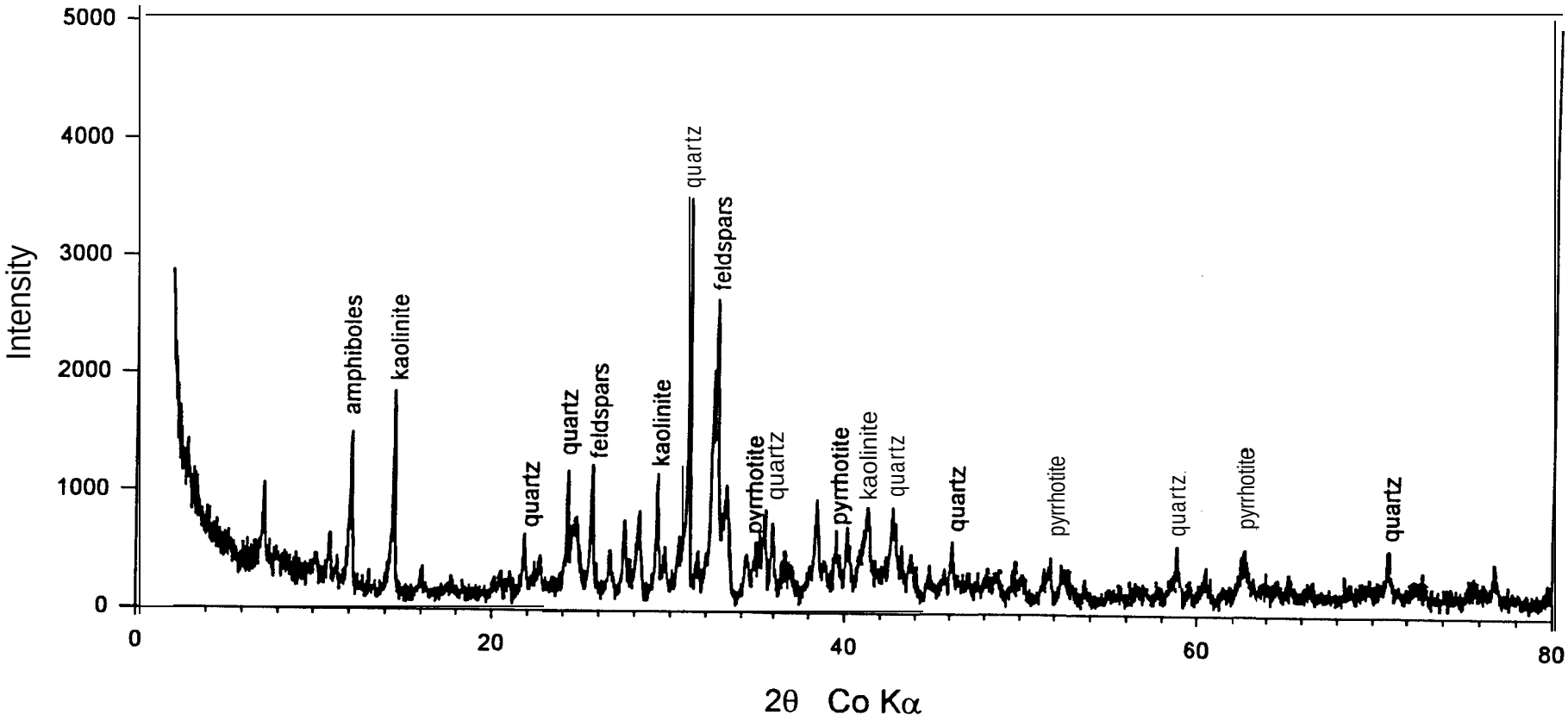

Figure 3.24 X-ray diffractogram of resuspended tailings in 80 cm water cover stirred at 140 rpm

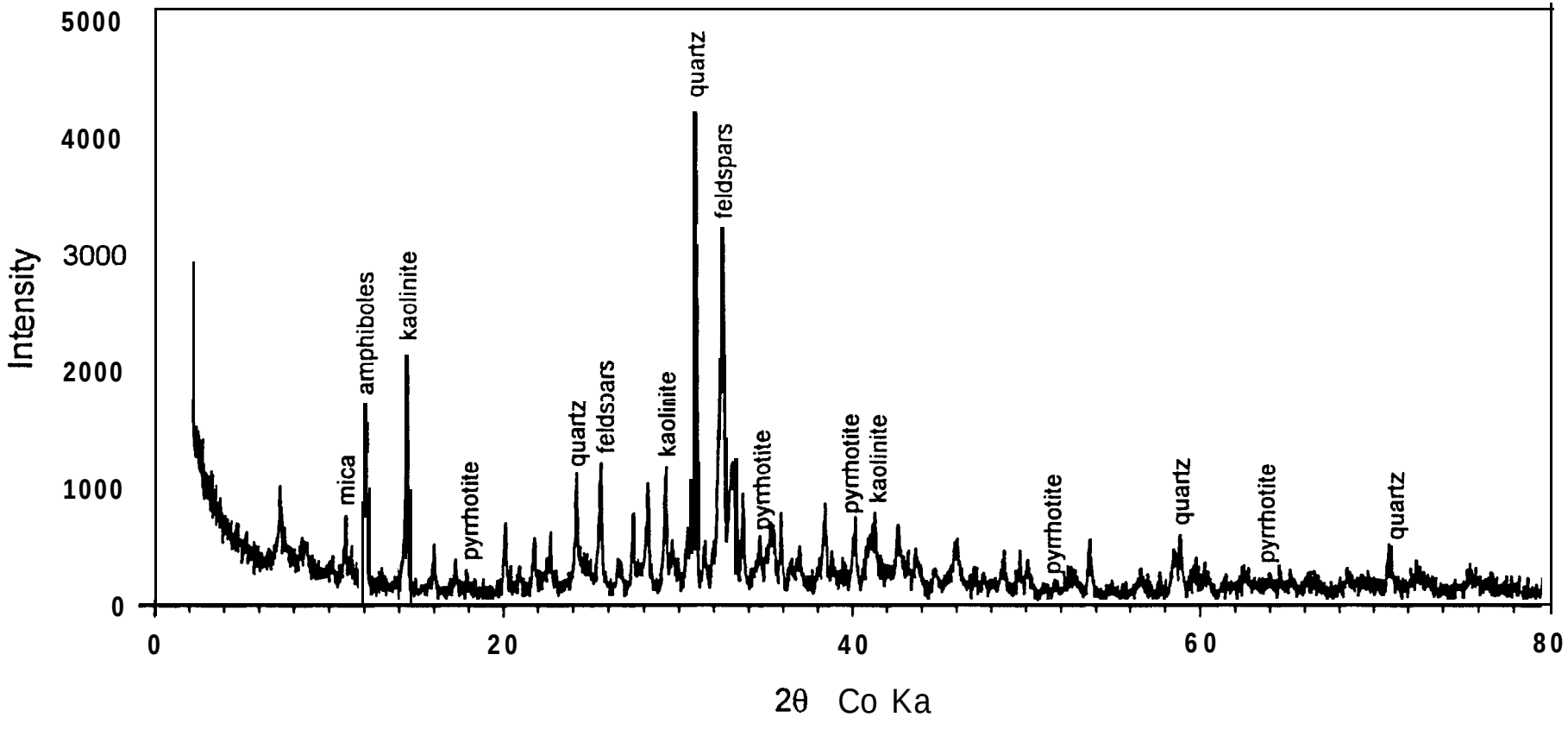

Figure 3.25 X-ray diffractogram of resuspended tailings in 60 cm water cover stirred at 200 rpm

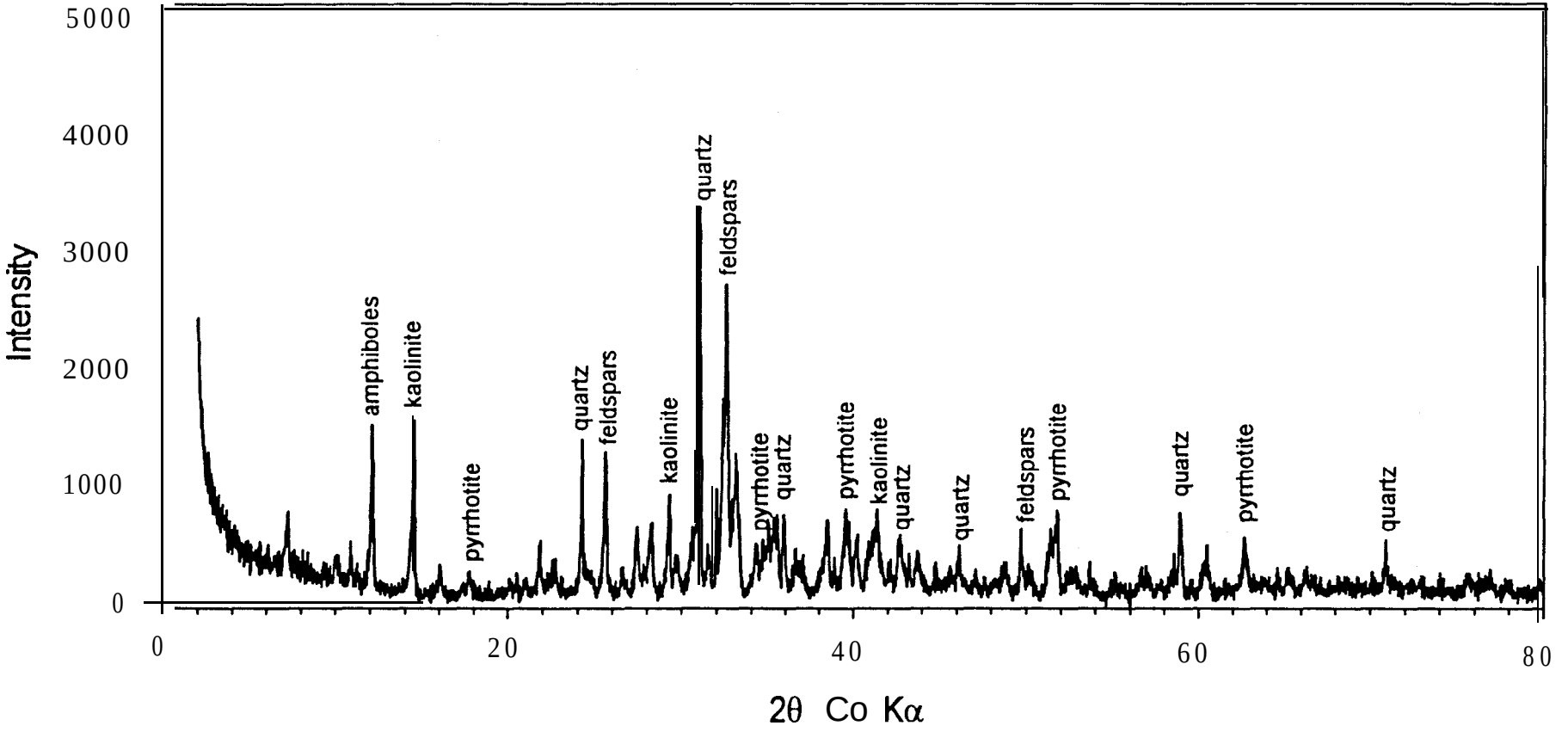

Figure 3.26 X-ray diffractogram of resuspended tailings in 60 cm water cover stirred at 170 rpm

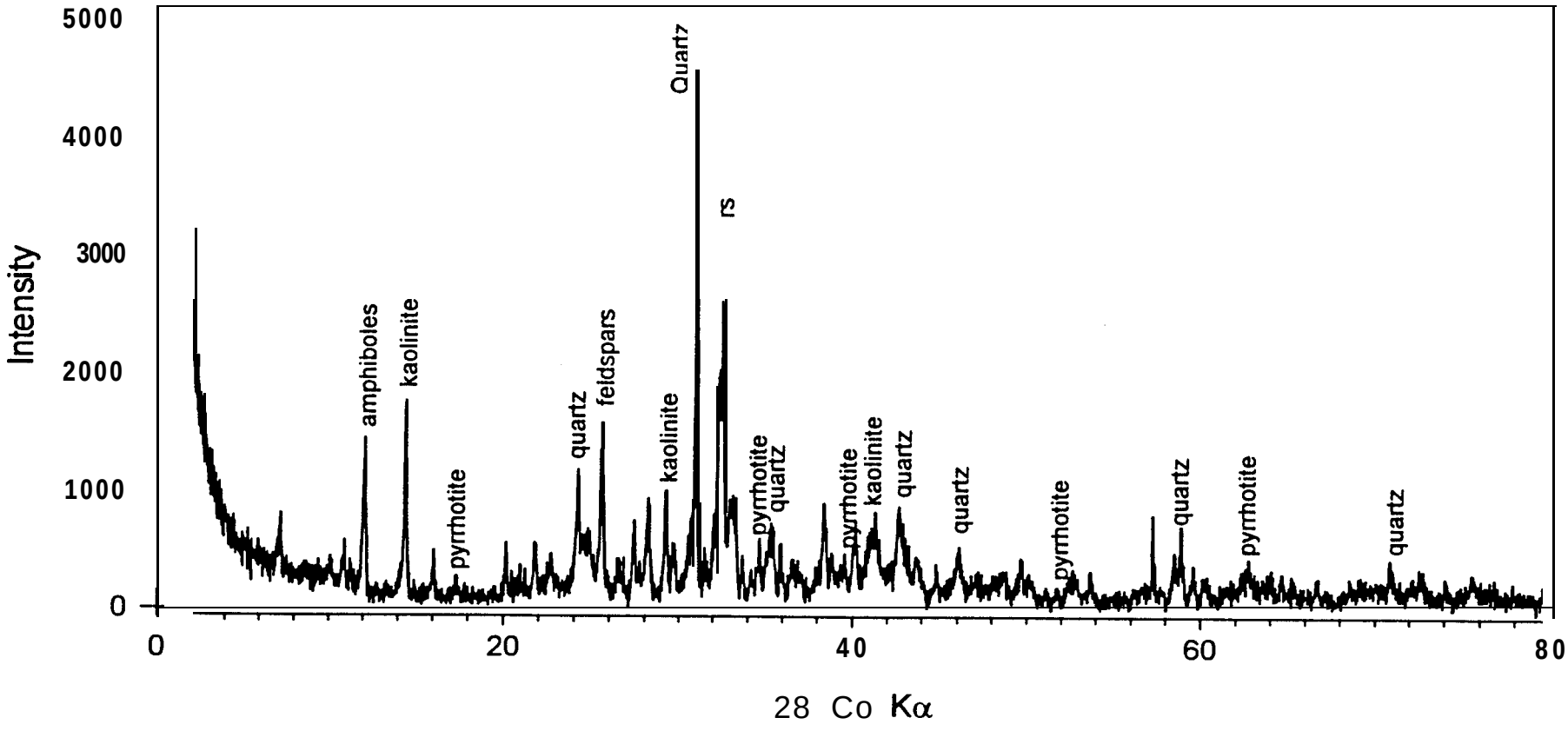

Figure 3.27 X-ray diffractogram of resuspended tailings in 60 cm water cover stirred at 140 rpm

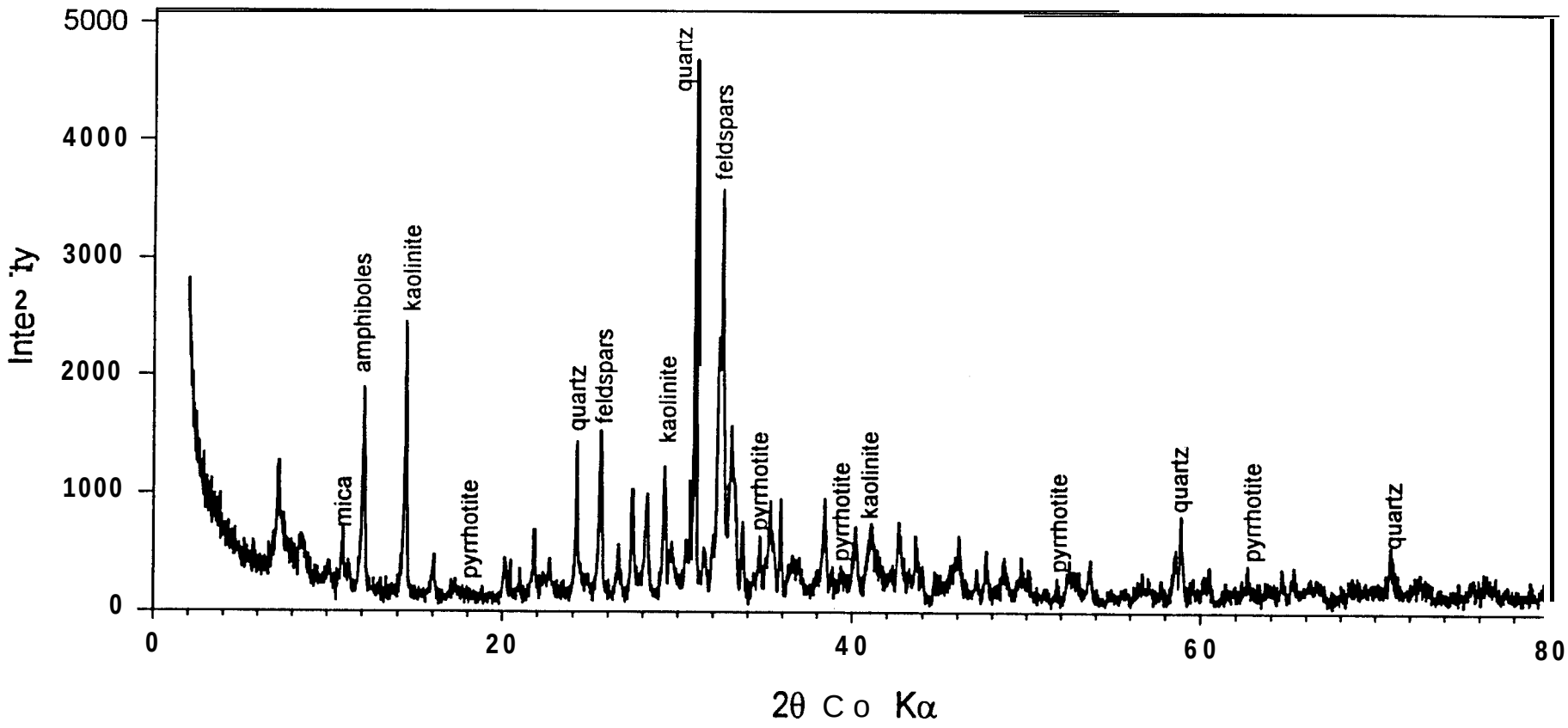

Figure 3.28 X-ray diffractogram of resuspended tailings in 45 cm water cover stirred at 200 rpm

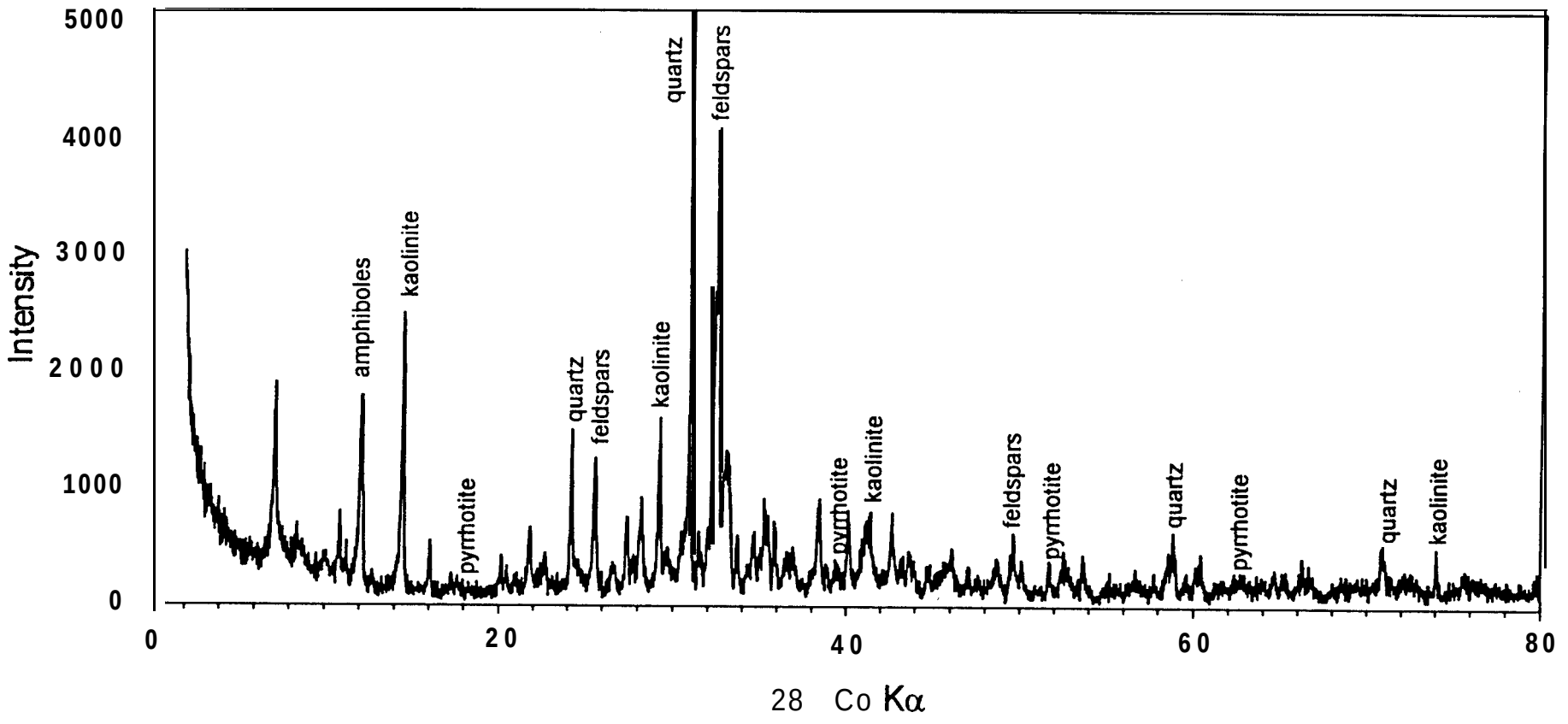

Figure 3.29 X-ray diffractogram of resuspended tailings in 45 cm water cover stirred at 170 rpm

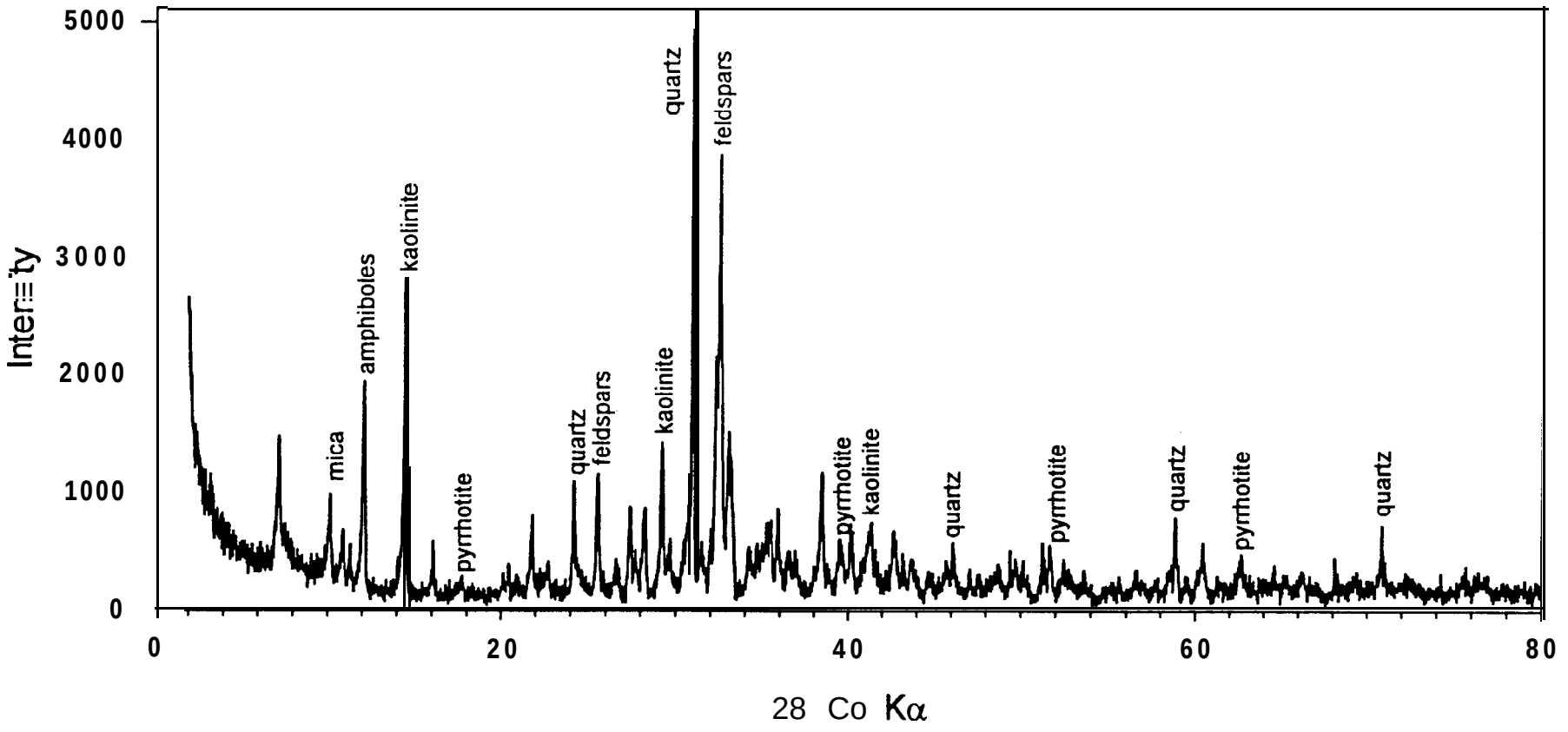

Figure 3.30 X-ray diffractogram of resuspended tailings in 45 cm water cover stirred at 140 rpm

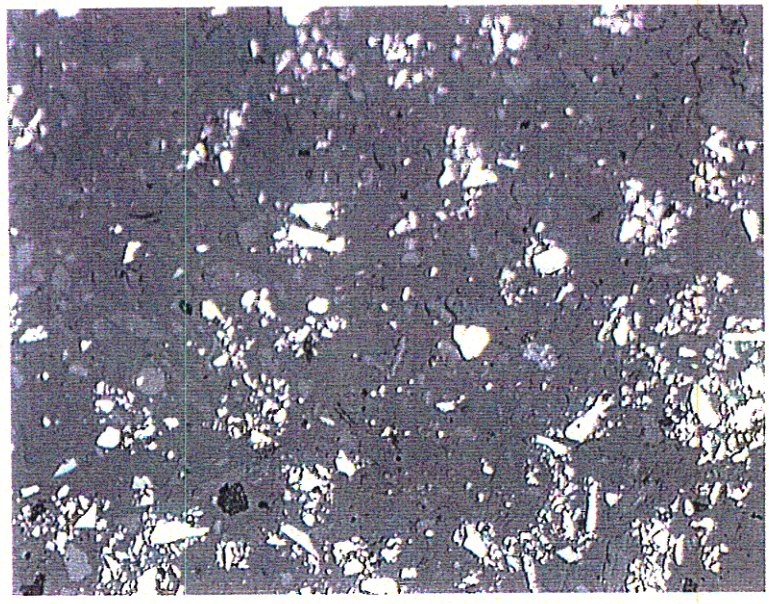

Figure 3.31 Optical photograph of resuspended particles in 80 cm water cover stirred at 140 rpm (20 cm above tailings surface)

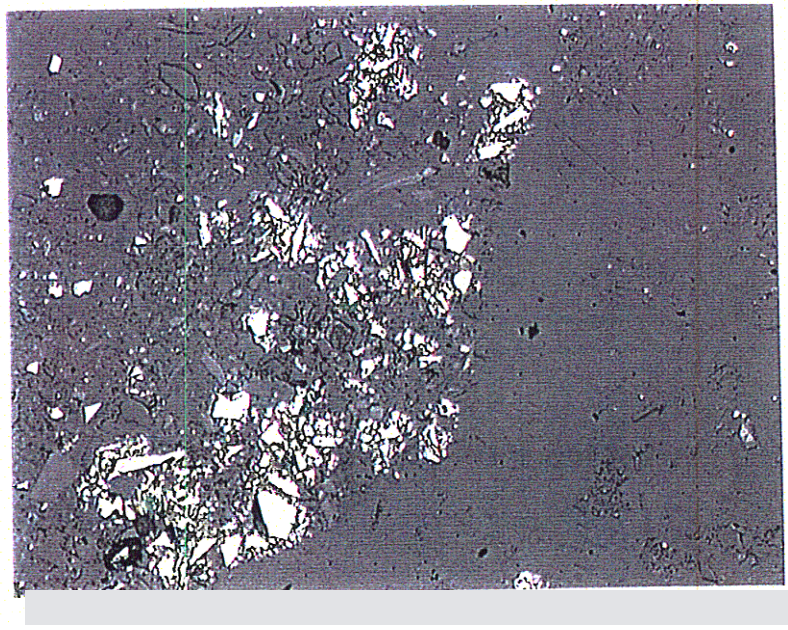

Figure 3.32 Optical photograph of resuspended particles in 80 cm water cover stirred at 140 rpm (40 cm above tailings surface)

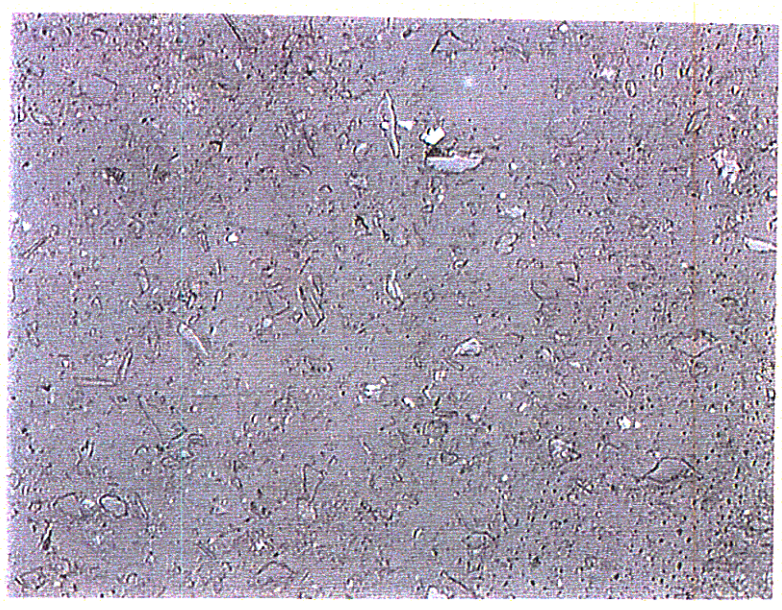

Figure 3.33 Optical photograph of resuspended particles in 60 cm water cover stirred at 200 rpm (20 cm above tailings surface)

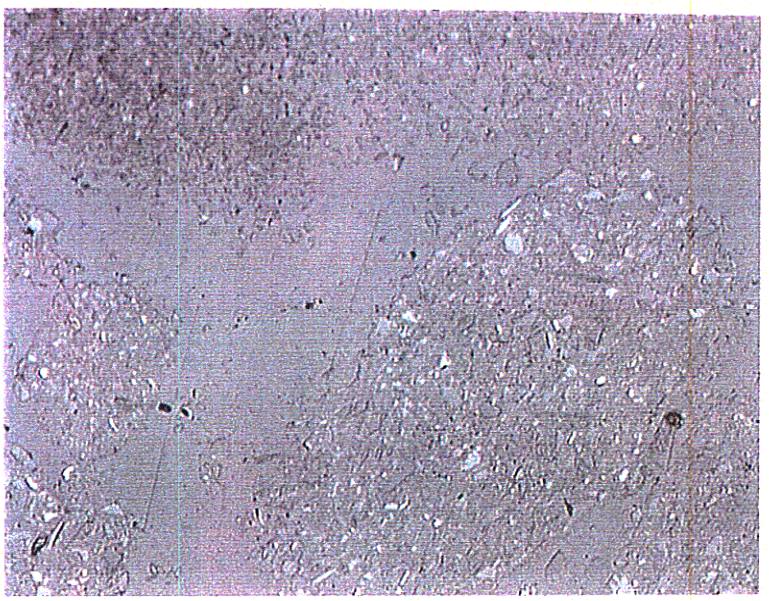

Figure 3.34 Optical photograph of resuspended particles in 60 cm water cover stirred at 200 rpm (40 cm above tailings surface)

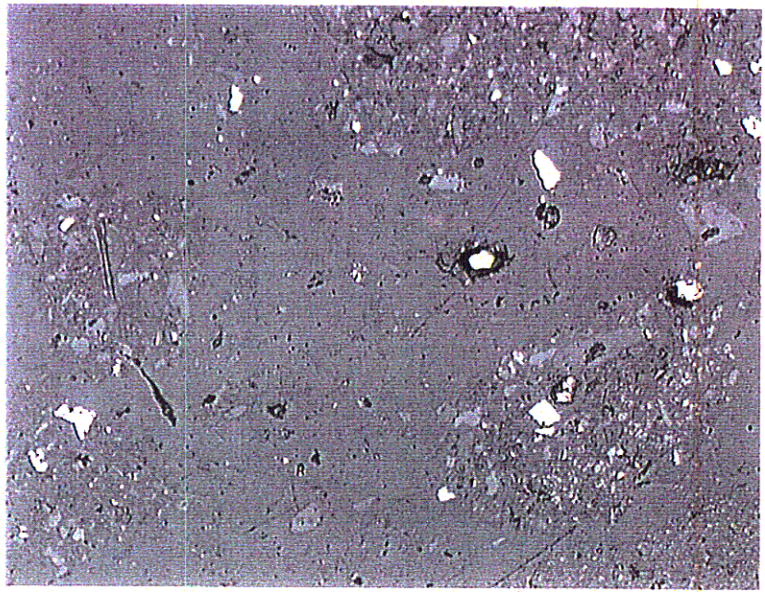

Figure 3.35 Optical photograph of resuspended particles in 60 cm water cover stirred at 140 rpm (20 cm above tailings surface)

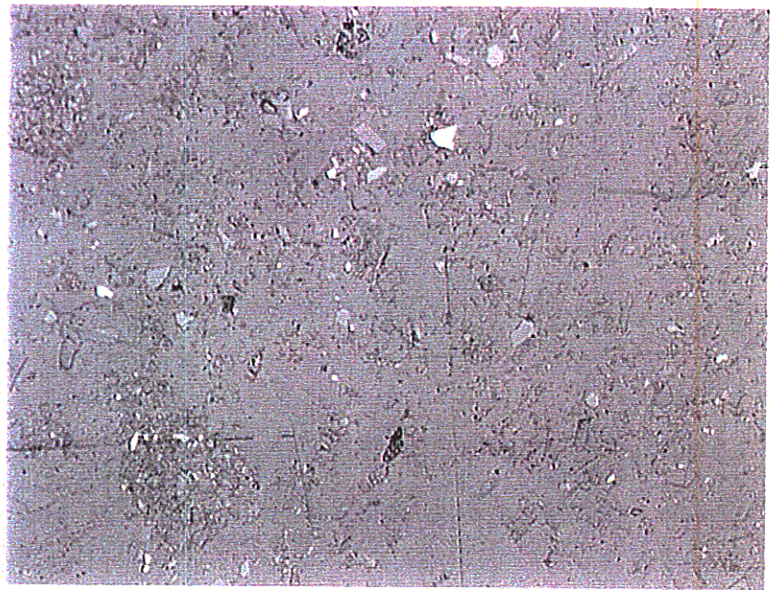

Figure 3.36 Optical photograph of resuspended particles in 60 cm water cover stirred at 140 rpm (40 cm above tailings surface)

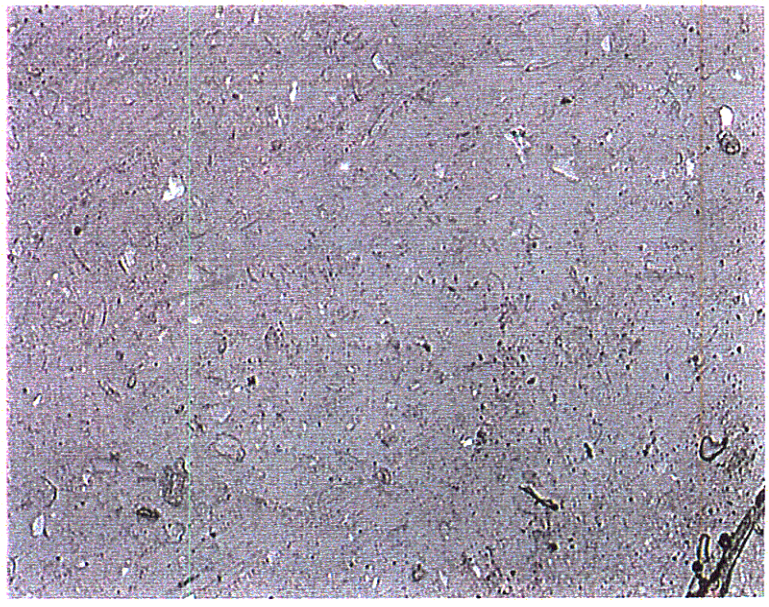

Figure 3.37 Optical photograph of resuspended particles in 45 cm water cover stirred at 200 rpm (20 cm above tailings surface)

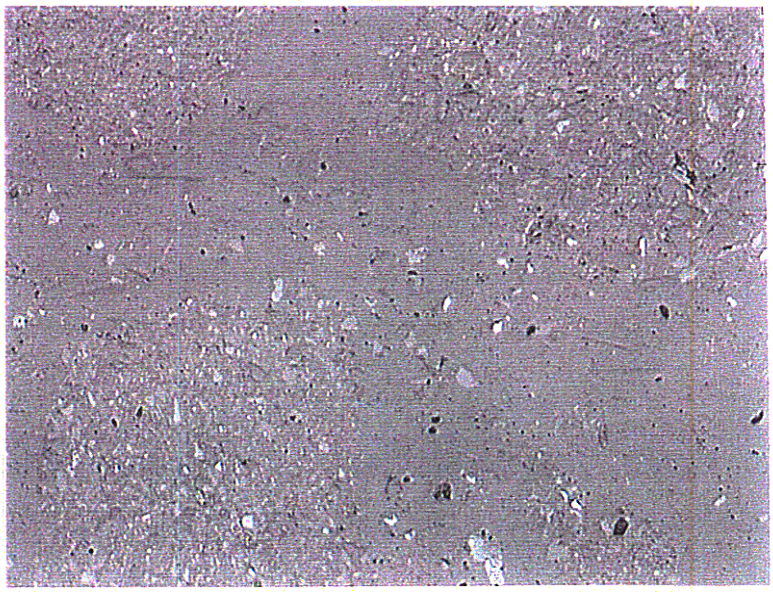

Figure 3.38 Optical photograph of resuspended particles in 45 cm water cover stirred at 200 rpm (40 cm above tailings surface)

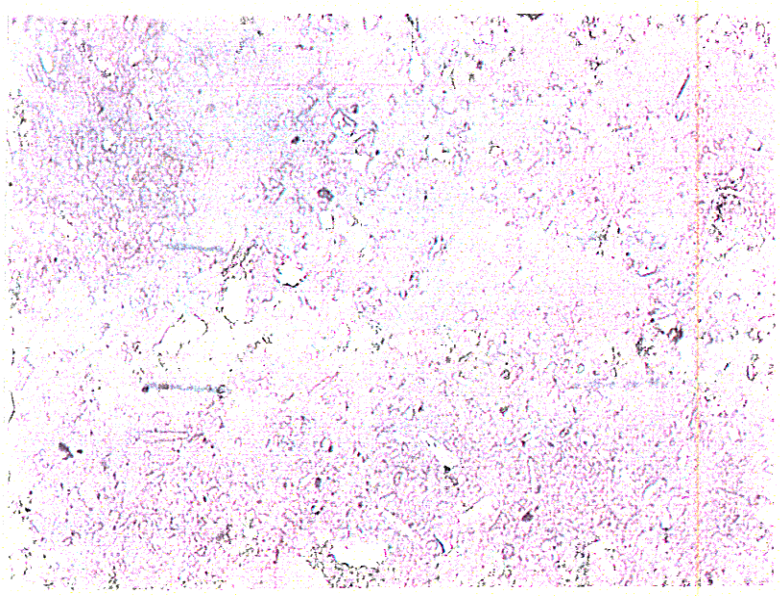

Figure 3.39 Optical photograph of resuspended particles in 45 cm water cover stirred at 140 rpm (20 cm above tailings surface)

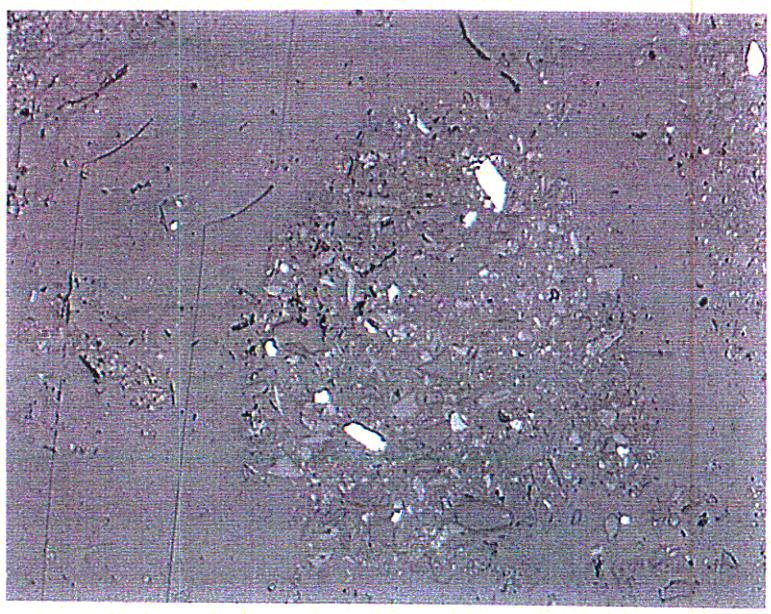

Figure 3.40 Optical photograph of resuspended particles in 45 cm water cover stirred at 140 rpm (40 cm above tailings surface)

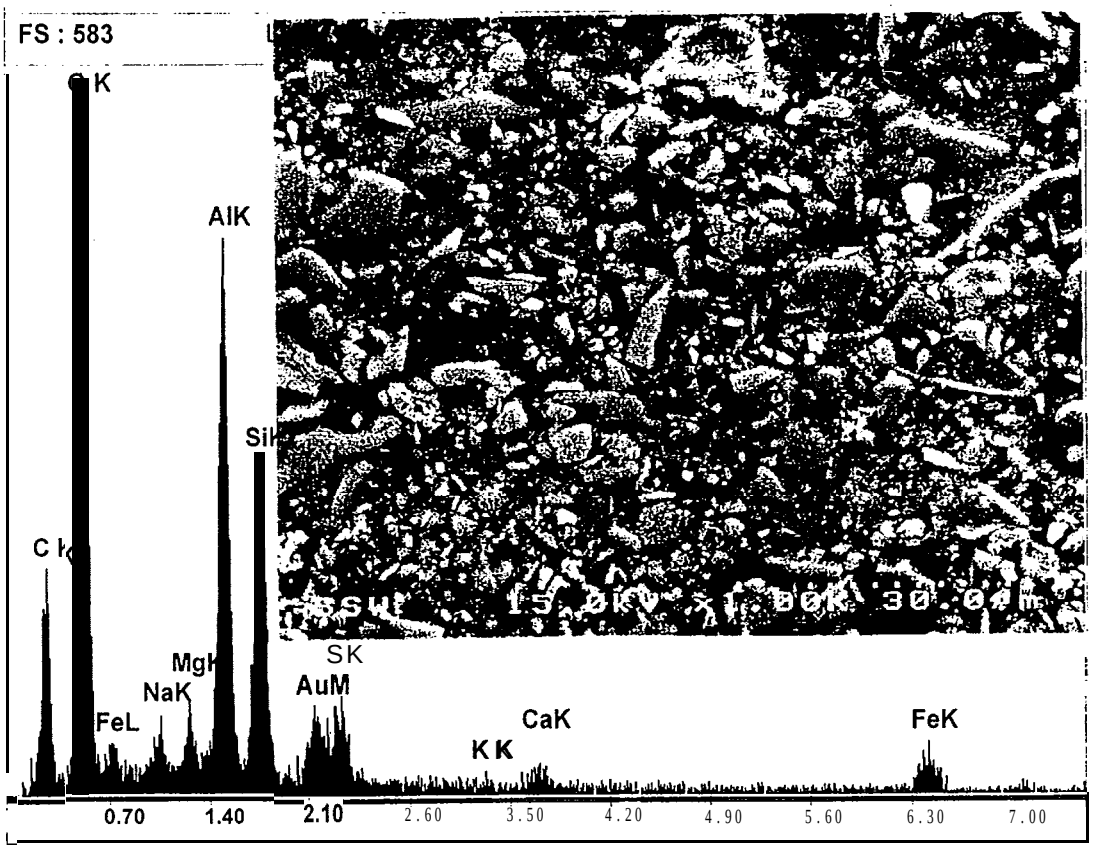

Element	Wt %	At %
C K	33.18	44.66
O K	43.15	43.60
NaK	1.22	0.85
MgK	1.02	0.68
AlK	8.85	5.30
SiK	5.50	3.21
AuM	3.25	0.27
SK	1.31	0.66
KK	0.13	0.05
CaK	0.45	0.18
FeK	1.84	0.53
Total	100.00	100.00

Figure 3.41 Scanning electron photomicrograph of resuspended particles in 80 cm water cover stirred at 140 rpm

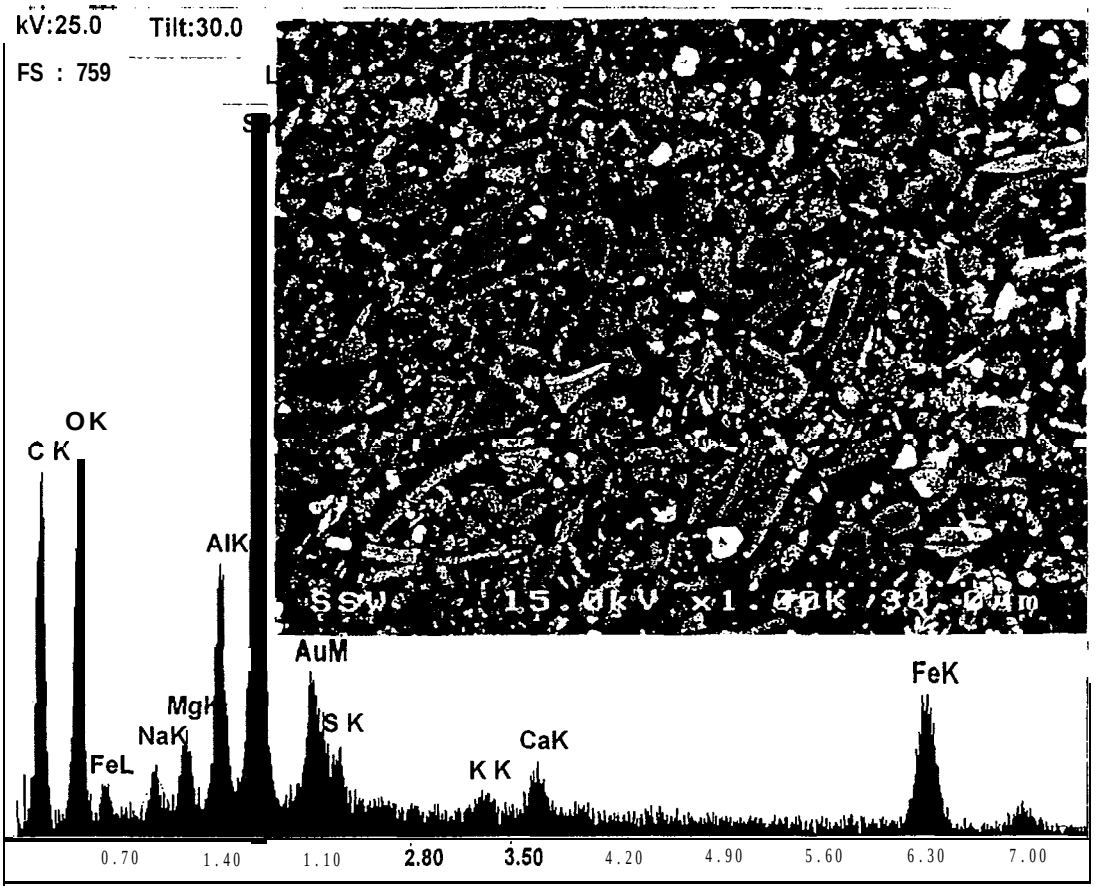

Element	Wt %	At %
C K	48.94	65.83
O K	22.09	22.30
NaK	0.00	0.00
MgK	1.32	0.88
AlK	3.67	2.20
SiK	9.57	5.50
AuM	5.85	0.48
S K	0.76	0.38
K K	0.48	0.20
CaK	0.93	0.38
FeK	6.40	1.85
Total	100.00	100.00

Figure 3.42 Scanning electron photomicrograph of resuspended particles in 60 cm water cover stirred at 170 rpm

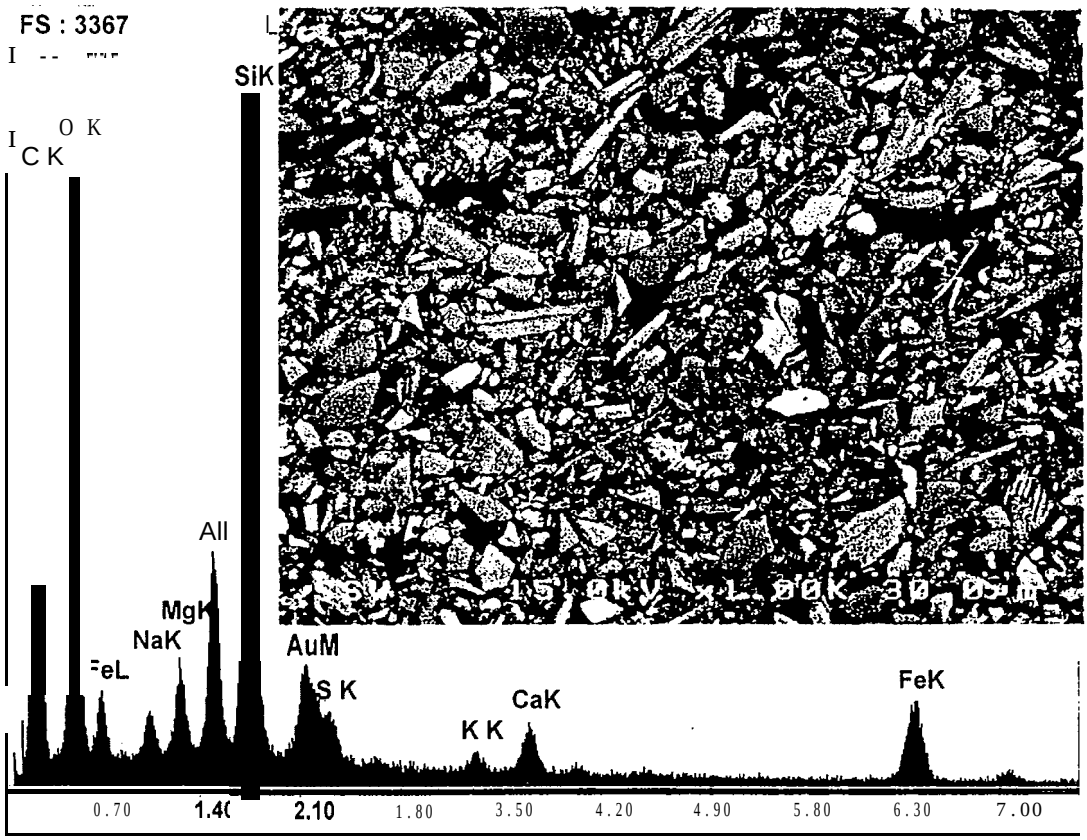

Element	Wt %	At %
C K	51.99	64.69
O K	29.53	27.58
NaK	0.90	0.59
MgK	1.16	0.72
AlK	2.30	1.27
SiK	6.73	3.58
AuM	3.20	0.24
S K	0.57	0.26
K K	0.25	0.10
CaK	0.66	0.24
FeK	2.71	0.72
Total	100.00	100.00

Figure 3.43 Scanning electron photomicrograph of resuspended particles in 45 cm water cover stirred at 170 rpm

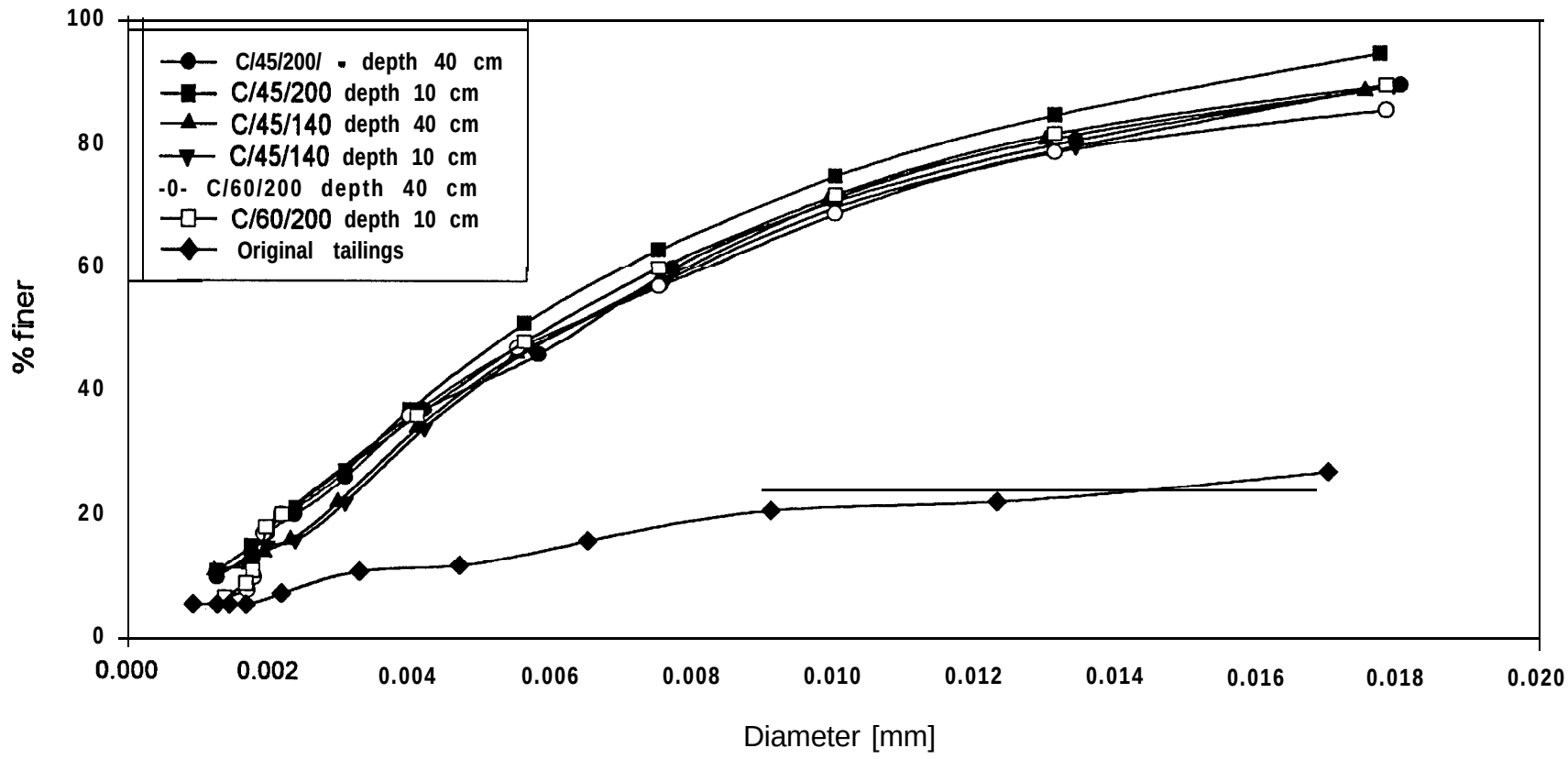

Figure 3.44 Particle size distributions of oxidized resuspended tailings

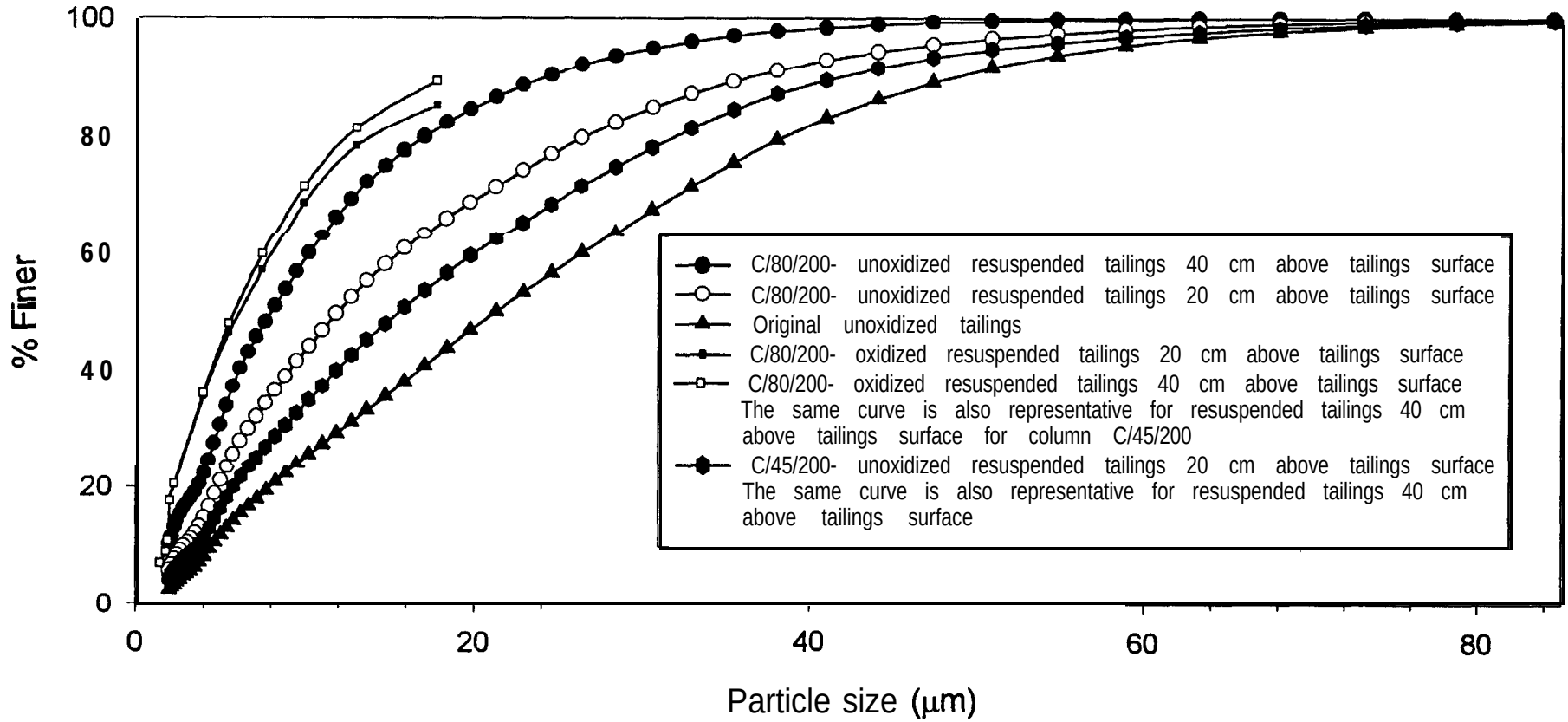

Figure 3.45 Particle size distributions of oxidized and unoxidized resuspended tailings

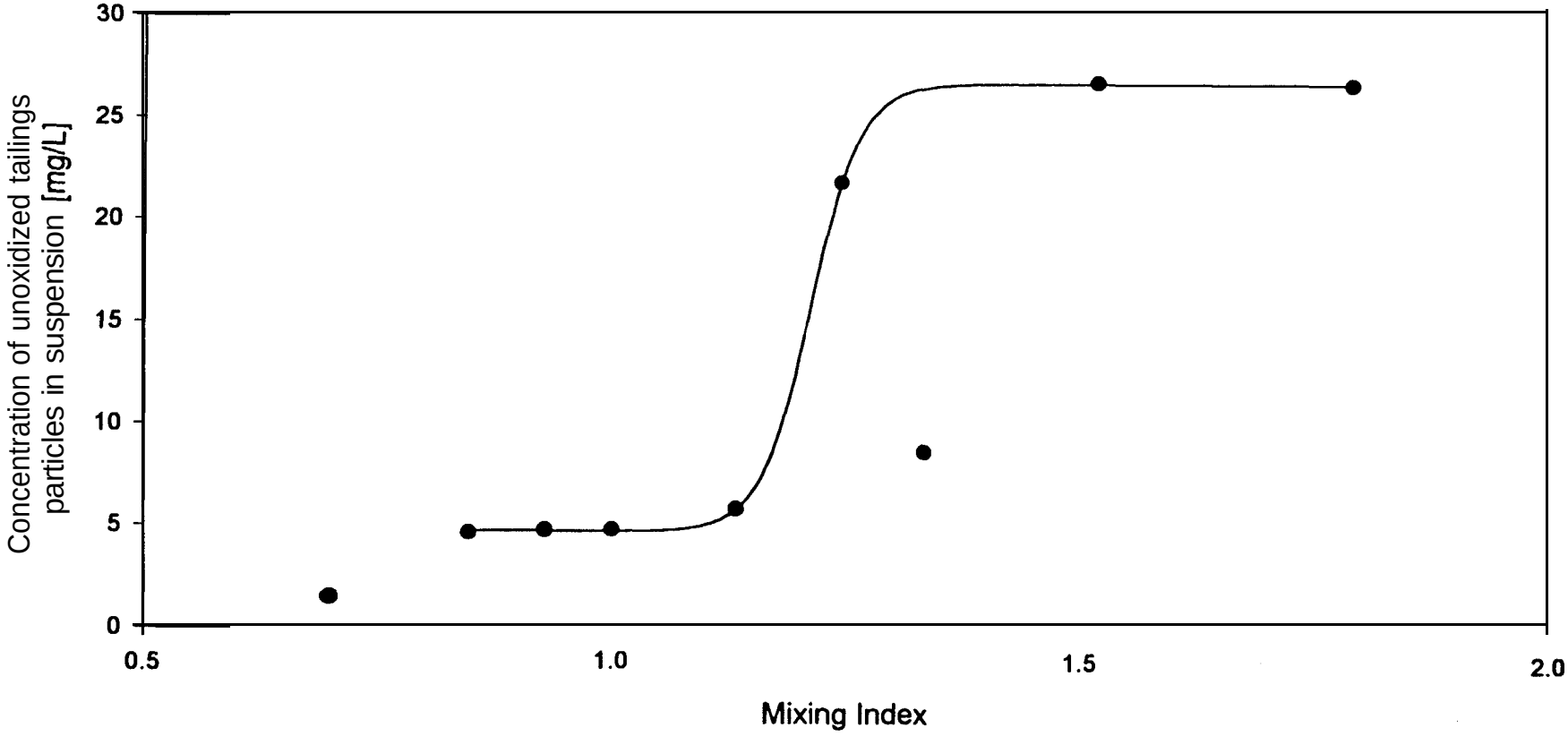

Figure 3.46 Variation of resuspended tailings concentration with mixing index

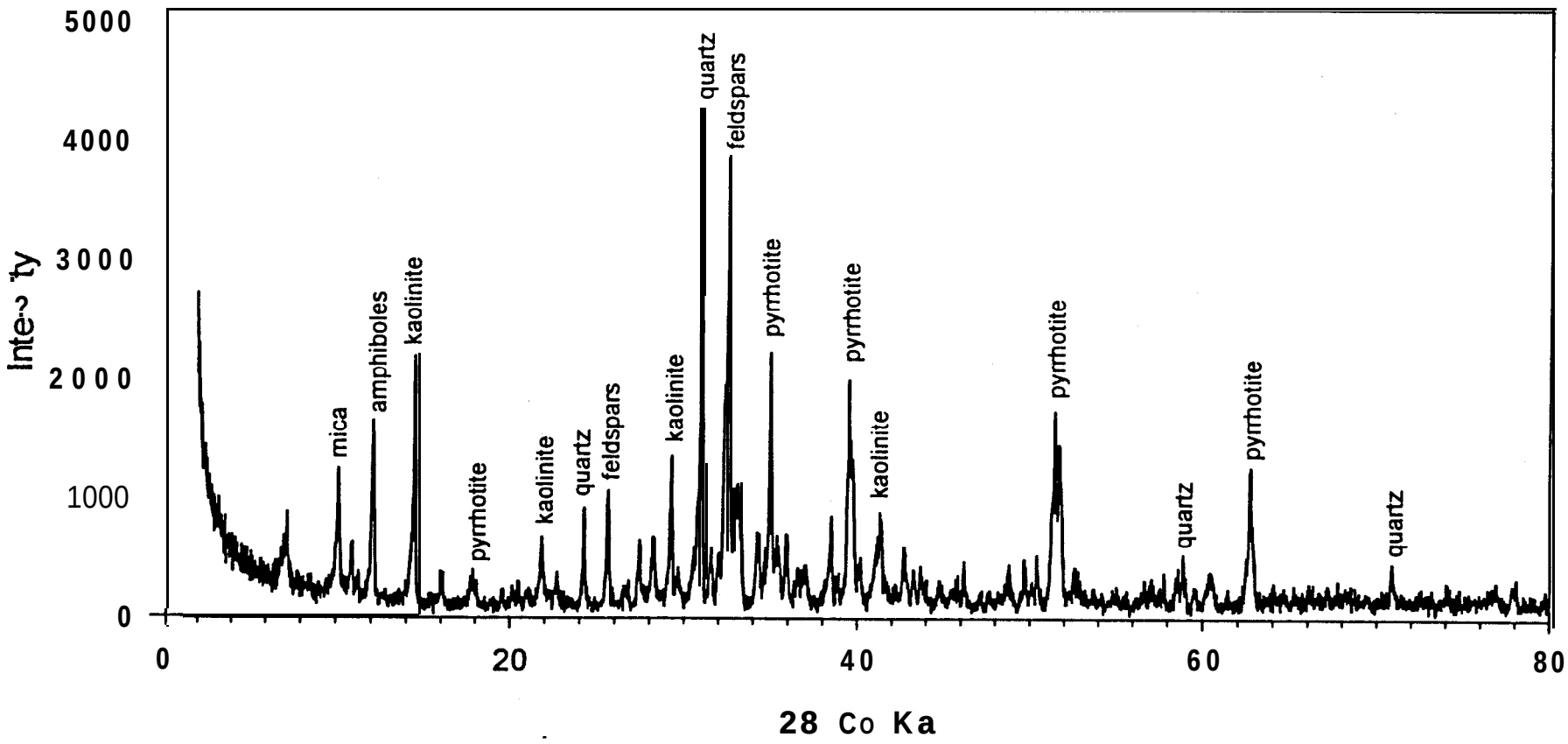

Figure 3.47 X-ray diffractogram of unoxidized resuspended tailings in 45 cm water cover stirred at 200 rpm (20 cm above tailings surface)

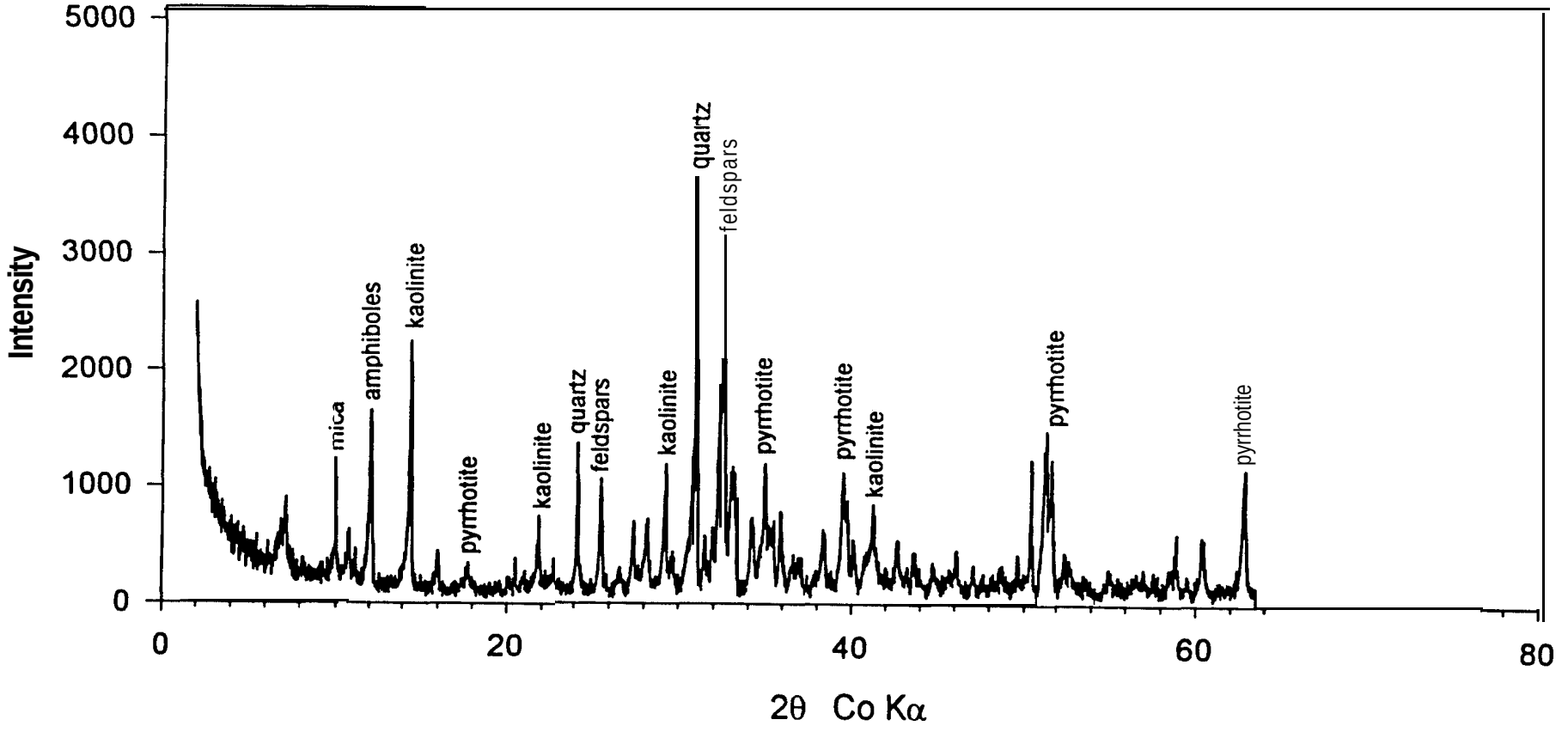

Figure 3.48 X-ray diffractogram of unoxidized resuspended tailings in 60 cm water cover stirred at 200 rpm (20 cm above tailings surface)

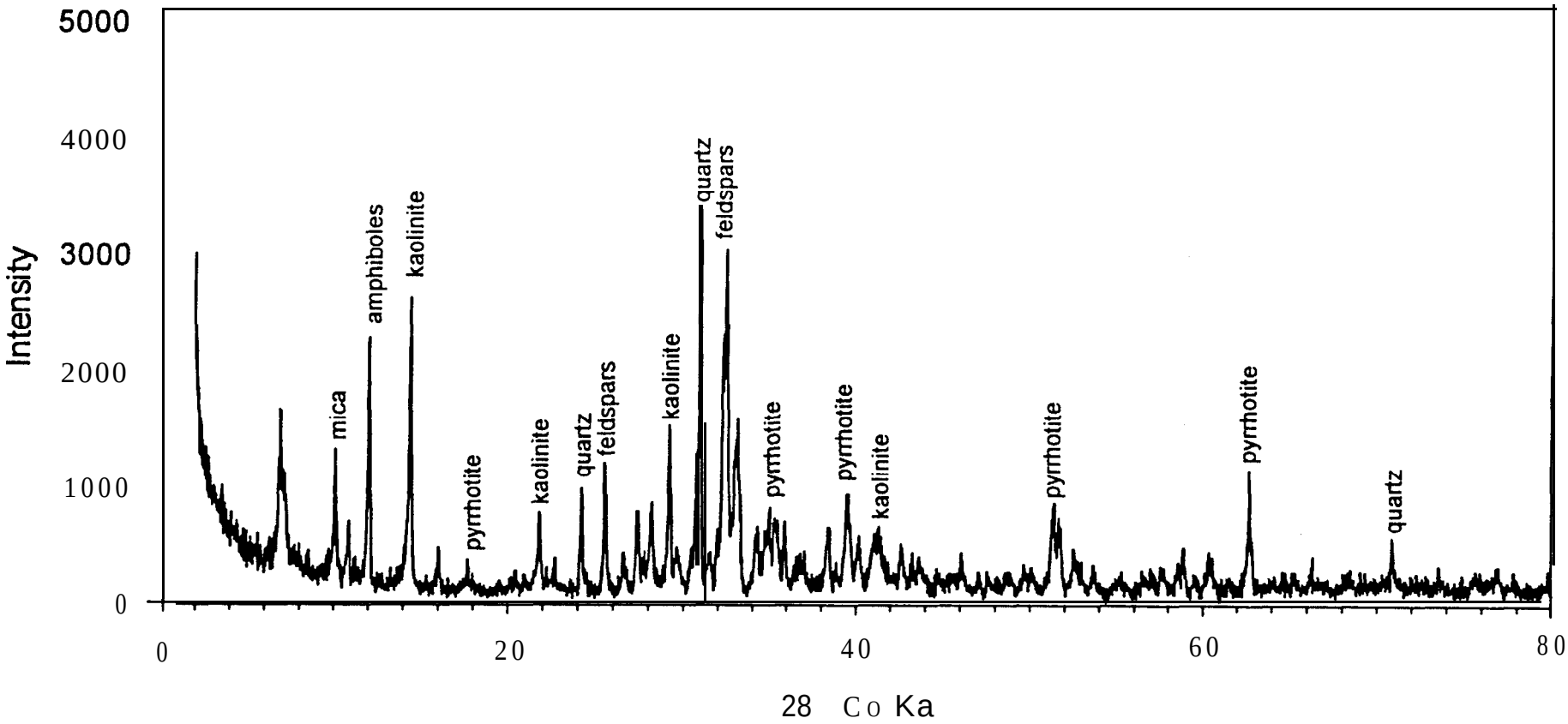

Figure 3.49 X-ray diffractogram of unoxidized resuspended tailings in 45 cm water cover stirred at 140 rpm (20 cm above tailings surface)

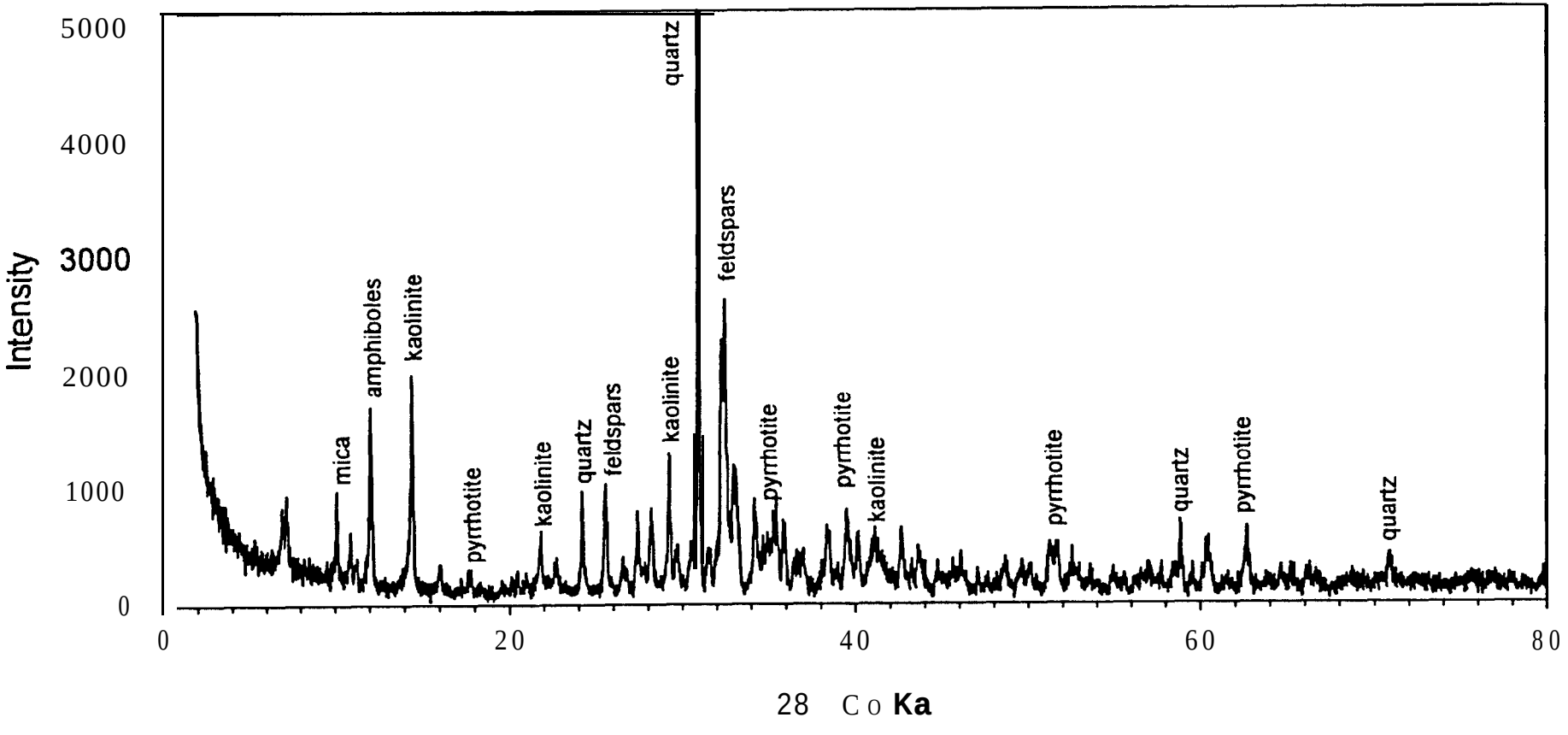

Figure 3.50 X-ray diffractogram of unoxidized resuspended tailings in 80 cm water cover stirred at 140 rpm (20 cm above tailings surface)

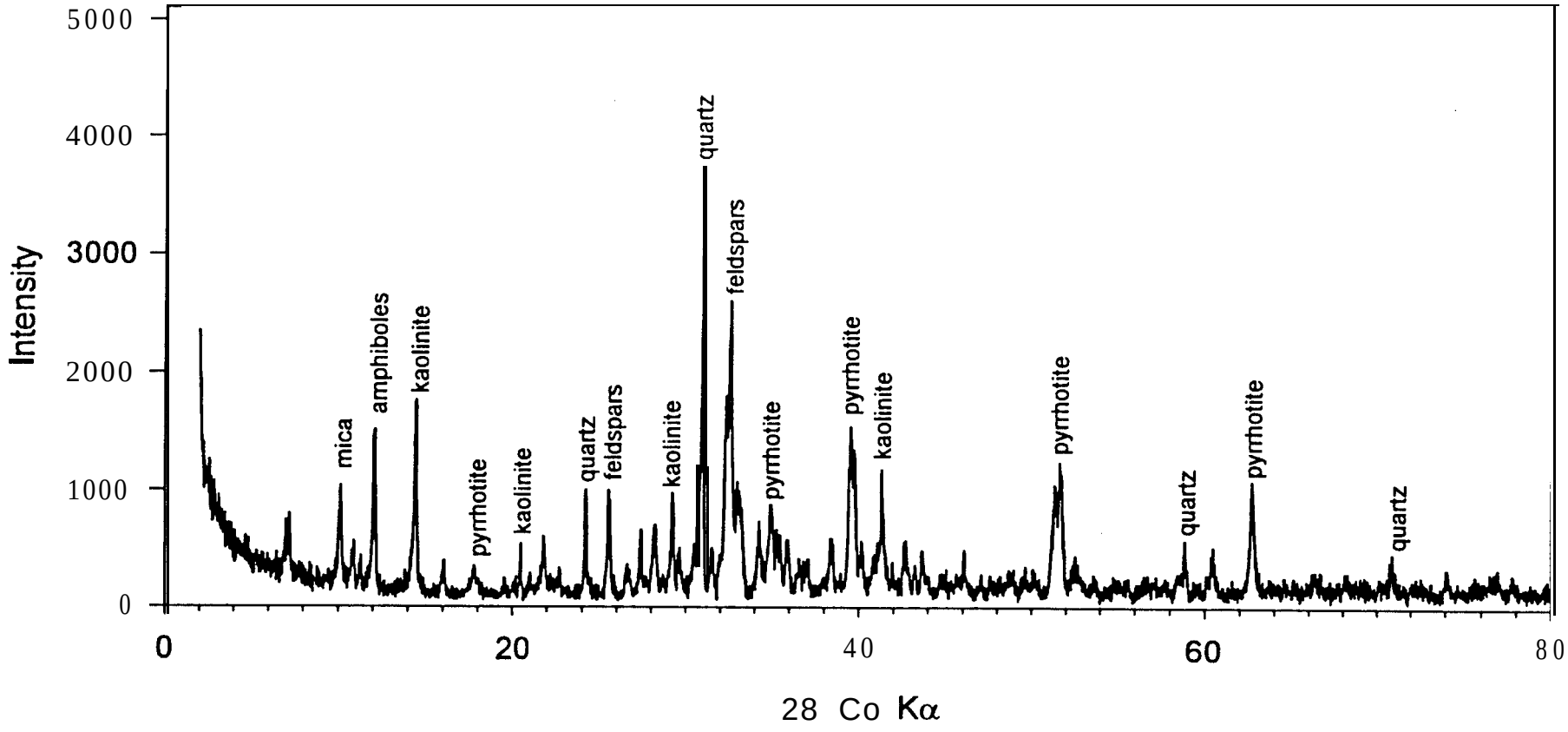

Figure 3.51 X-ray diffractogram of unoxidized resuspended tailings in 45 cm water cover stirred at 200 rpm (40 cm above tailings surface)

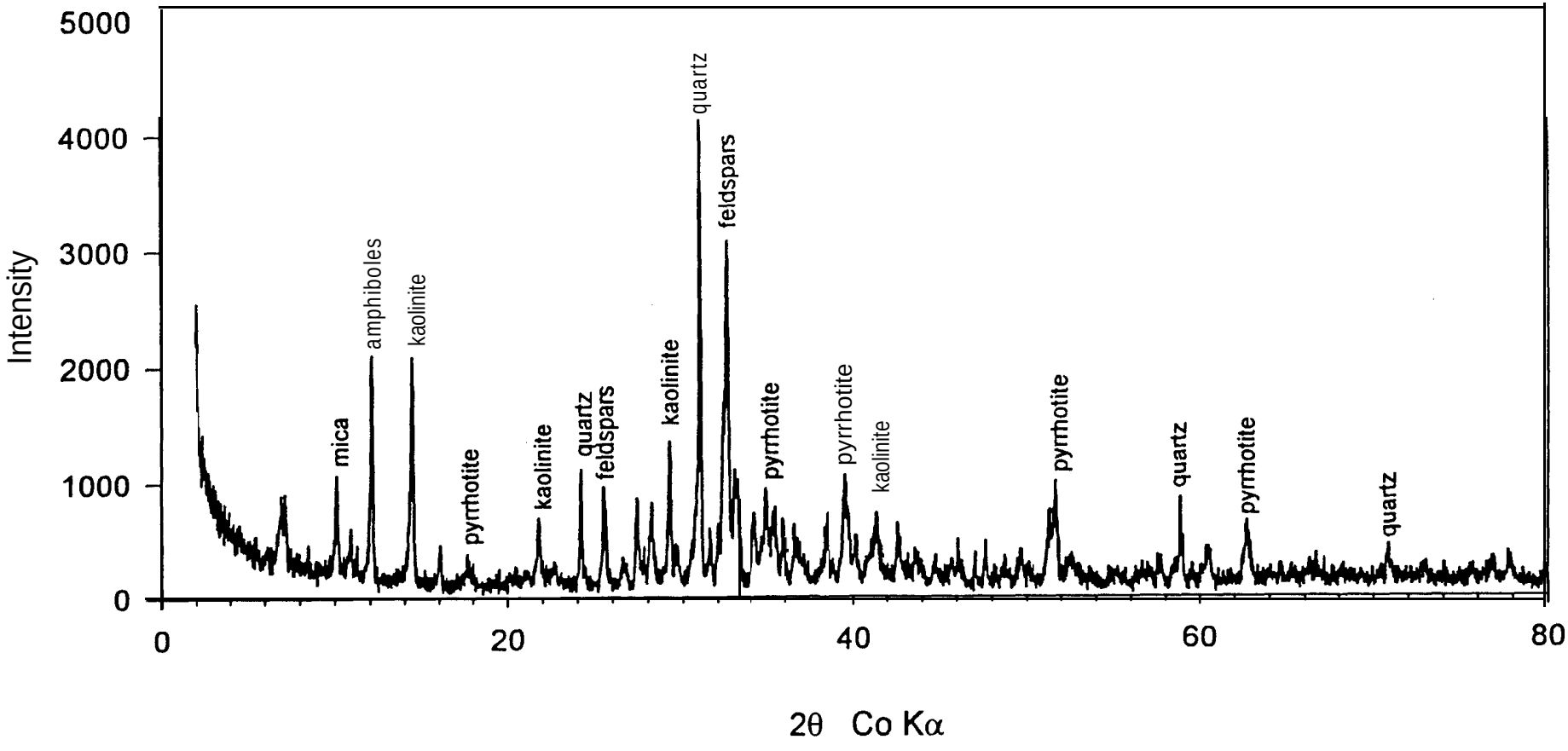

Figure 3.52 X-ray diffractogram of unoxidized resuspended tailings in 60 cm water cover stirred at 200 rpm (40 cm above tailings surface)

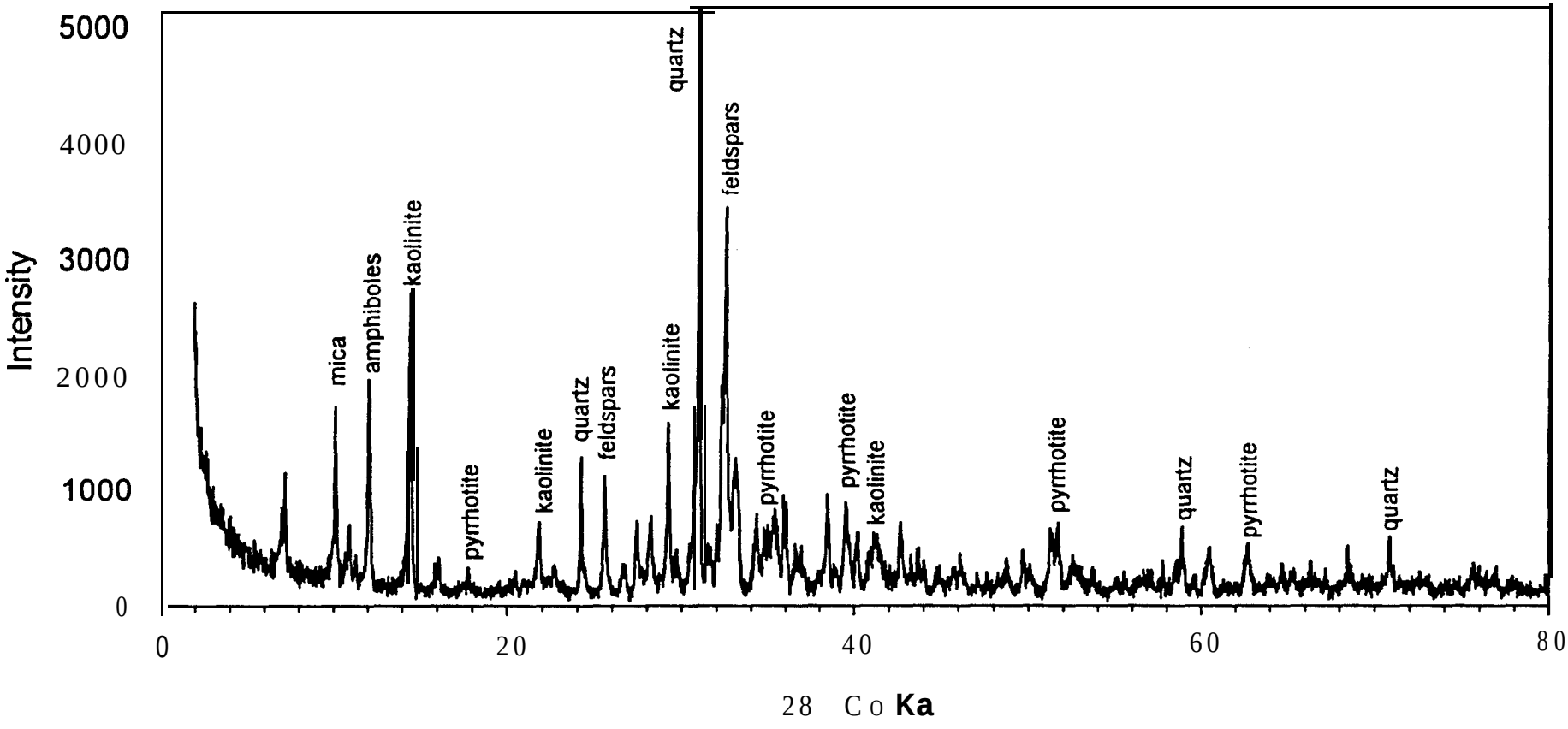

Figure 3.53 X-ray diffractogram of unoxidized resuspended tailings in 45 cm water cover stirred at 140 rpm (40 cm above tailings surface)

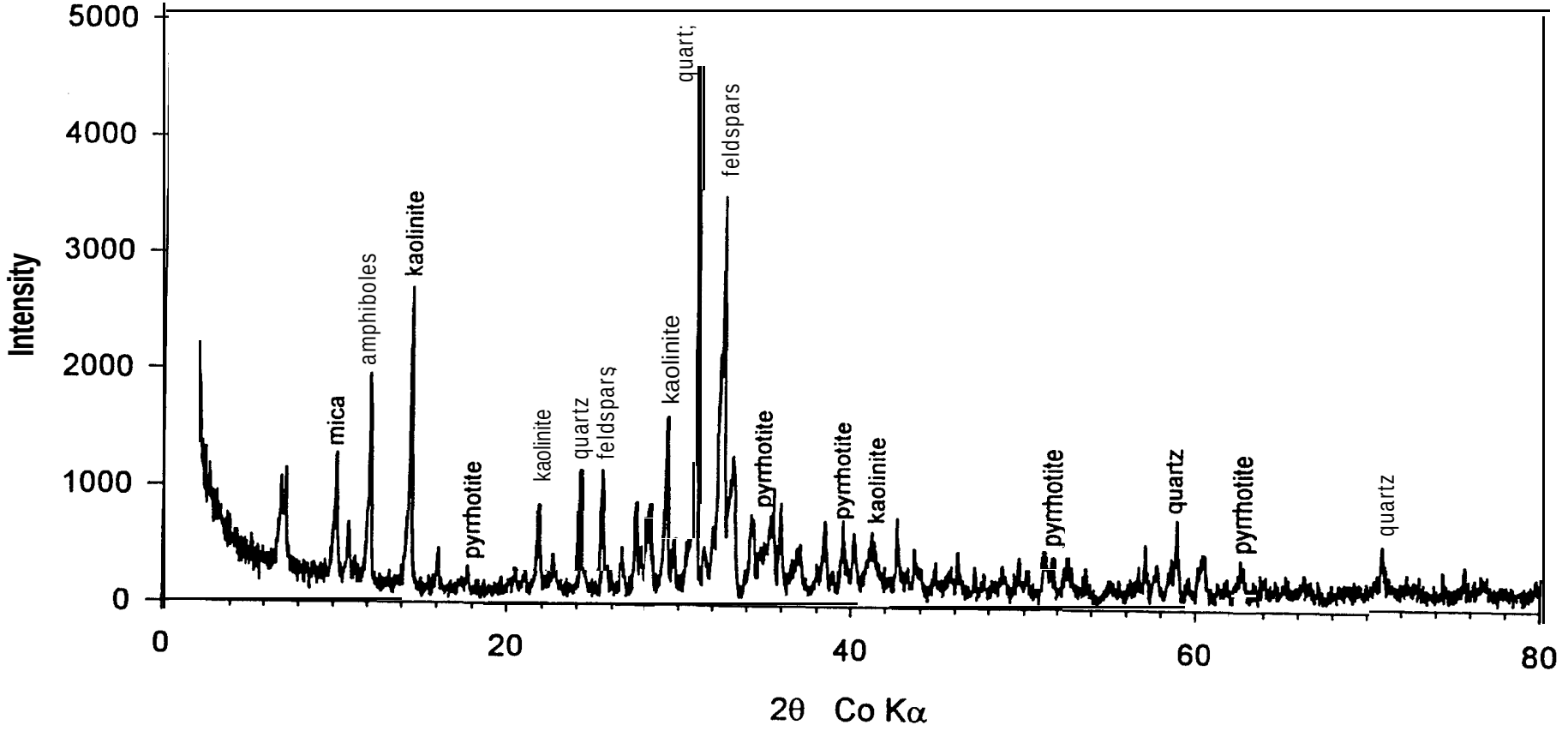

Figure 3.54 X-ray diffractogram of unoxidized resuspended tailings in 60 cm water cover stirred at 140 rpm (40 cm above tailings surface)

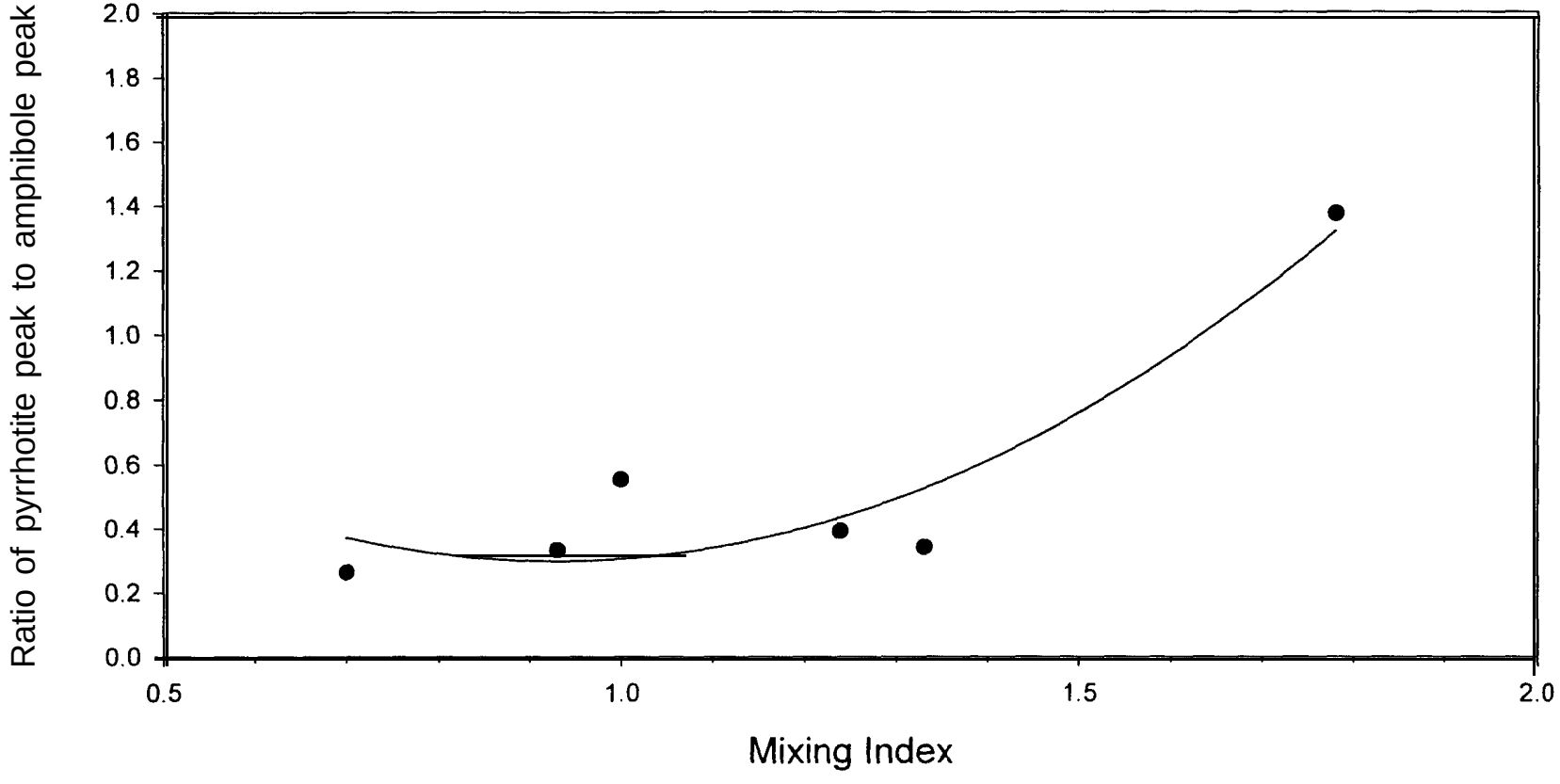

Figure 3.55 Ratio of pyrrhotite to amphibole peak intensities versus mixing index

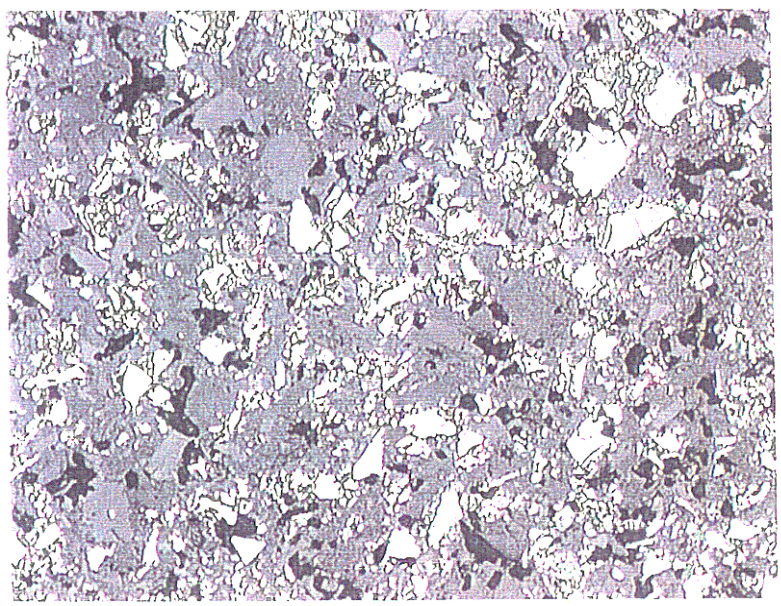

Figure 3.56 Optical photograph of surface of tailings in 80 cm water cover stirred at 140 rpm

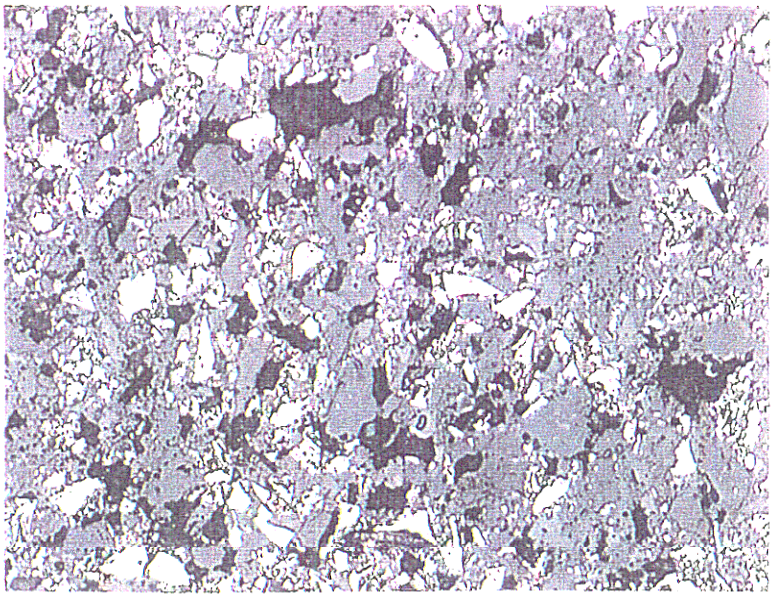

Figure 3.57 Optical photograph of surface of tailings in static 80 cm water cover

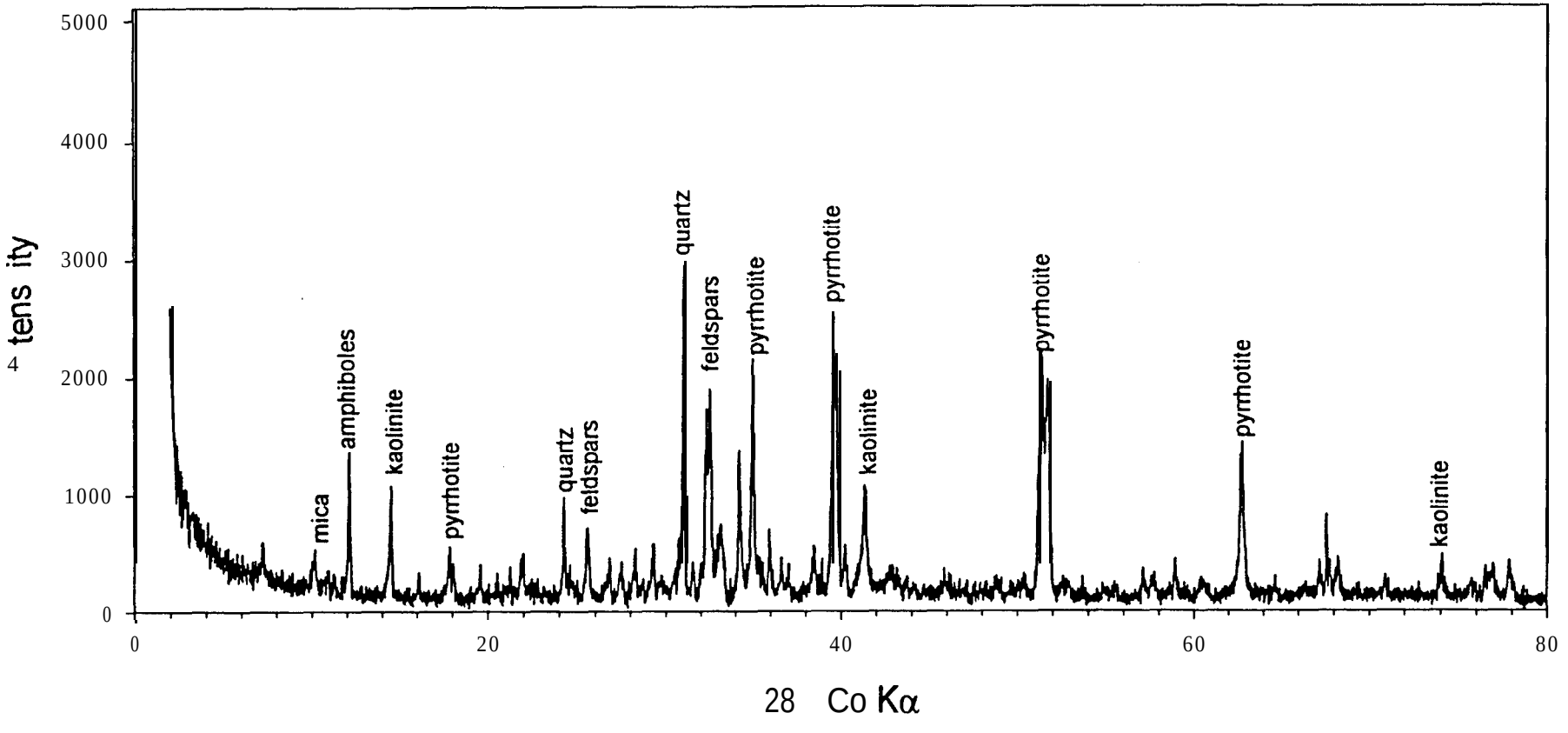

Figure 3.58 X-ray diffractogram of surface of undisturbed tailings underlying 80 cm water cover stirred at 170 rpm

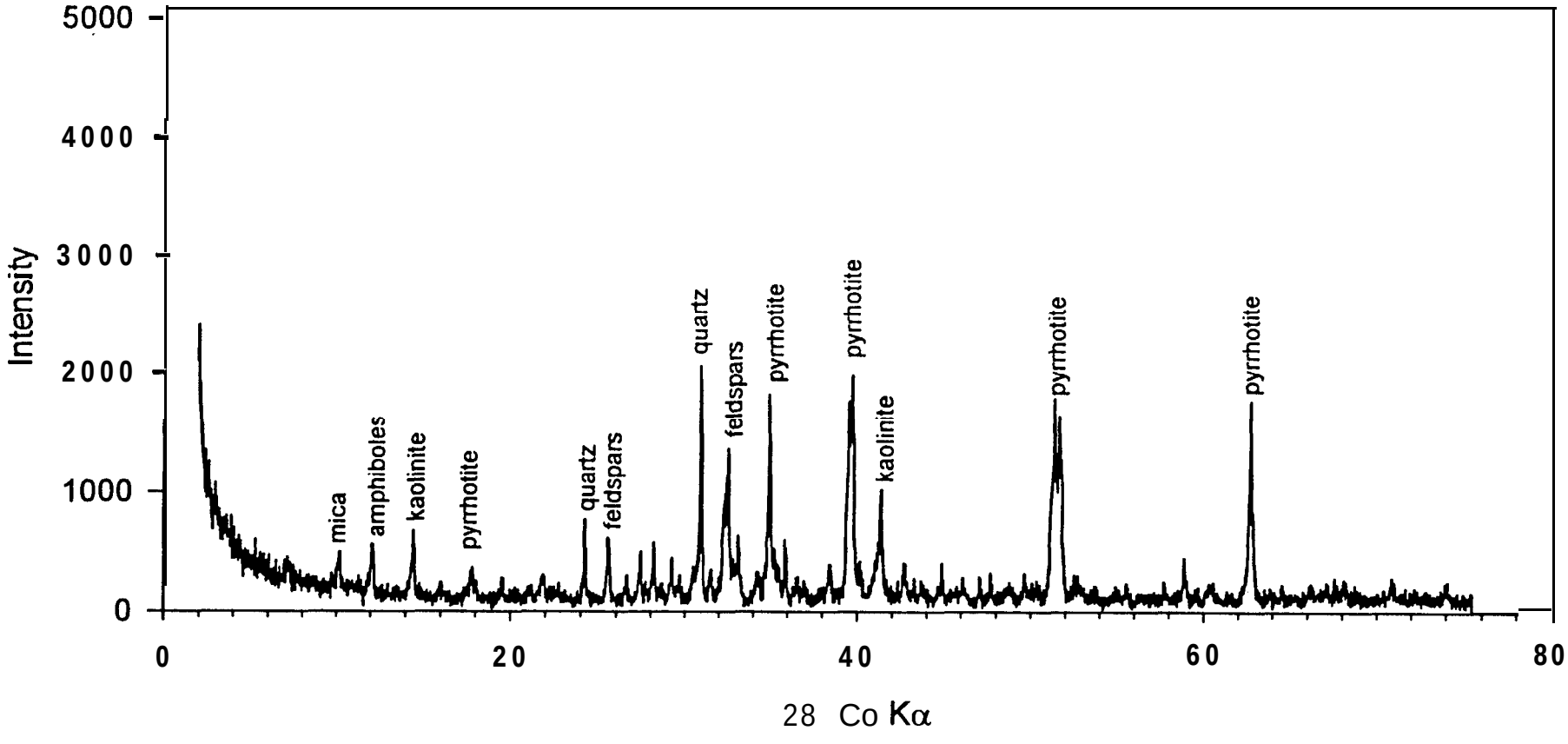

Figure 3.59 X-ray diffractogram of surface of undisturbed tailings underlying 80 cm water cover stirred at 140 rpm

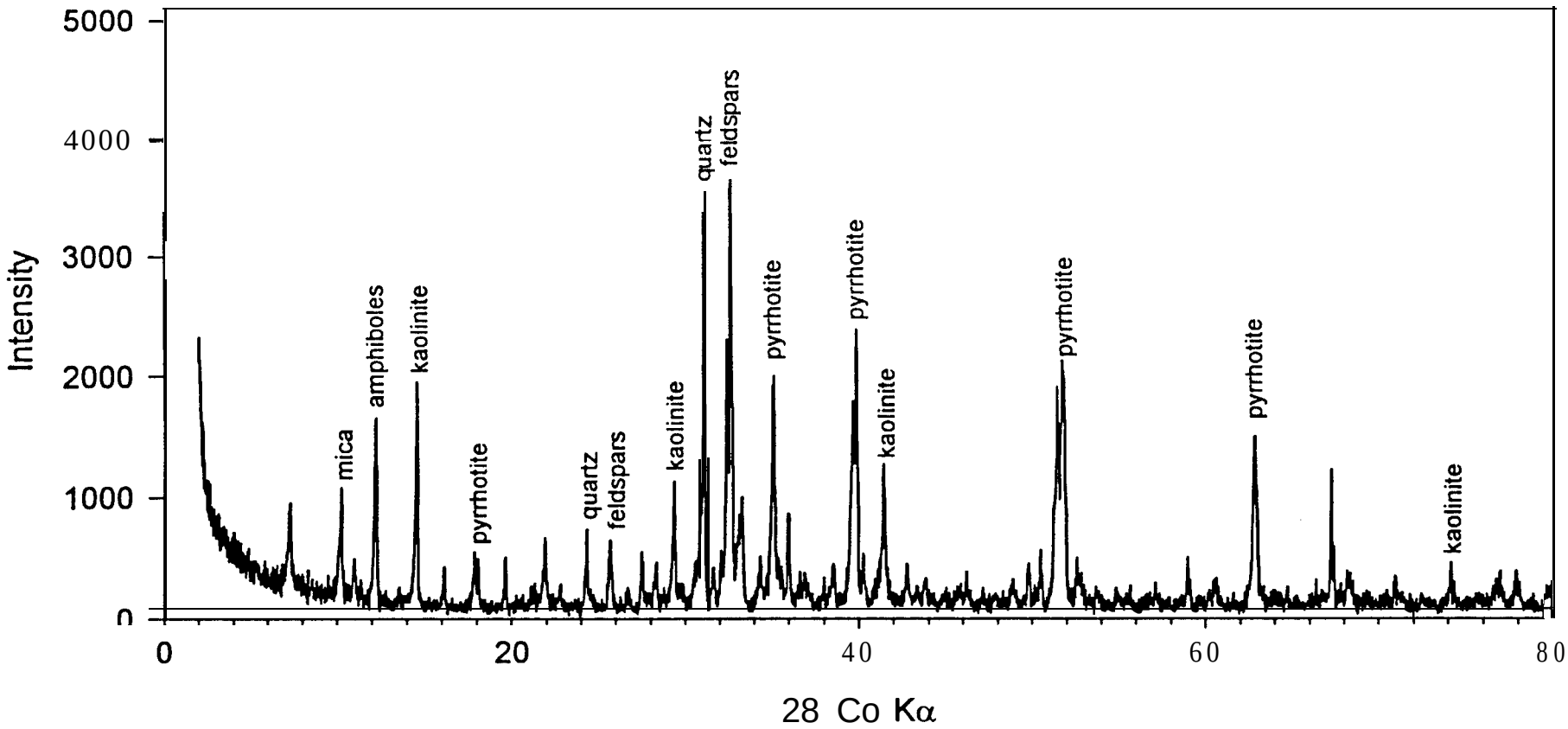

Figure 3.60 X-ray diffractogram of surface of undisturbed tailings underlying 60 cm water cover stirred at 170 rpm

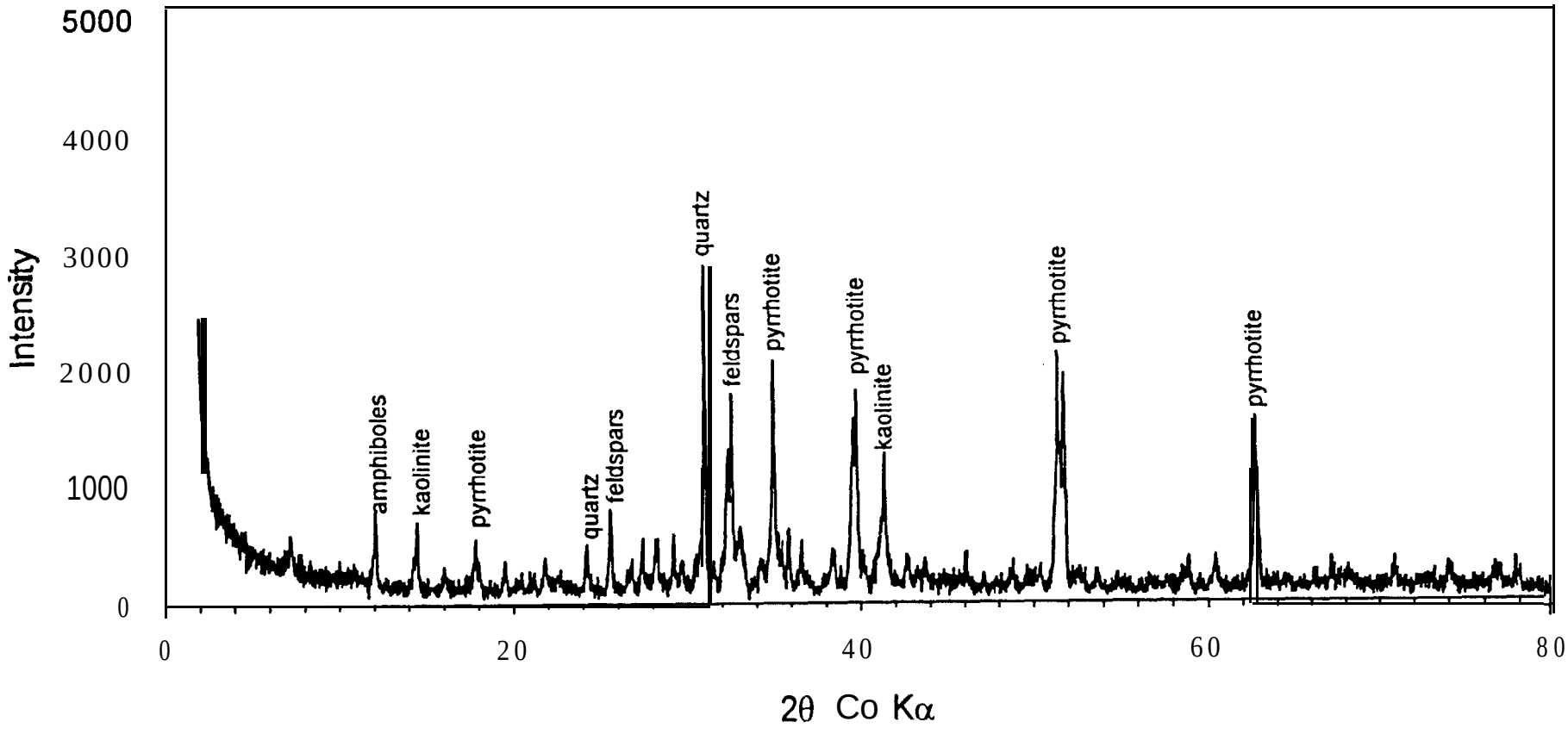

Figure 3.61 X-ray diffractogram of surface of undisturbed tailings underlying 45 cm water cover stirred at 170 rpm

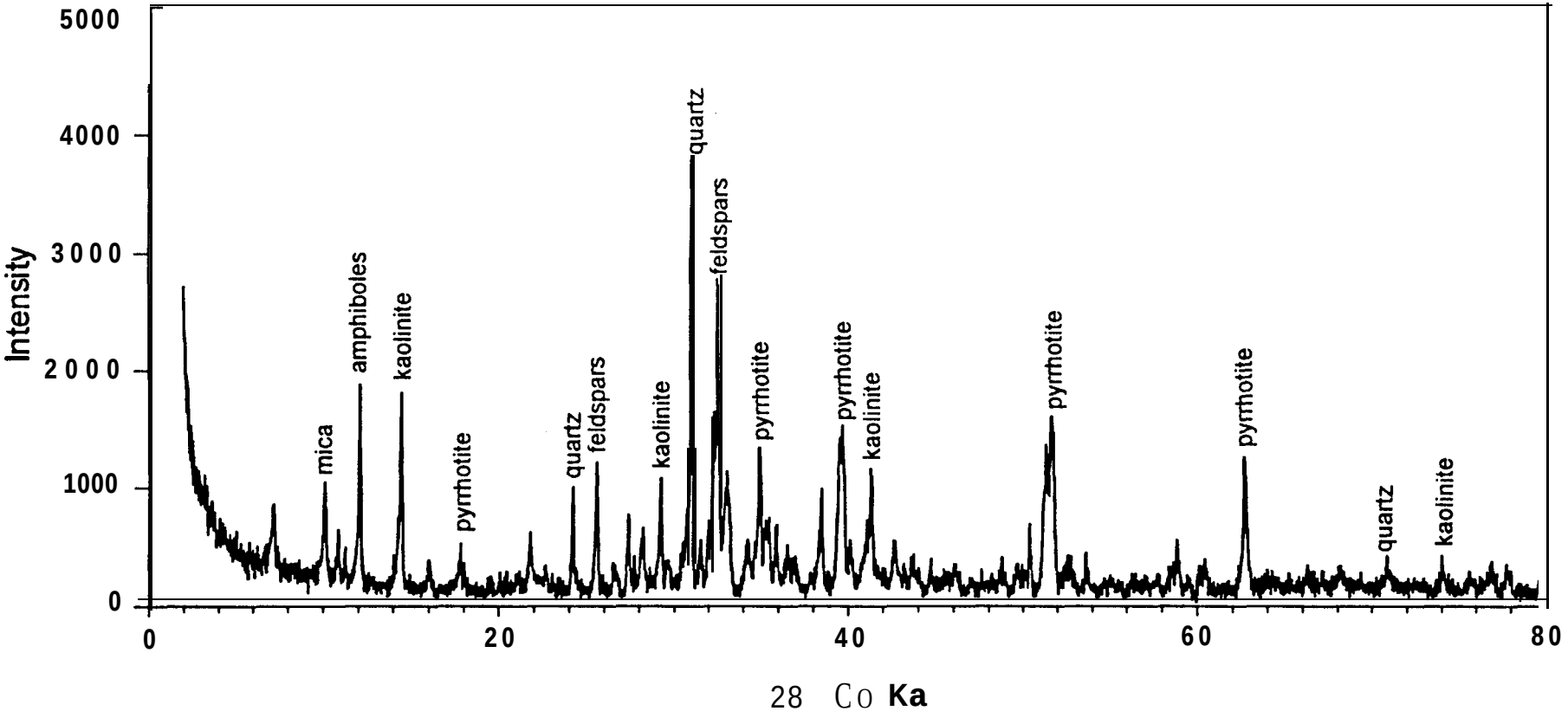

Figure 3.62 X-ray diffractogram of surface of undisturbed tailings underlying static 80 cm water cover

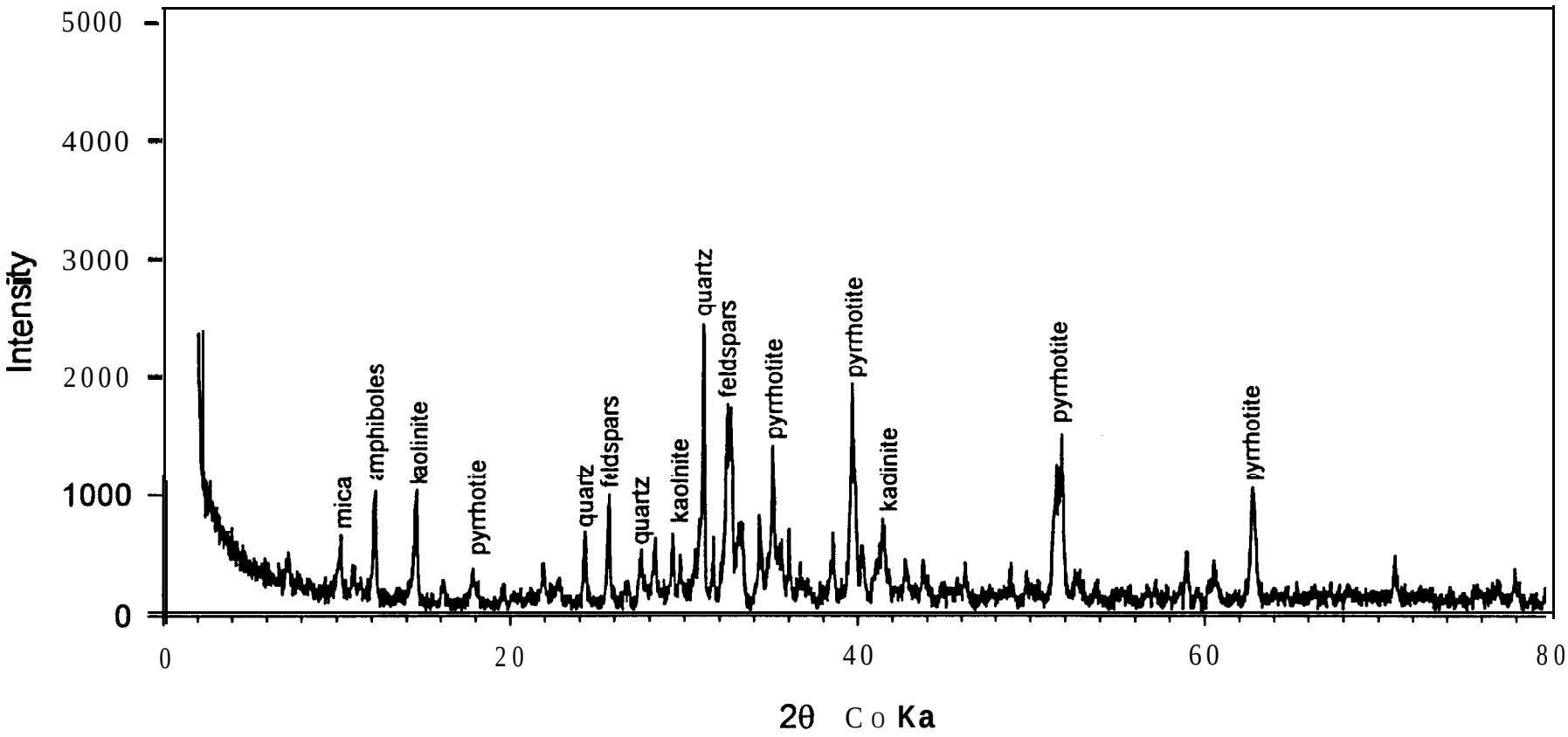

Figure 3.63 X-ray diffractogram of surface of undisturbed tailings underlying static 45 cm water cover

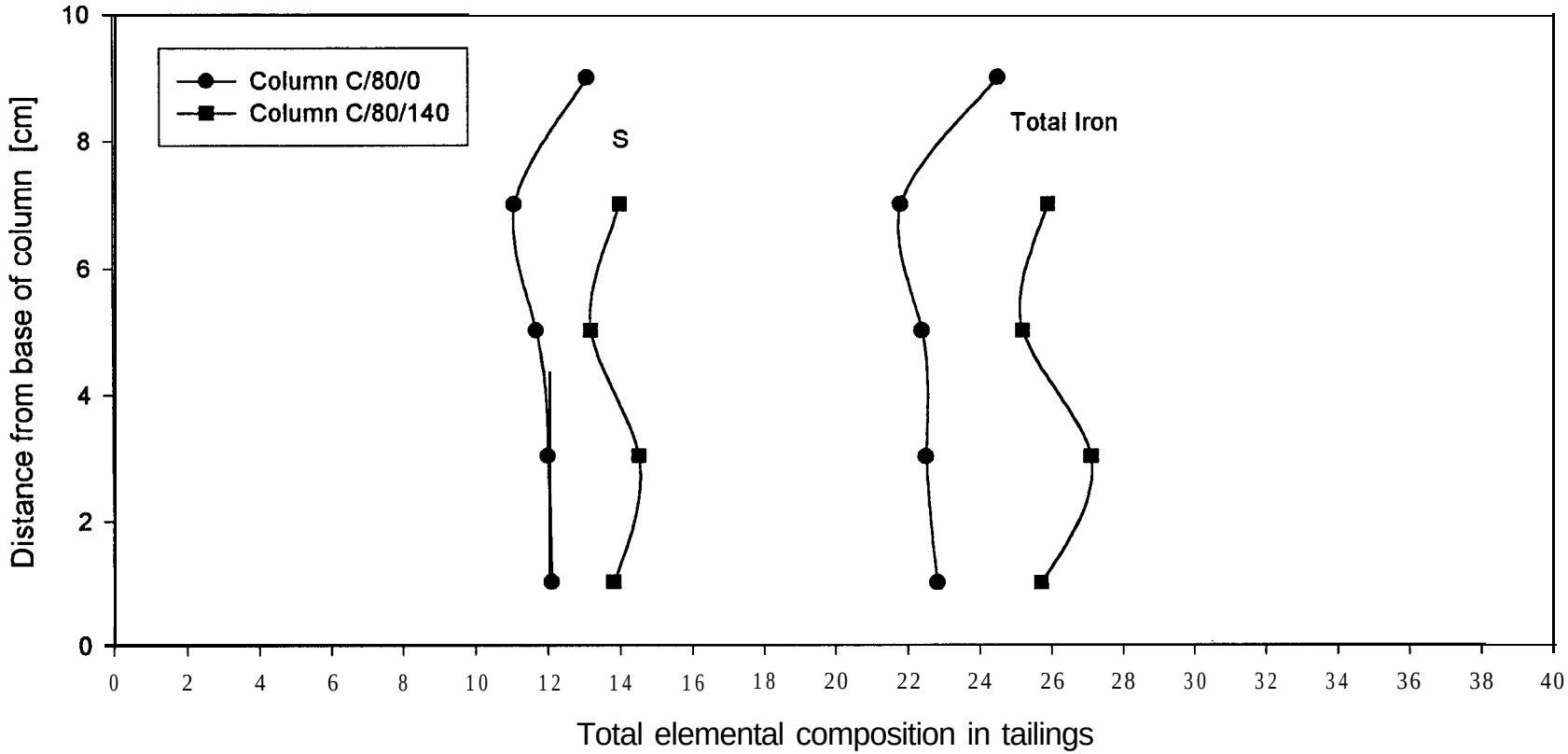

Figure 3.64 Total Fe and S profiles in undisturbed tailings below static 80 cm water cover and cover stirred at 140 rpm

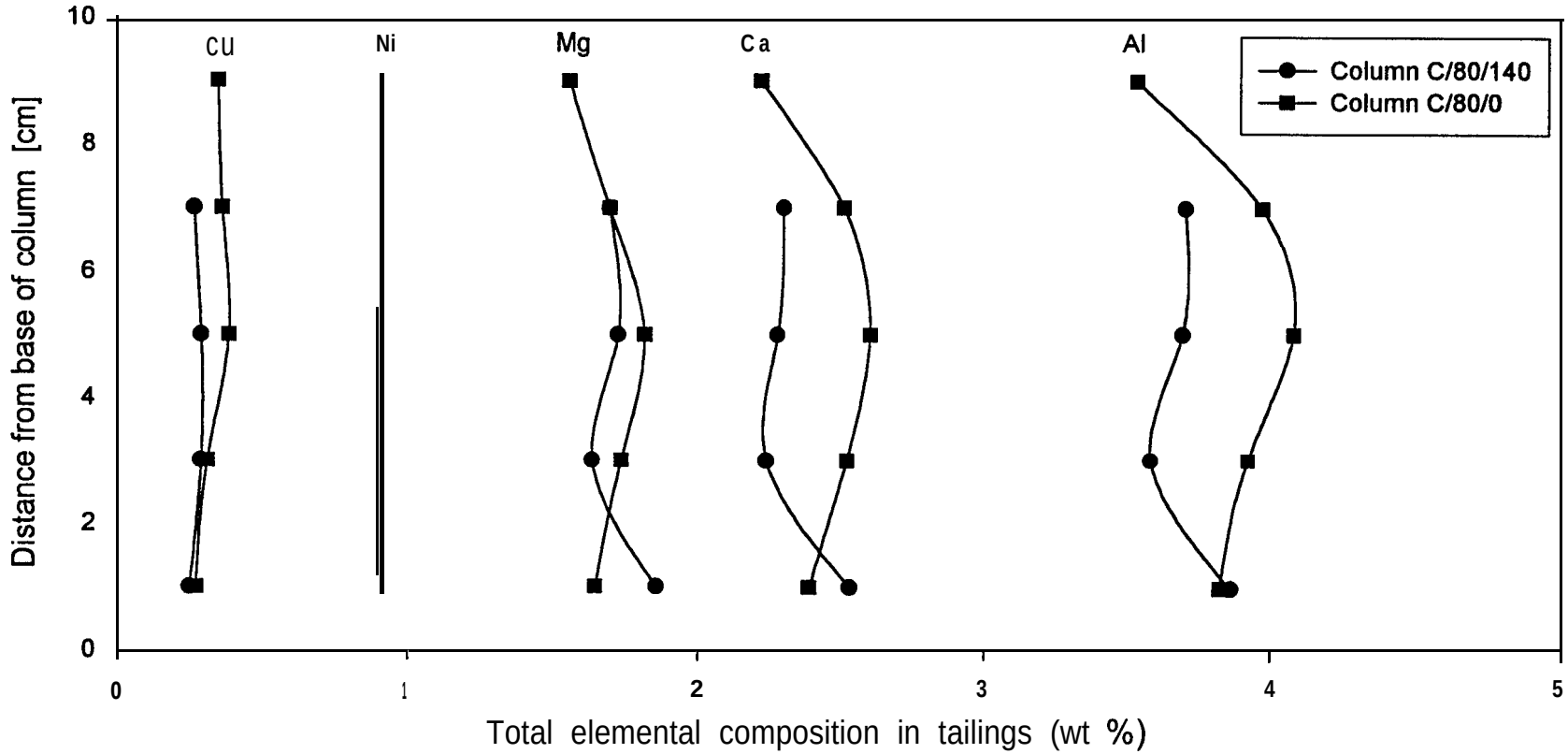

Figure 3.65 Total Cu, Ni, Aℓ, Mg and Ca profiles in undisturbed tailings below static 80 cm water cover and cover stirred at 140 rpm

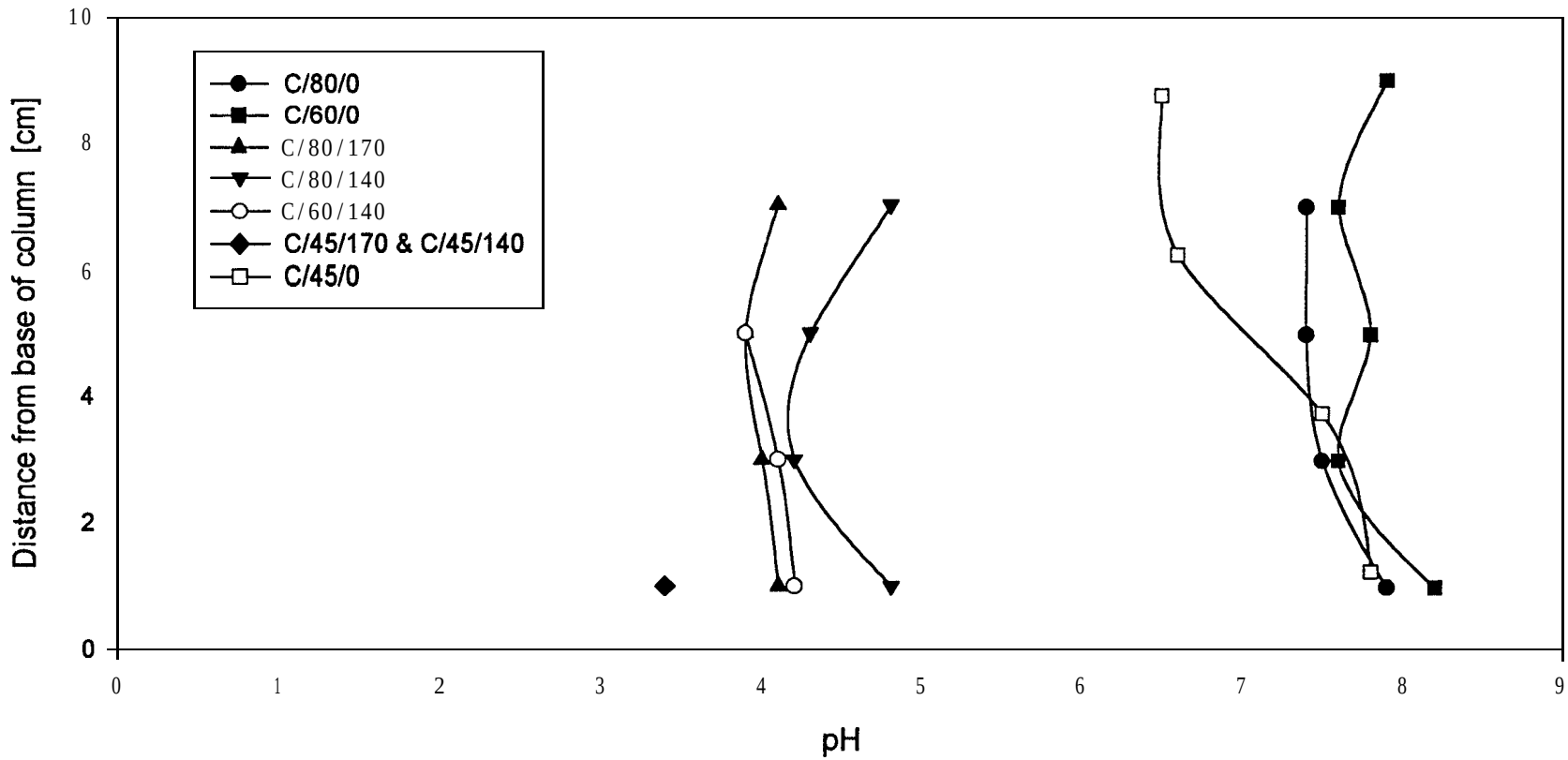

Figure 3.66 pH profile for tailings pore water

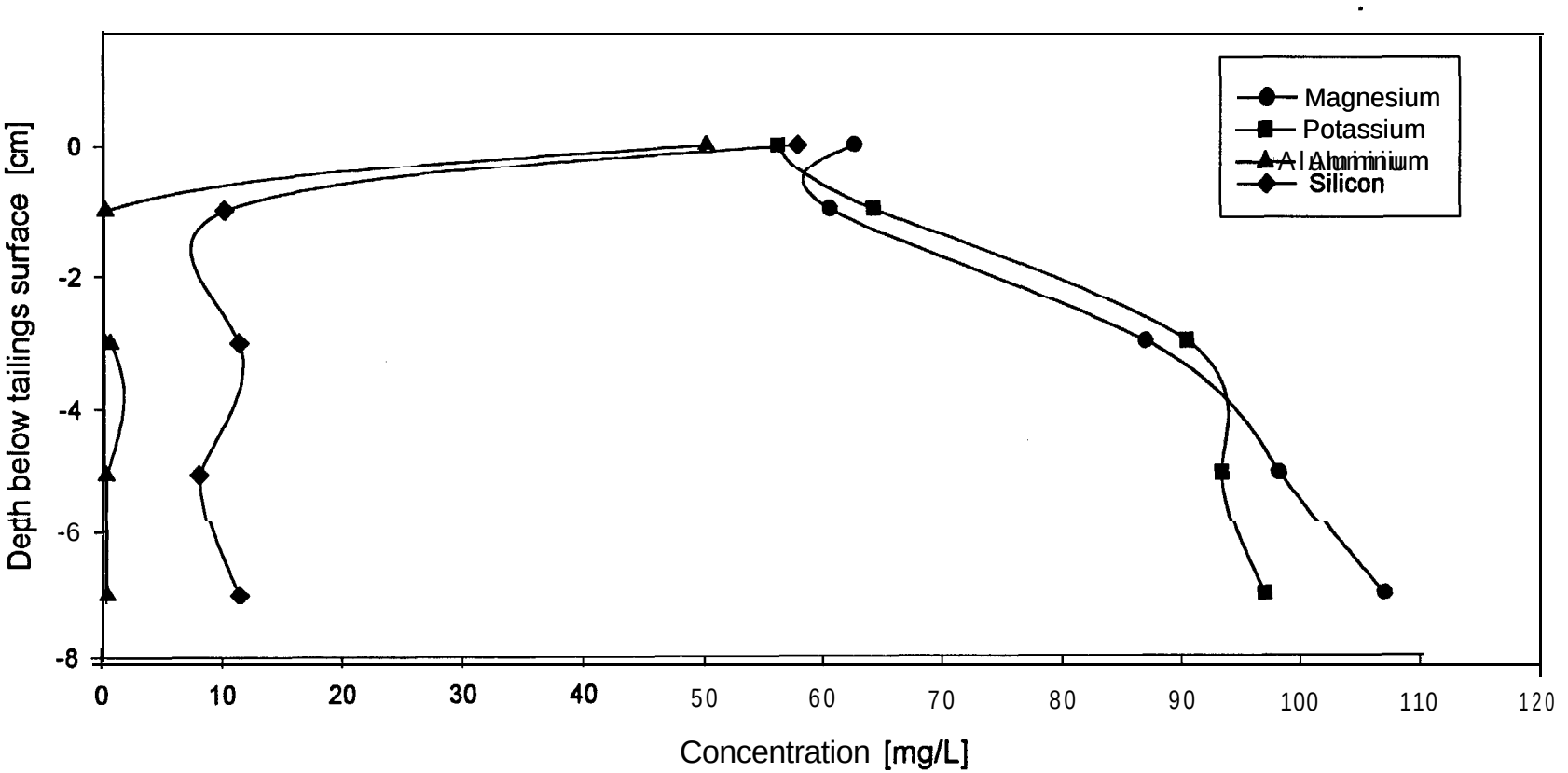

Figure 3.67 Mg, K, Aℓ and Si concentration profiles for tailings pore water below 80 cm water cover stirred at 140 rpm

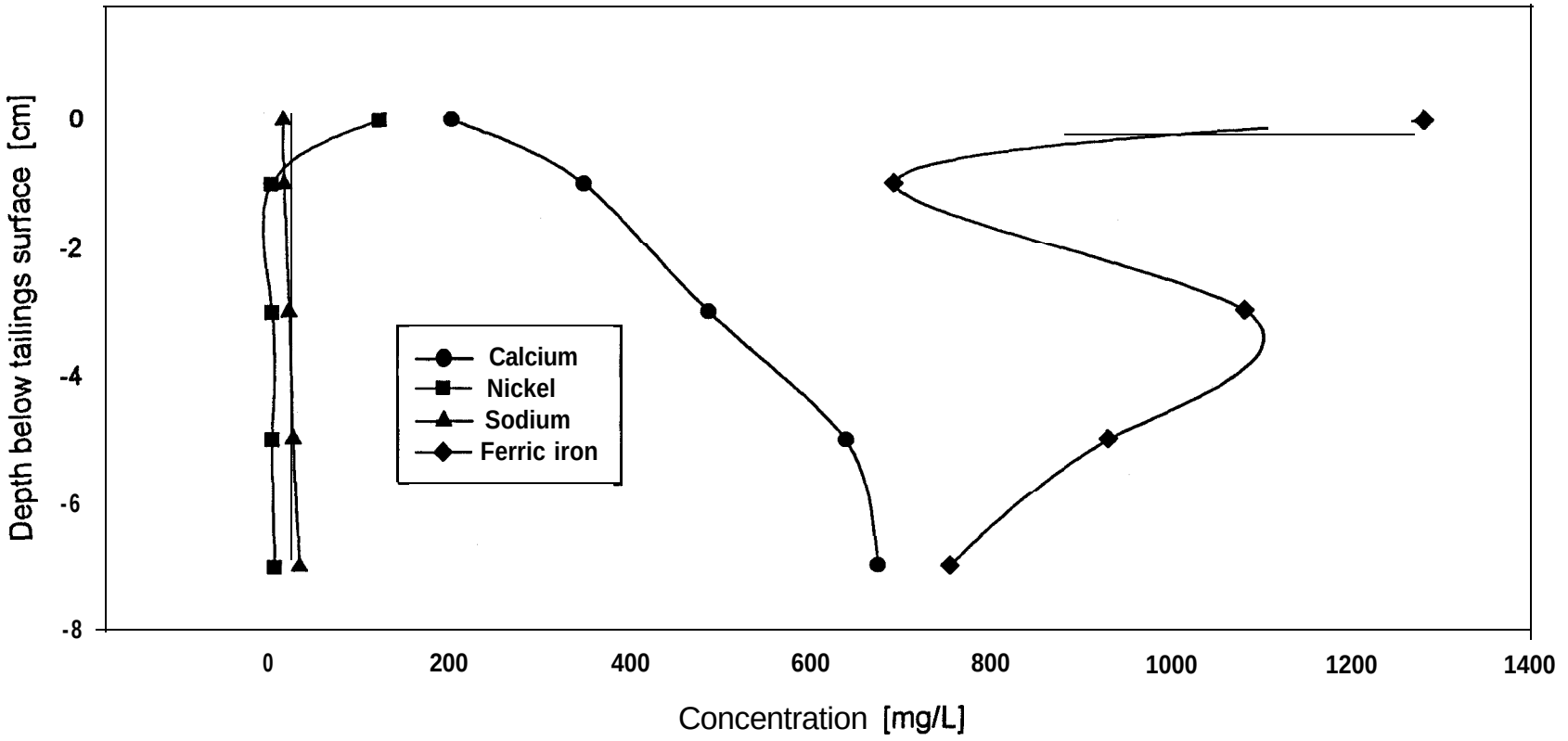

Figure 3.68 Ca, Ni, Na and Fe^{3+} concentration profiles for tailings pore water below 80 cm water cover stirred at 140 rpm

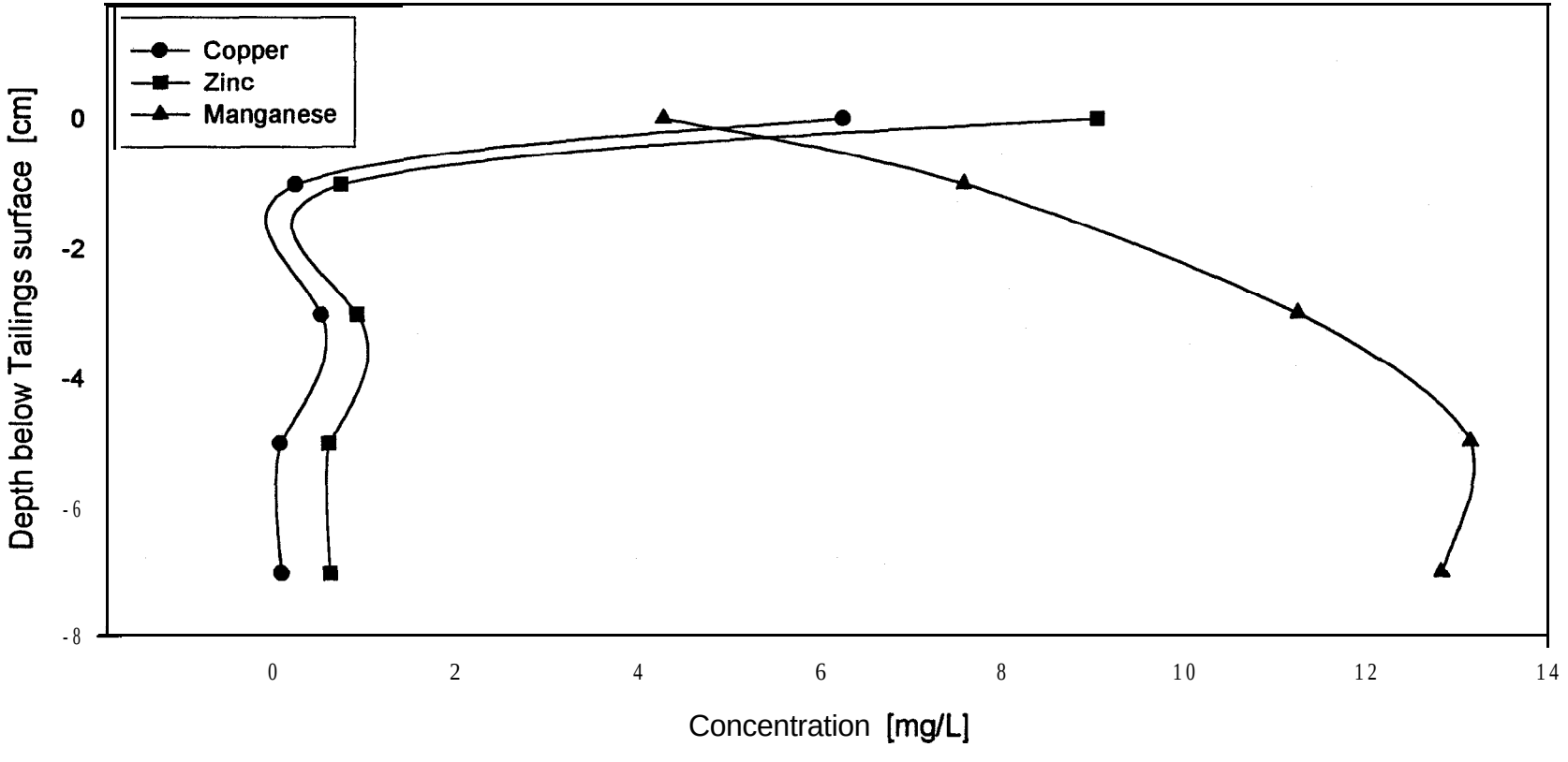

Figure 3.69 Cu, Zn and Mn concentration profiles for tailings pore water below 80 cm water cover stirred at 140 rpm

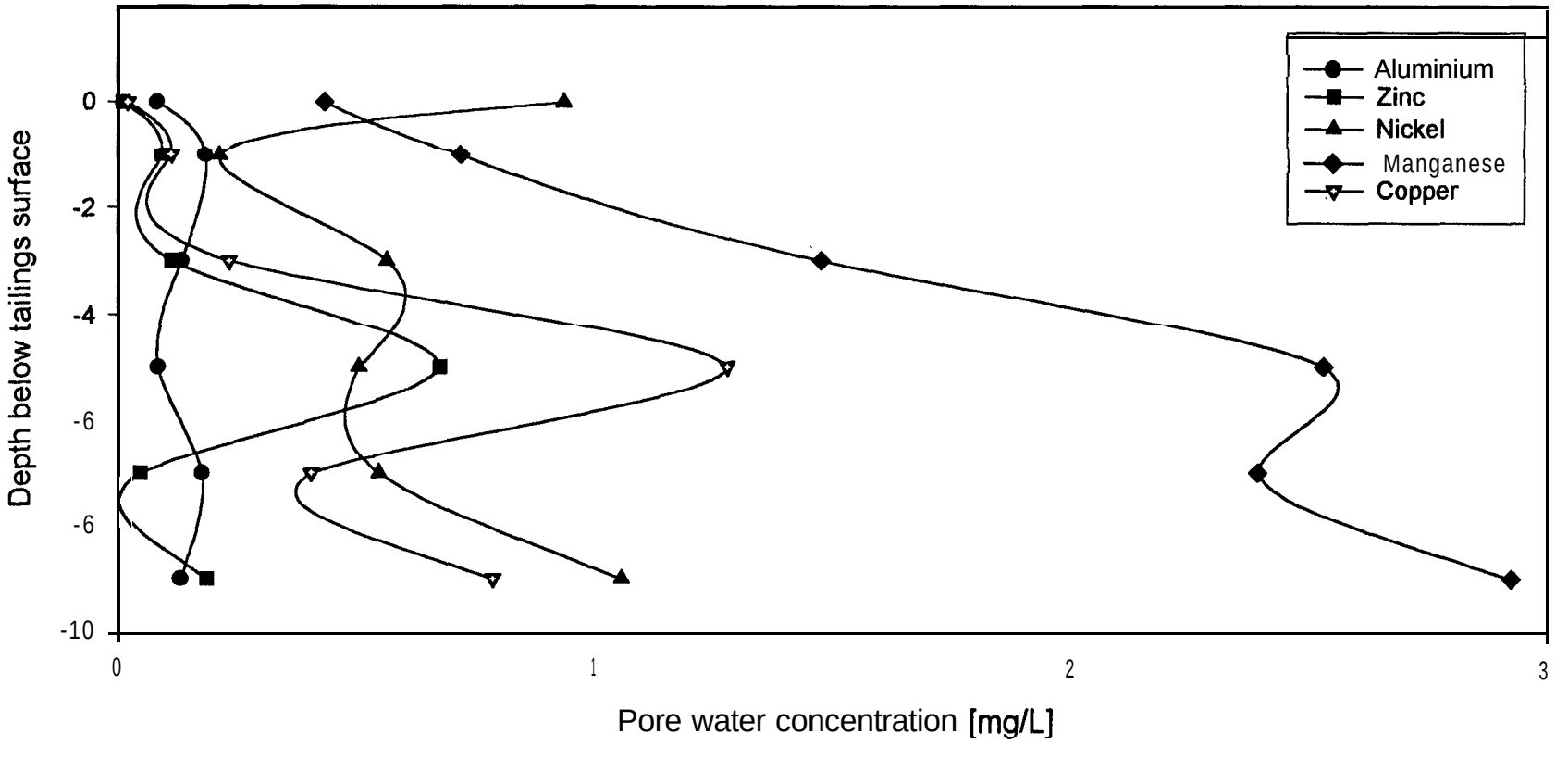

Figure 3.70 A!, Zn, Ni, Mn and Cu concentration profiles for tailings pore water below static 80 cm water cover

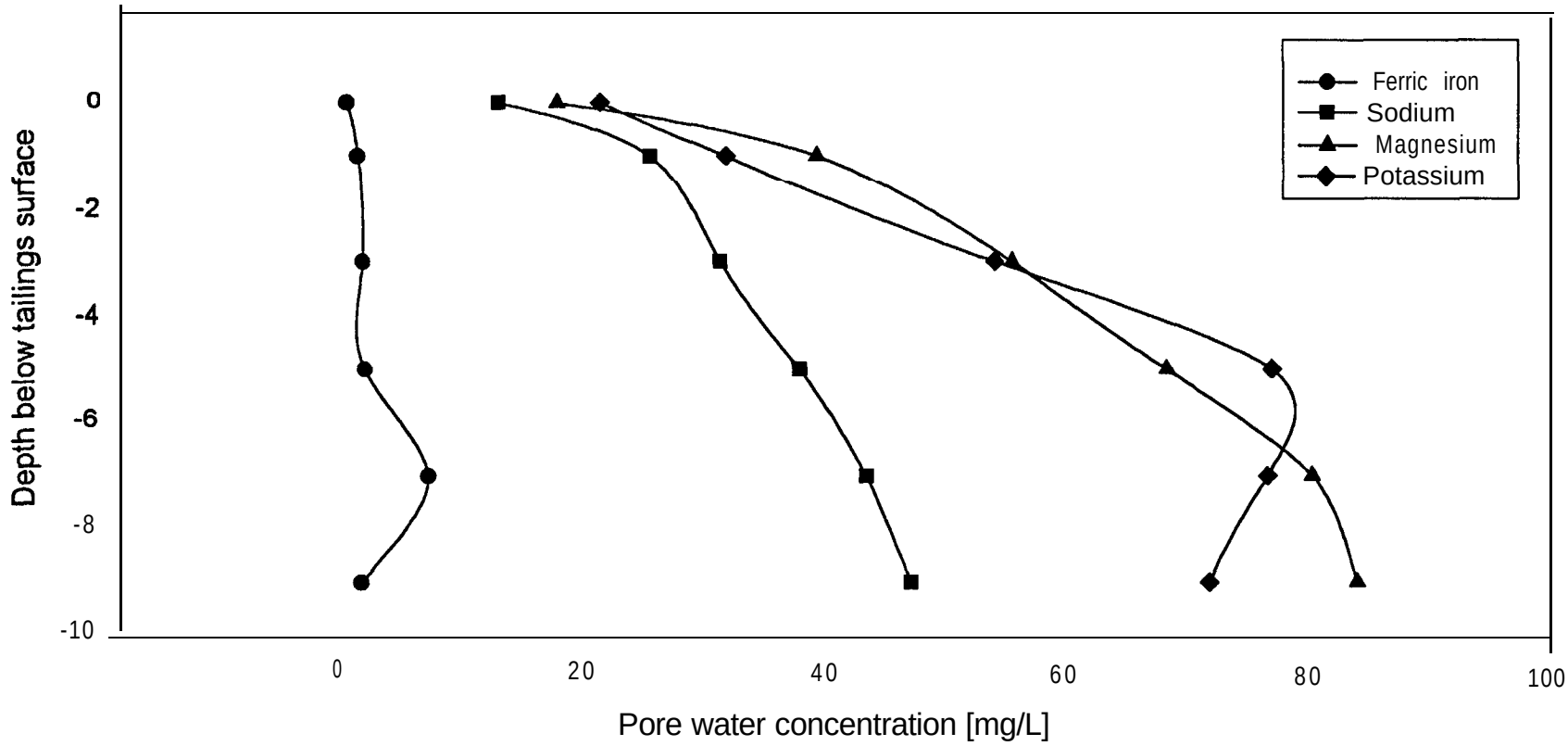

Figure 3.71 Fe^{3+}, Na, Mg and K concentration profiles for tailings pore water below static 80 cm water cover

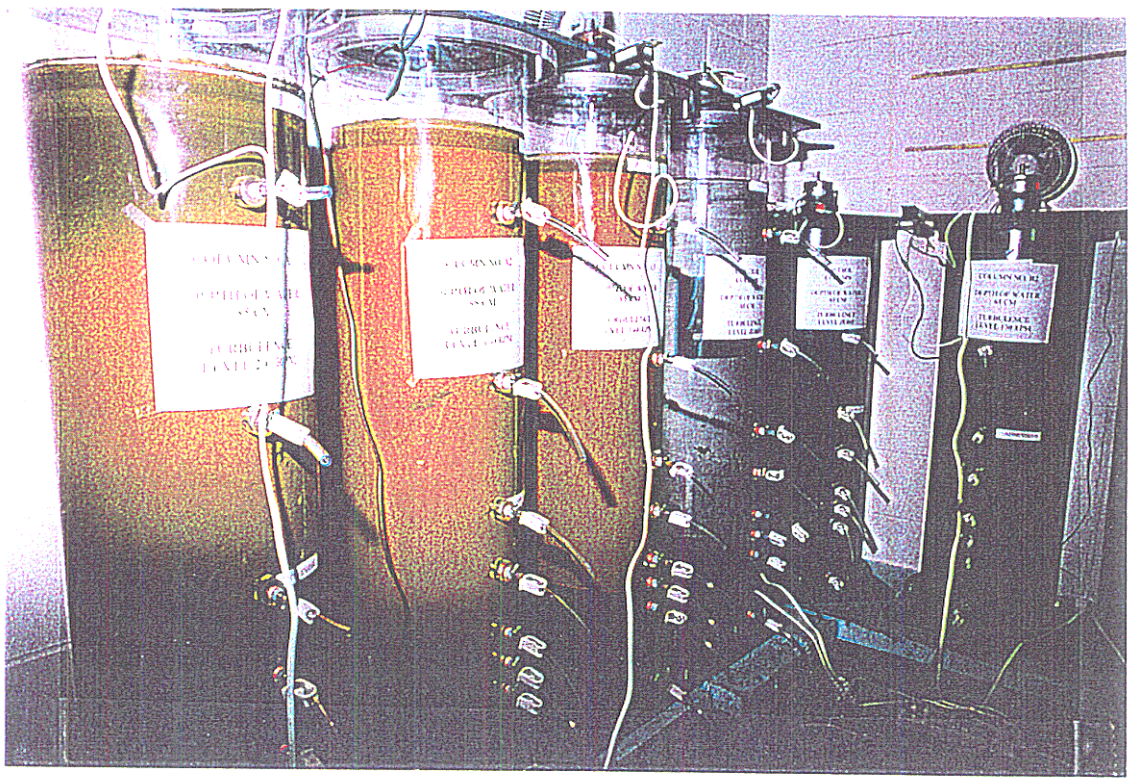

Figure 3.72 Photograph of Plexiglas columns showing yellowish brown film of suspended particle coating on side walls

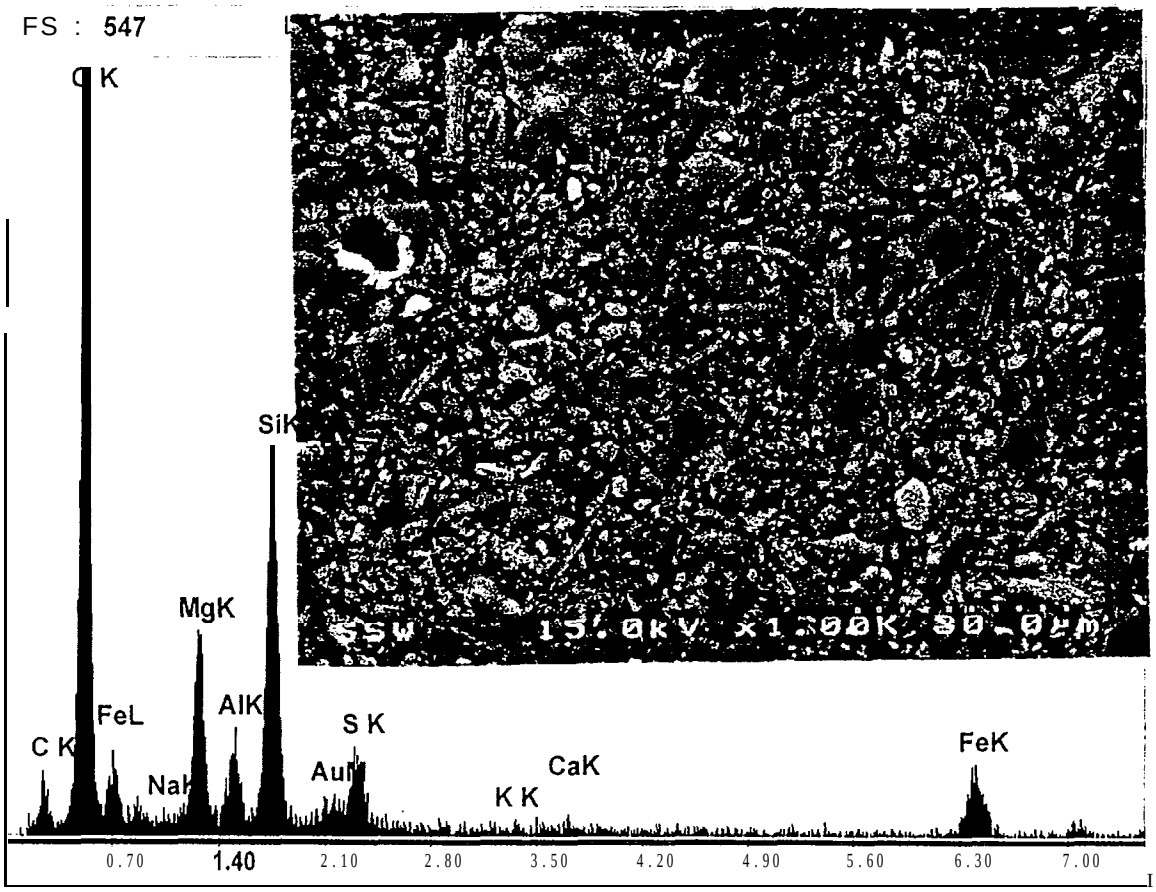

Element	Wt %	At %
C K	15.15	22.24
O K	55.06	60.67
NaK	0.30	0.23
MgK	7.16	5.19
AlK	2.77	1.81
SiK	10.88	6.83
AuM	0.94	0.08
SK	1.73	0.95
KK	0.26	0.12
CaK	0.45	0.20
FeK	5.29	1.67
Total	100.00	100.00

Figure 3.73 Scanning electron photomicrograph of precipitate in 60 cm water cover stirred at 200 rpm indicating the presence of iron oxyhydrode

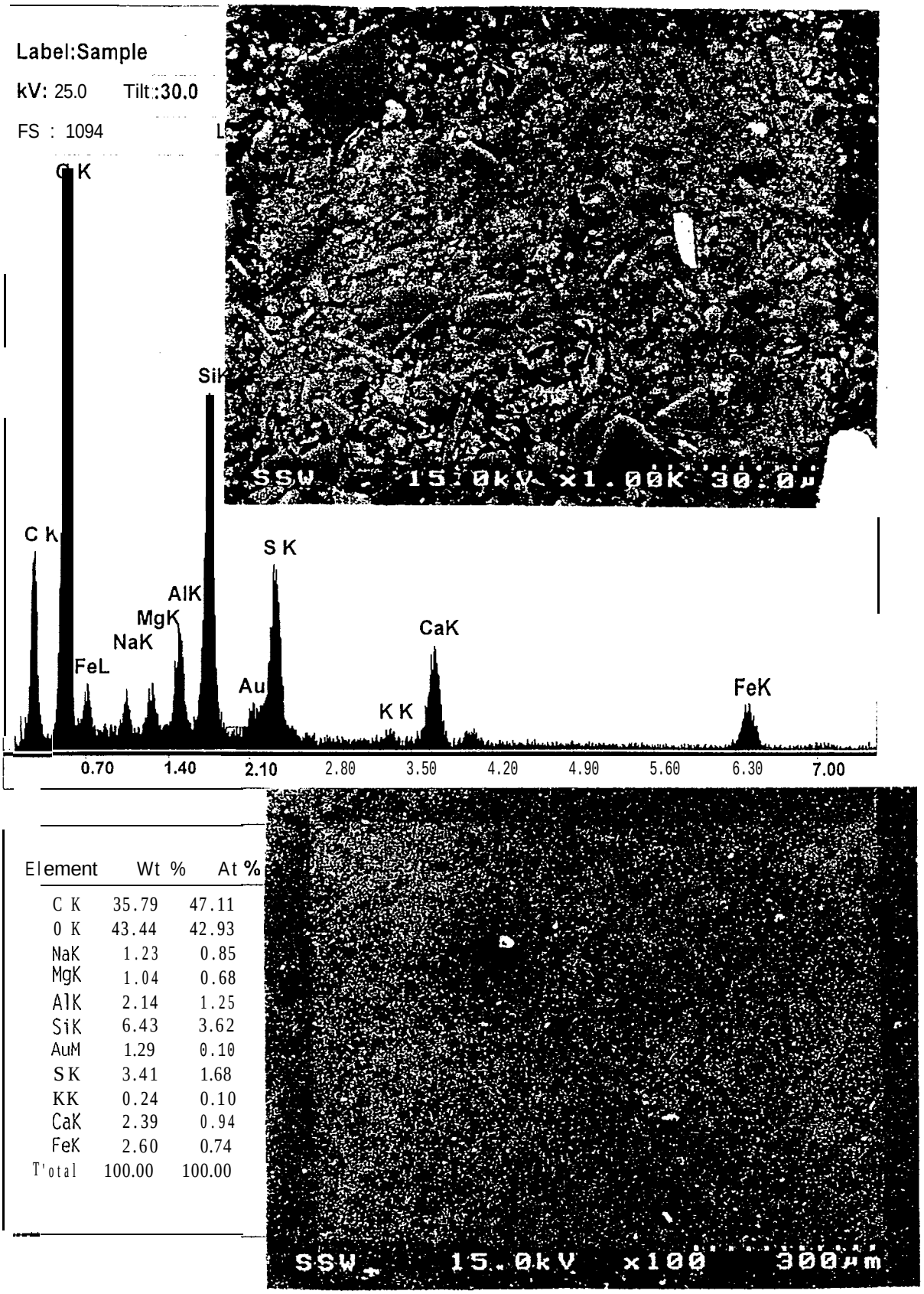

Element	Wt %	At %
C K	35.79	47.11
O K	43.44	42.93
NaK	1.23	0.85
MgK	1.04	0.68
AlK	2.14	1.25
SiK	6.43	3.62
AuM	1.29	0.10
S K	3.41	1.68
K K	0.24	0.10
CaK	2.39	0.94
FeK	2.60	0.74
Total	100.00	100.00

Figure 3.74 Scanning electron photomicrograph of precipitate in 60 cm water cover stirred at 200 rpm indicating the presence of gypsum

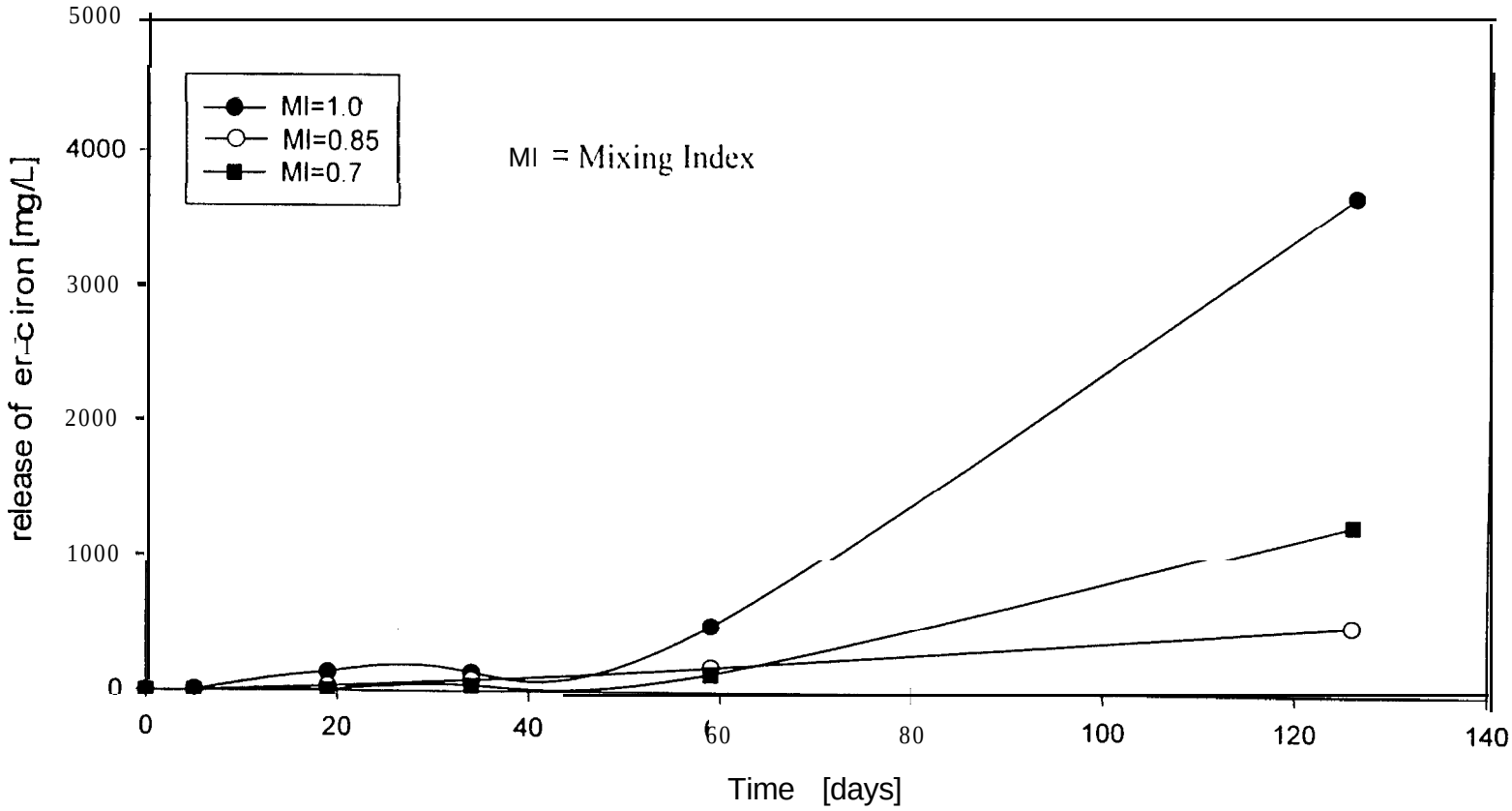

Figure 3.75 Variation of ferric iron concentration in 80 cm water cover

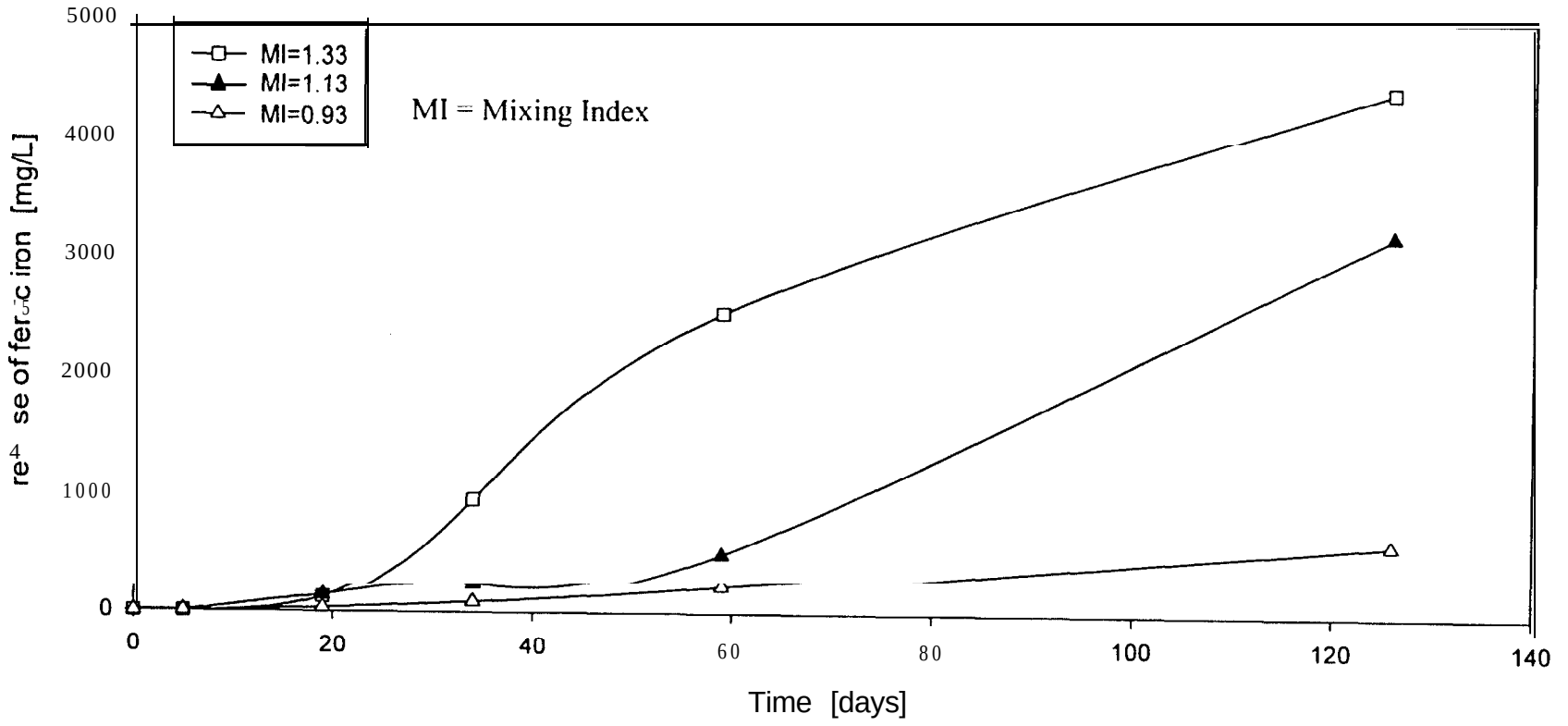

Figure 3.76 Variation of ferric iron concentration in 60 cm water cover

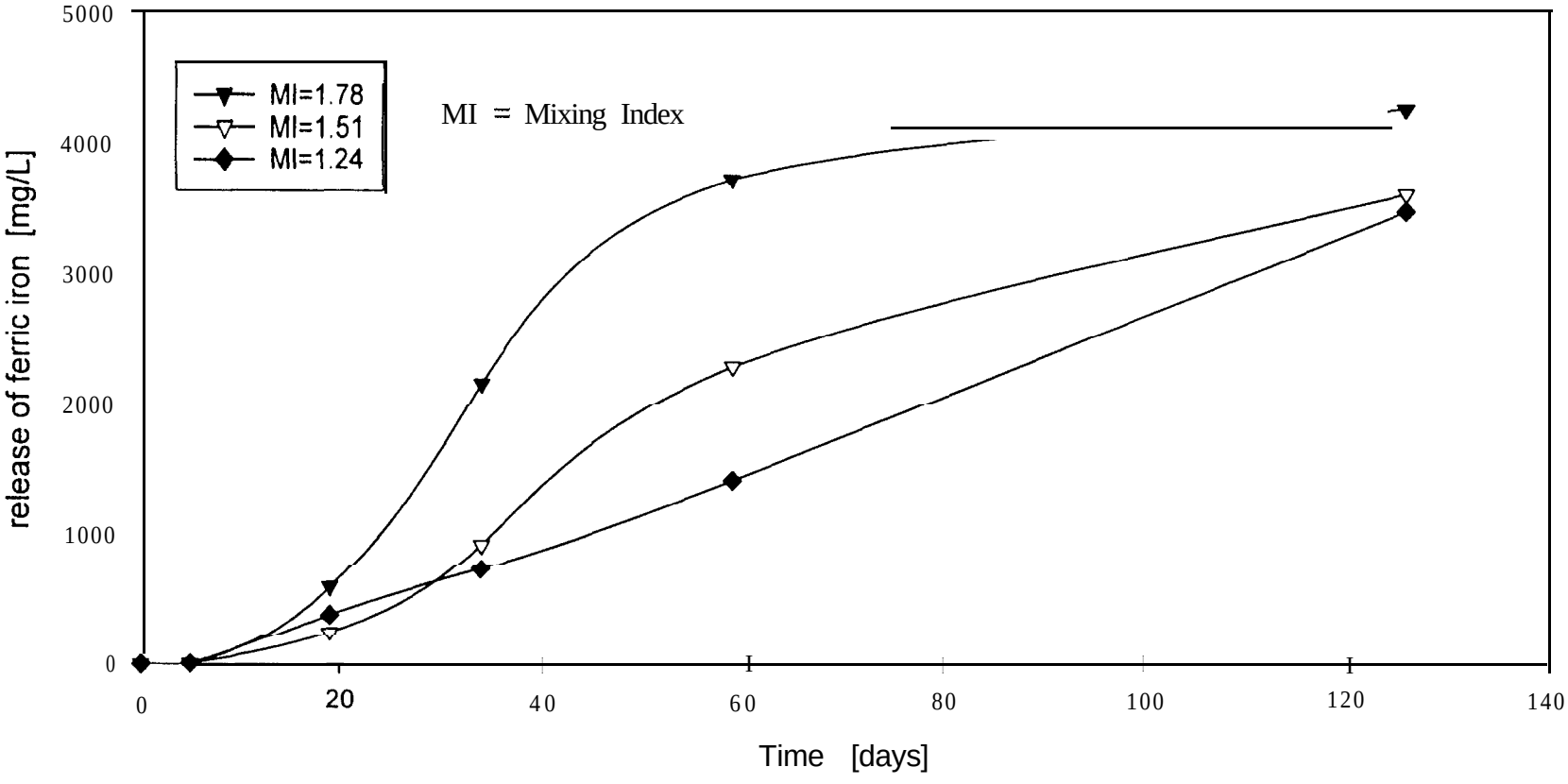

Figure 3.77 Variation of ferric iron concentration in 45 cm water cover

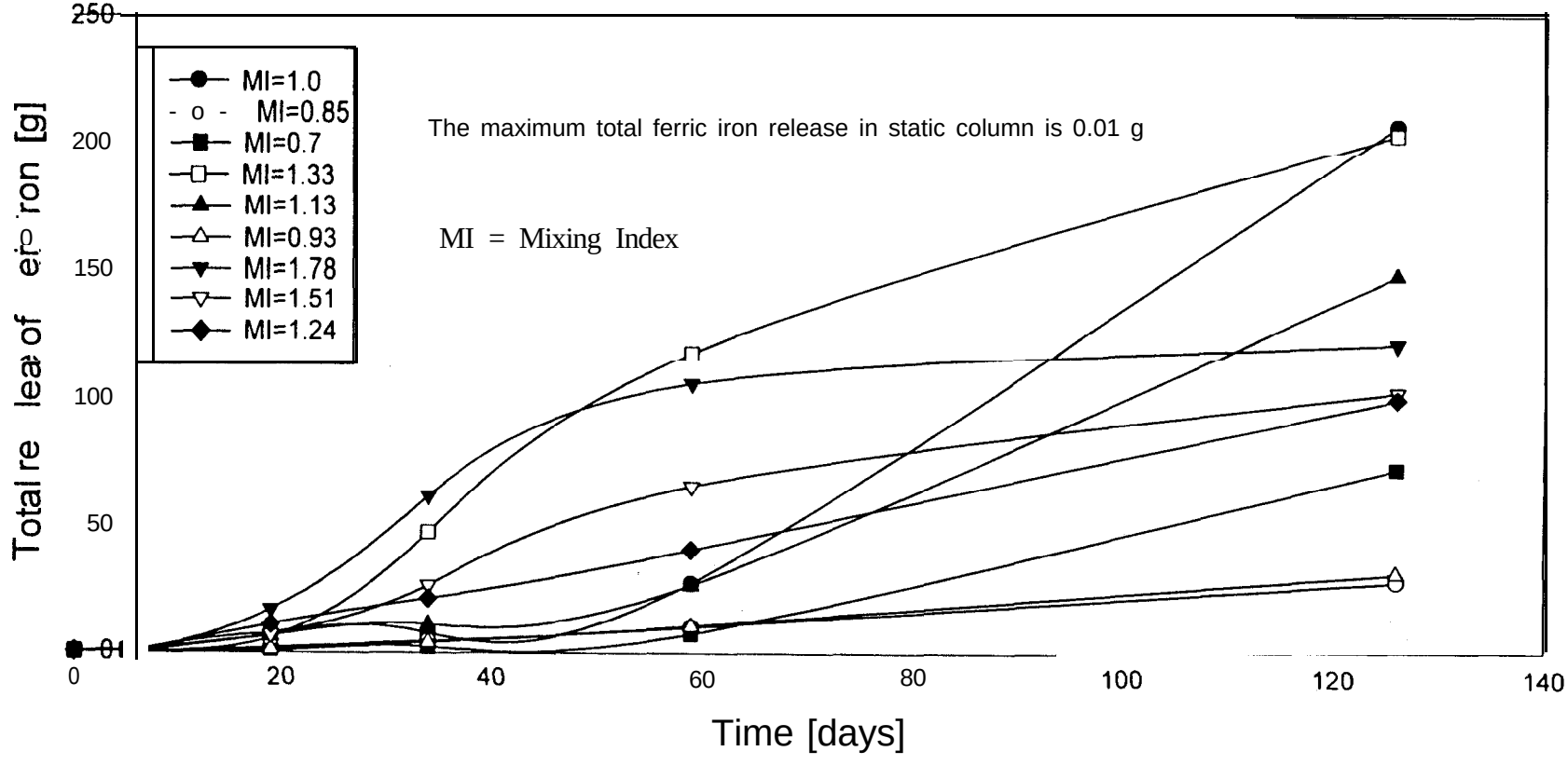

Figure 3.78 Variation of ferric iron release with time and mixing index

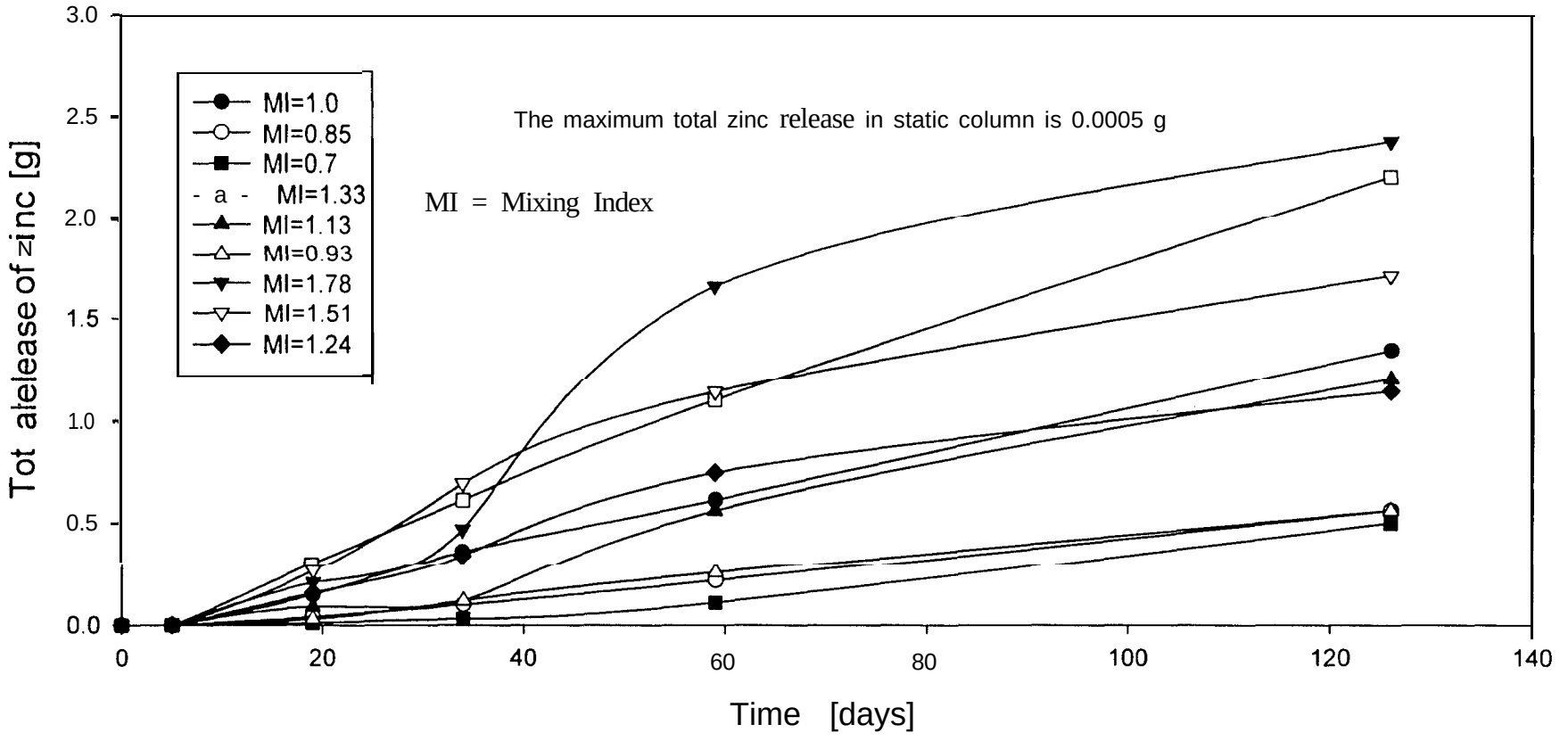

Figure 3.79 Variation of zinc release with time and mixing index

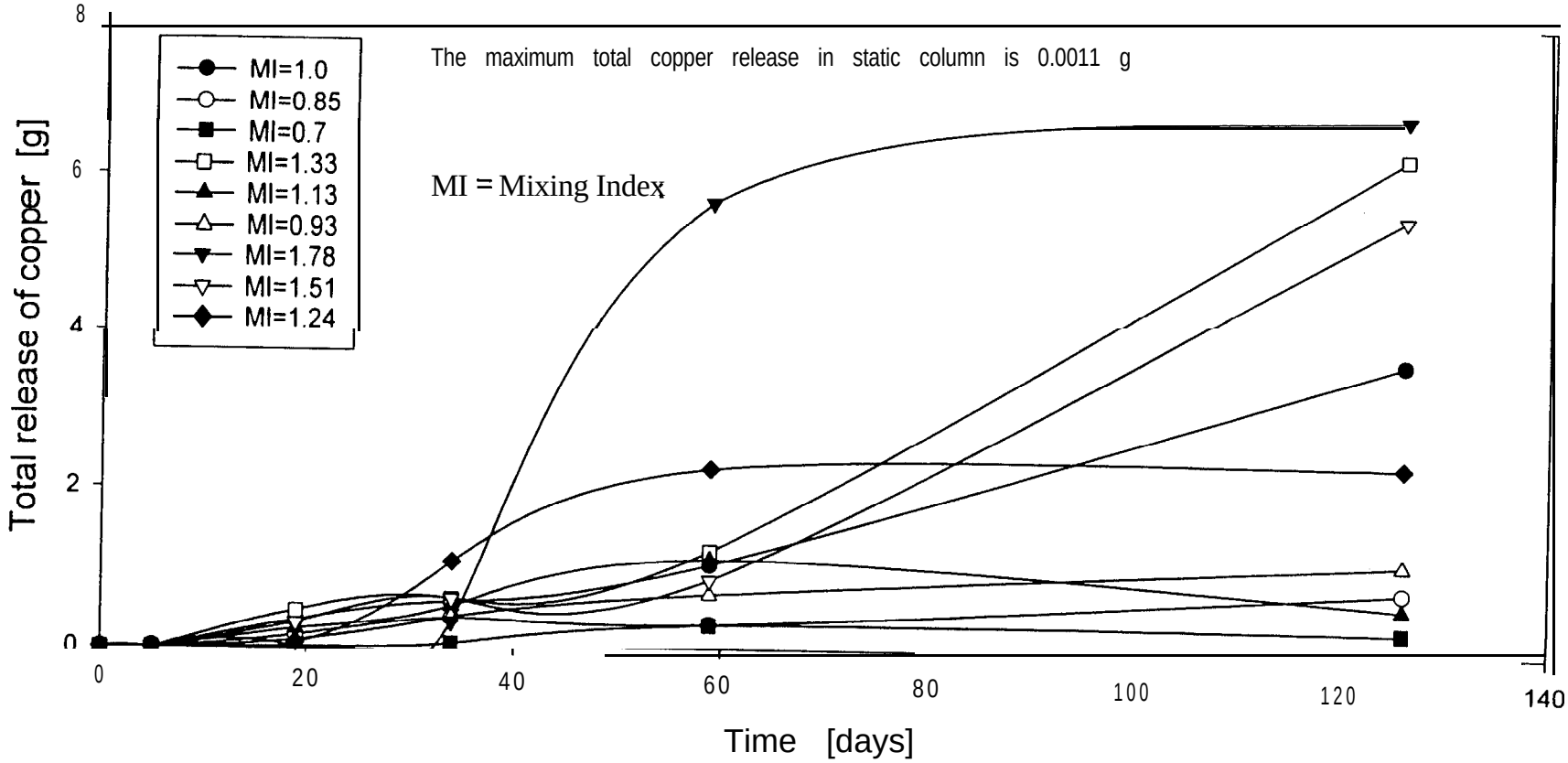

Figure 3.80 Variation of copper release with time and mixing index

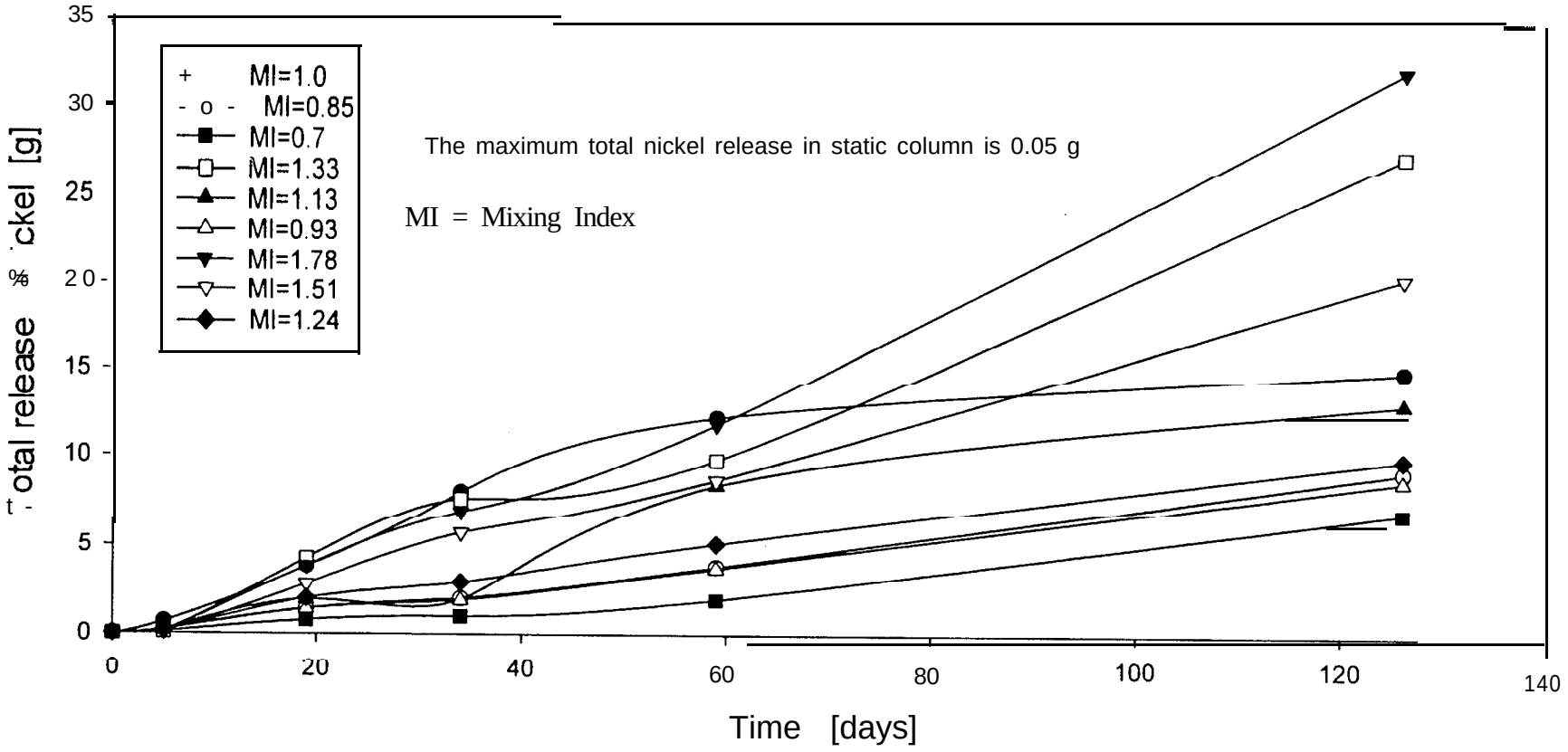

Figure 3.81 Variation of nickel release with time and mixing index

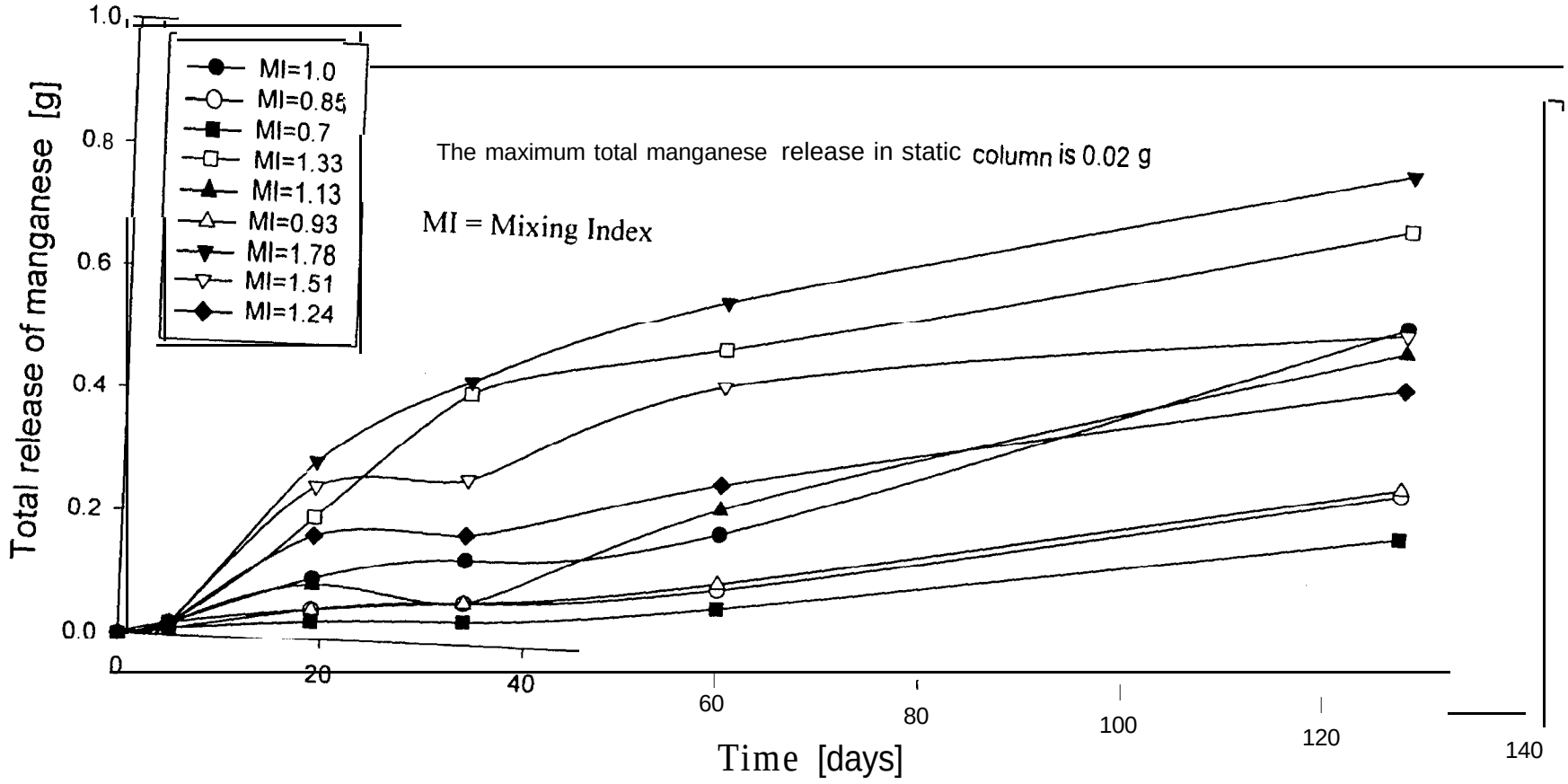

Figure 3.82 Variation of manganese release with time and mixing index

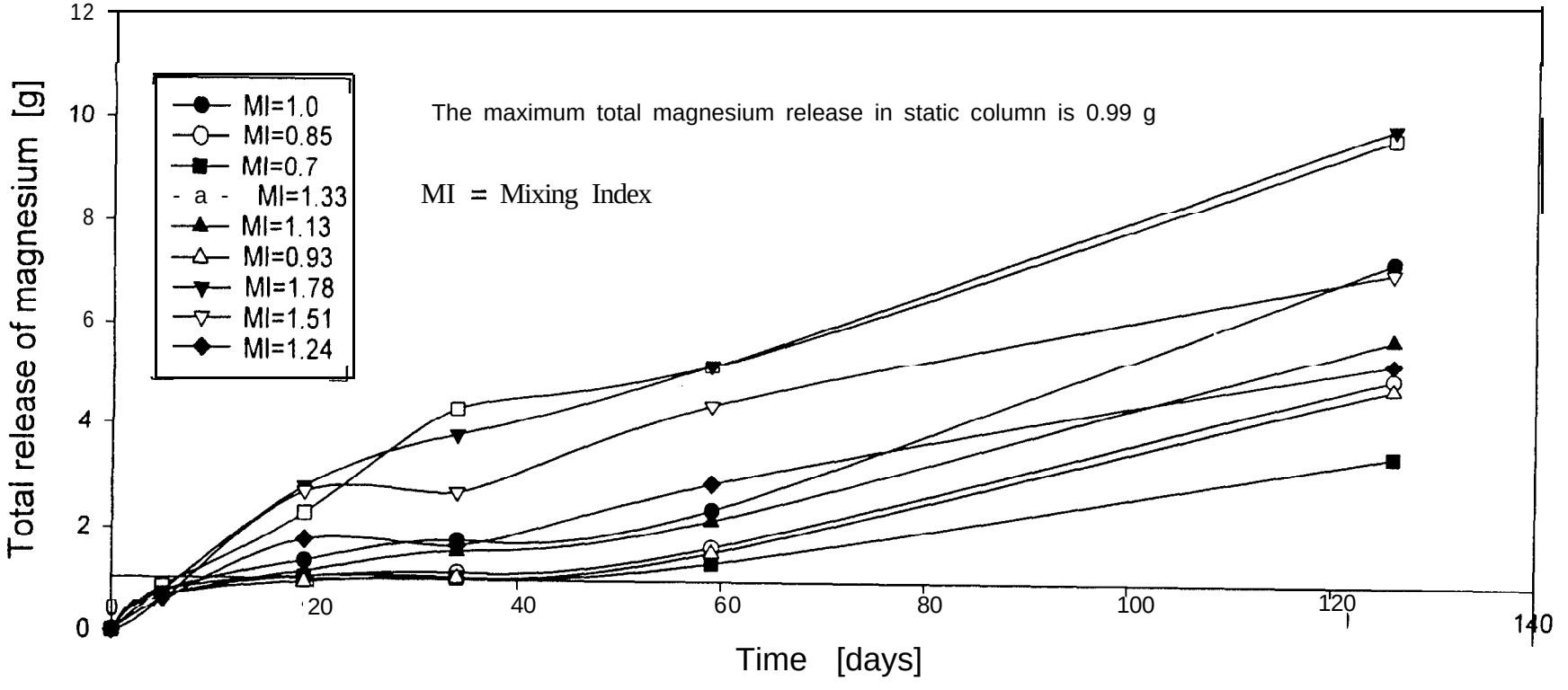

Figure 3.83 Variation of magnesium release with time and mixing index

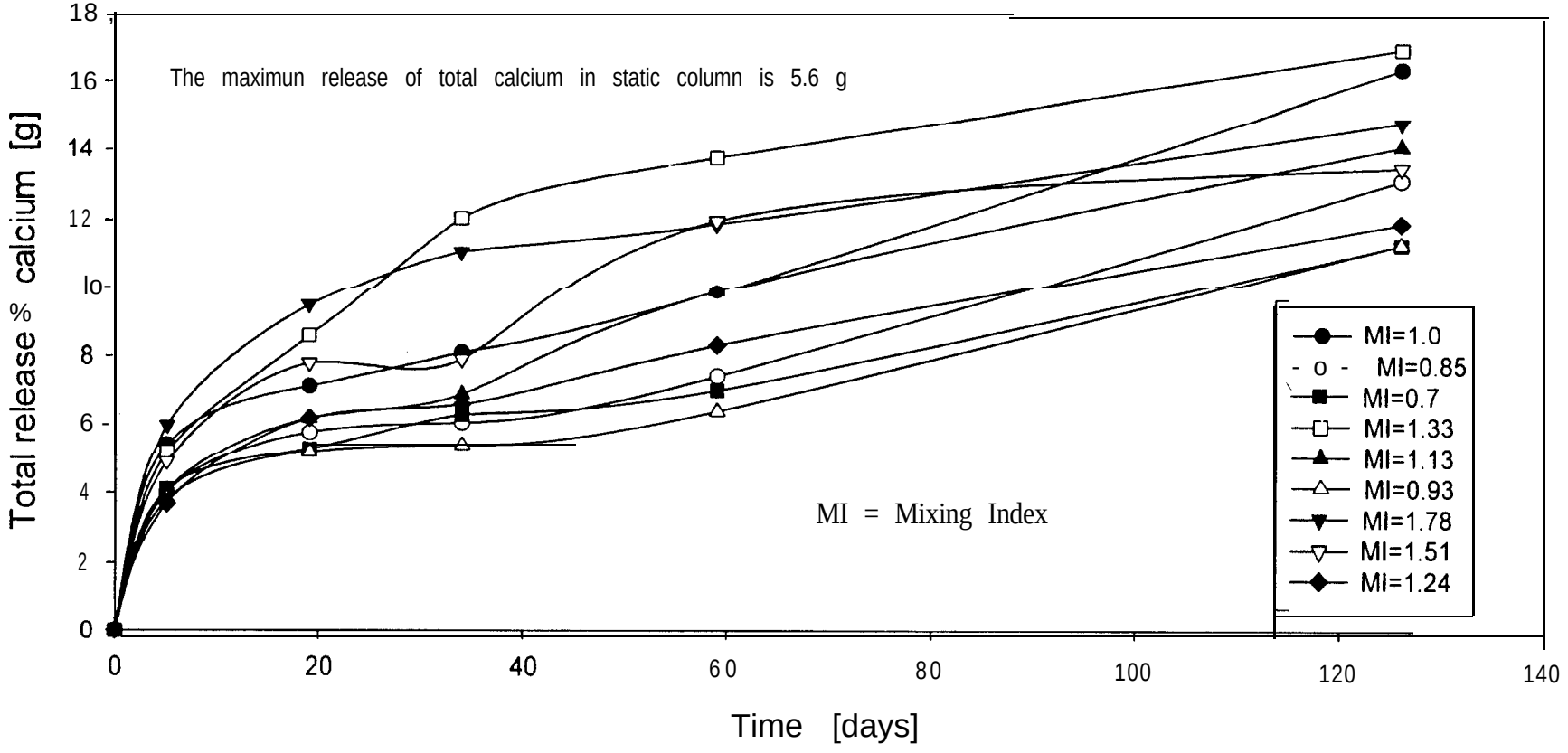

Figure 3.84 Variation of calcium release with time and mixing index

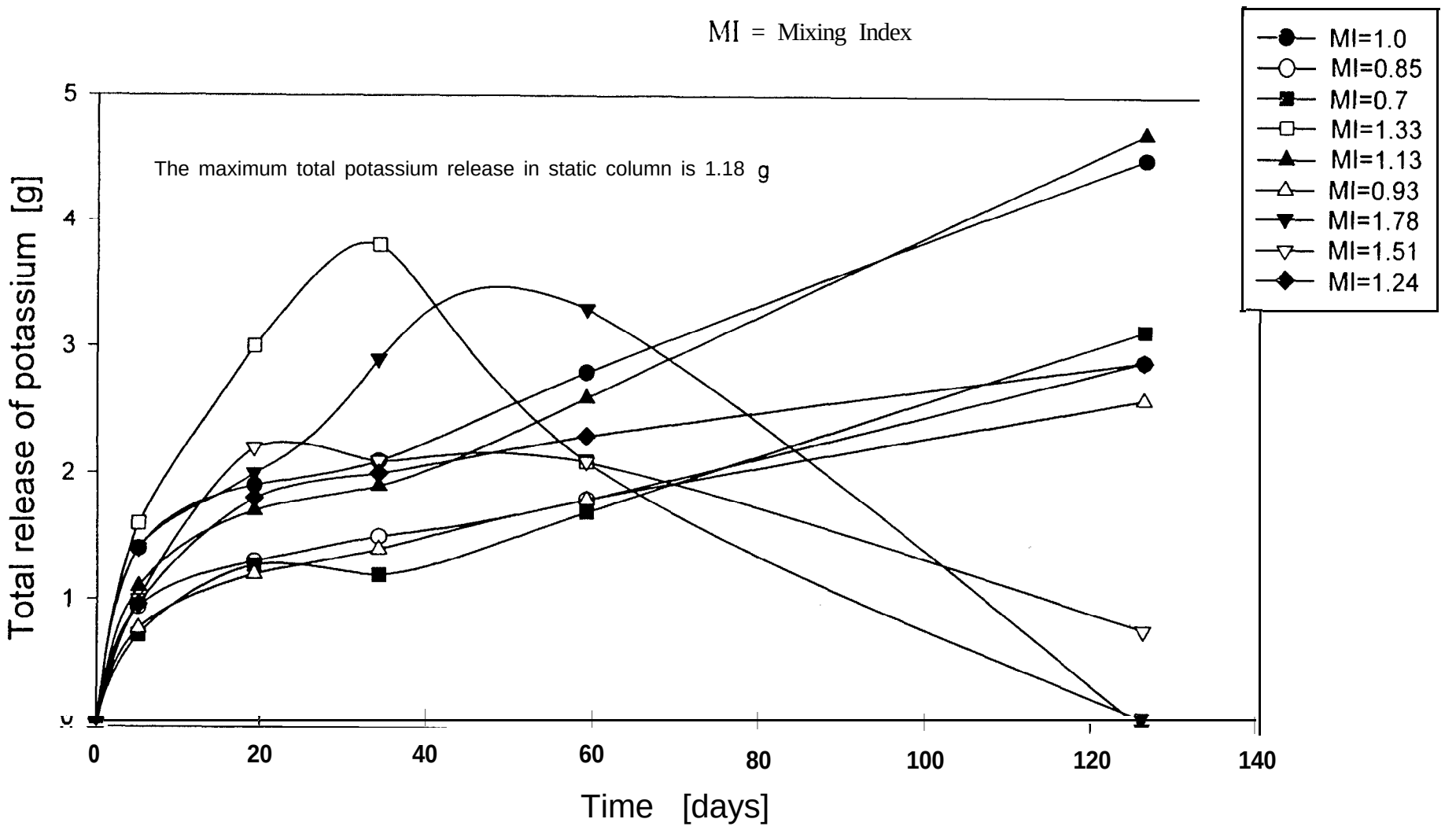

Figure 3.85 Variation of potassium release with time and mixing index

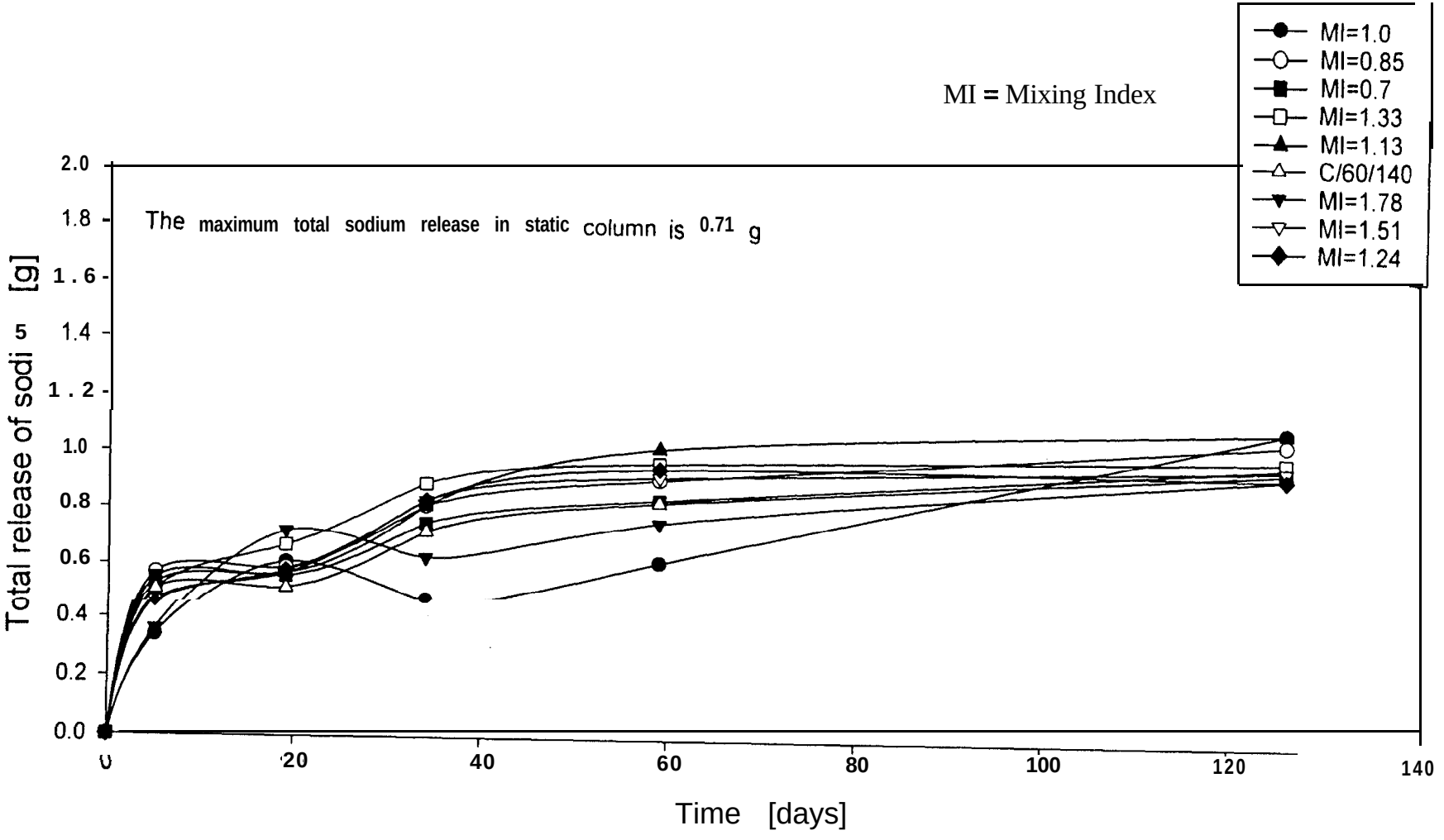

Figure 3.86 Variation of sodium release with time and mixing index

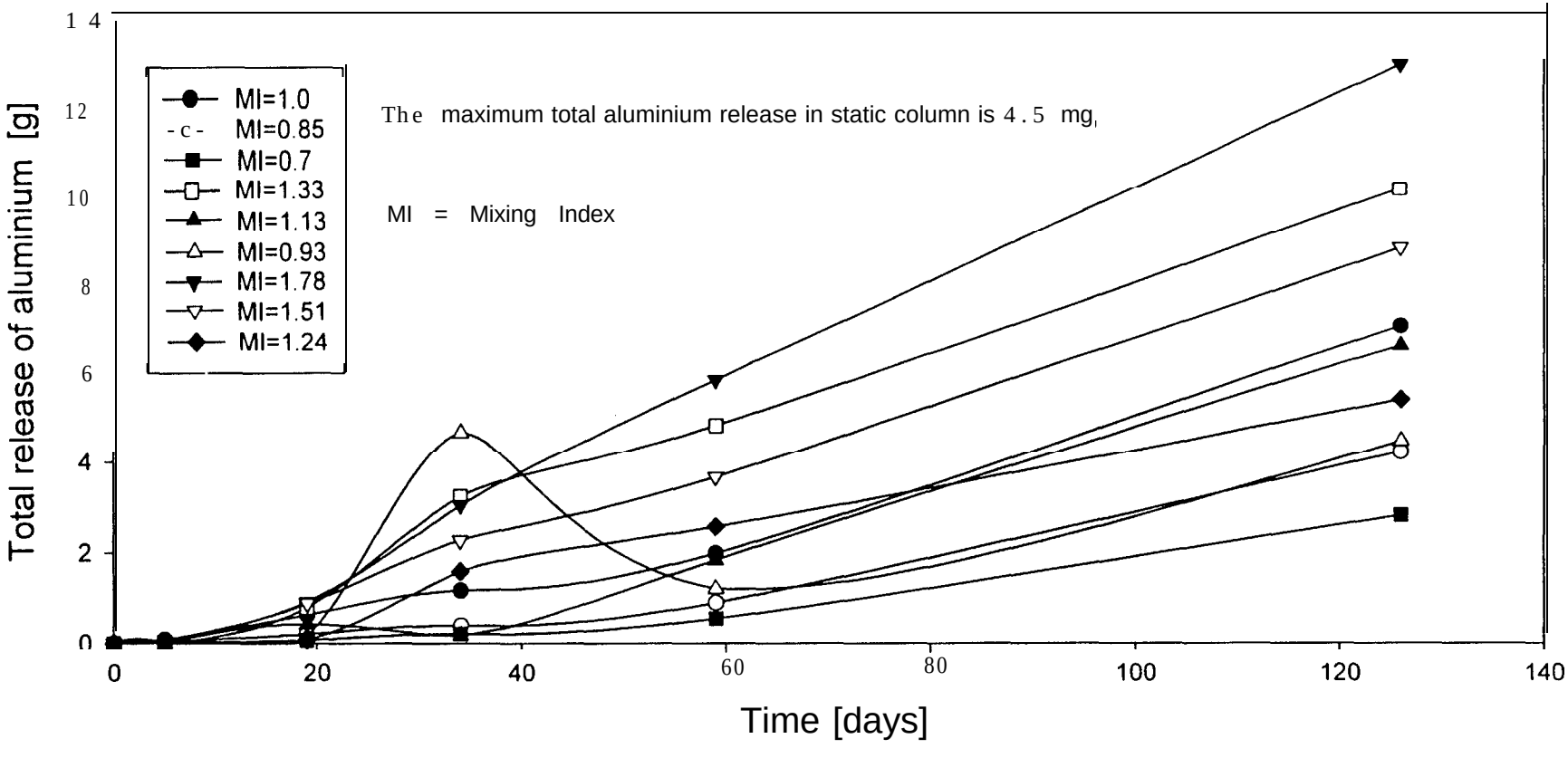

Figure 3.87 Variation of aluminium release with time and mixing index

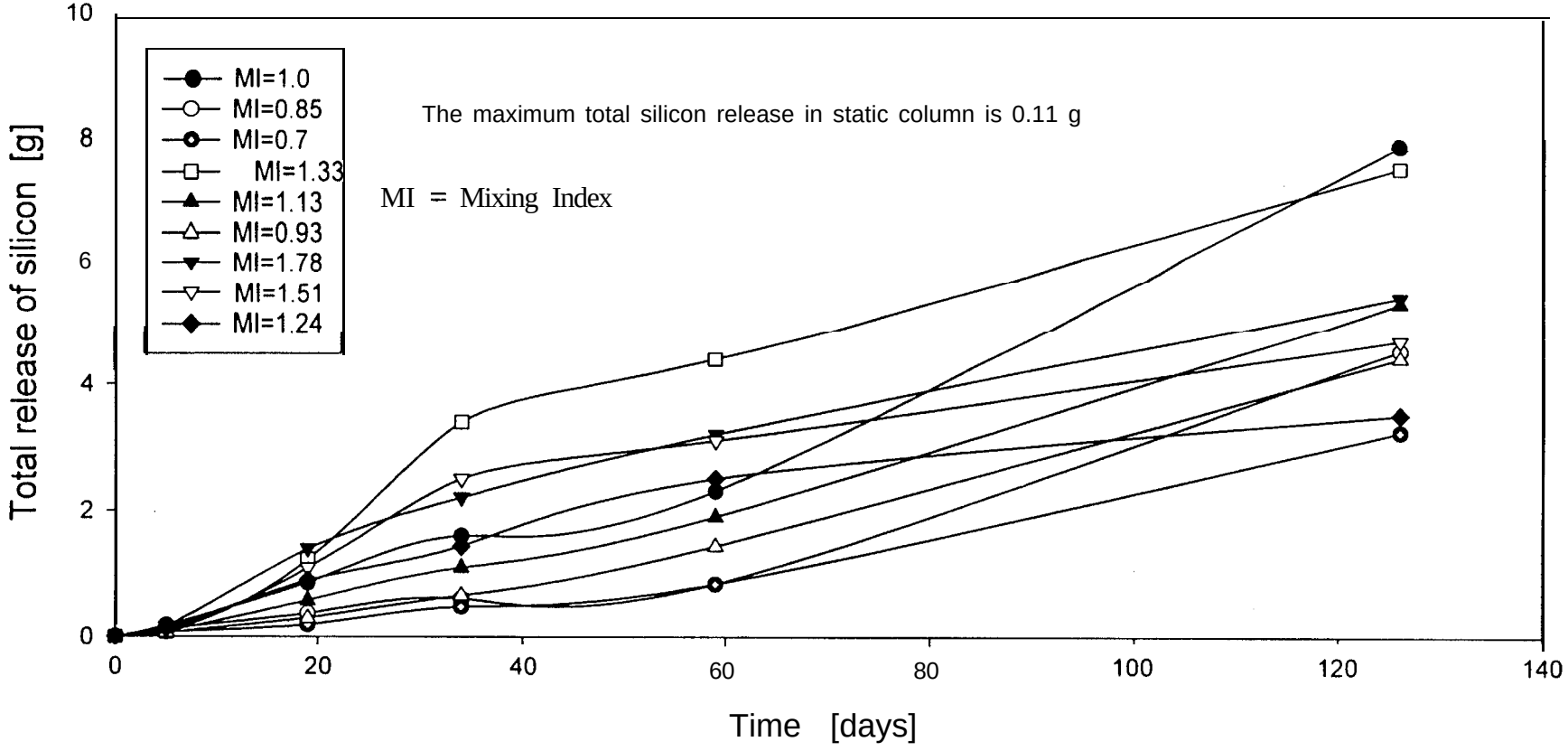

Figure 3.88 Variation of silicon release with time and mixing index

4. ANALYSIS AND DISCUSSION

4.1 Resuspension

When stresses are created on the surface of flooded tailings, the tailings particles are sent into suspension if the shear stress exceeds the critical shear stress. This critical shear stress, which initiates sediment motion, is unique for each type of tailings. Due to the cohesive nature of sulphide mine tailings, the critical shear stress cannot de determined experimentally using the Shields diagram, since Shields criterion for the initiation of sediment motion is valid only for non-cohesive particles (Shields, 1936). No validated theoretical formulations exist at present to determine the initiation of sediment motion for cohesive particles. Hence, the critical shear stress has to be determined experimentally. Straight flumes, commonly used for experimental research on non-cohesive sediments (Krishnappan, 1993), such as sand and gravel, are not suitable for cohesive sediments (silt and clay). Cohesive sediments are usually transported in a flocculated form consisting of agglomerations of particles held together by electrochemical surface forces and other bonding mechanisms. The flocs are usually fragile and are susceptible to breakage by the impellers of re-circulating pumps that are normally used in straight flumes. Furthermore, the transport processes of cohesive sediments are time-dependent processes with time scales ranging from hours to days; investigations of such large time-scale processes using straight flumes are not practical, as they would require excessively long flumes. An alternate approach is to use circular flumes and to generate the flow by moving the flow boundaries rather than the fluid.

The results presented in this report show that as the degree of mixing increases, greater quantities of tailings particles are sent into suspension. Furthermore, the amount of sulphide (pyrrhotite) particles sent into suspension increases with the degree of mixing. This is because sulphide particles tend to have a high specific gravity and require higher surface stresses to put them into suspension. This implies that when experiments are conducted to determine the onset of sediment motion, the particles sent into suspension must be analyzed chemically and mineralogically to differentiate between sulphides and gangue minerals (such as silicates). Silicates are not susceptible to oxidation and may not pose the same threat of acid and metal contamination of the

environment as reactive sulphides. Significant resuspension of silicate particles in a water cover could, however, lead to unacceptably high turbidity. Silicates tend to have a lower gravity than sulphides; hence, the use of an experimental, critical shear stress to predict the onset of sediment motion is quite conservative.

4.2 Oxidation of Suspended Tailings

The results of the present show that significant quantities of tailings particles sent into suspension do indeed oxidize. The following evidence confirms oxidation:

a) The pH of the water cover was found to decrease with time for all stirred columns from a value of about 7.6 to an average value of 2.7. The pH of the static column essentially remained at 7.5;

b) Dissolved oxygen (DO) concentration in the stirred water cover decreases with time from 8.33 mg/L and stabilizes to an average value of 0.5 mg/L. DO in the static water cover decreases from 8.33 mg/L to 6.5 mg/L at the end of the experiments. Thus more oxygen is consumed in the stirred water cover than in the static water cover;

c) Electrical conductivity and sulphate in the water cover in all stirred columns increase with time, and is considerably greater than the values obtained in the static columns. Increase in electrical conductivity is confirmed by observed increase in metal concentrations in the water cover;

d) The average specific gravity of resuspended tailings is 2.7, while that of the original tailings and the tailings at rest is 3.89. The higher specific gravity reflects the presence of heavier sulphide minerals such as pyrrhotite. This suggests that considerable amount of pyrrhotite present in the resuspended tailings is depleted through oxidation, resulting in a lower specific gravity;

e) Particle size analysis of the resuspended particles show that at least 80 % of the resuspended particles are finer than 0.018 mm, whereas only 30 % of the original tailings particles were finer than 0.018 mm. This suggests that the resuspended particles weather and reduce in size as a result of oxidation;

f) X-ray diffraction analysis of the resuspended particles collected at the end of the experiments gives much lower pyrrhotite peak intensities than those of the original tailings and tailings at rest. This confirms more extensive consumption of pyrrhotite in the resuspended tailings than in the tailings at rest;

g) Total elemental analysis of the resuspended particles, collected at the end of the experiments, show a drastic decrease in the amount of iron and sulphur compared to those in the original and static tailings. This again indicates the resuspended tailings particles oxidize considerably more than tailings at rest;

h) Optical microscope photographs and scanning electron photomicrographs of the resuspended particles showed negligible presence of pyrrhotite grains, compared to the original and static tailings, thereby confirming that resuspended tailings particles oxidize considerably more than tailings at rest;

i) Metal release in the water cover is considerably greater in stirred columns than in columns that are not stirred. This confirms that the products of pyrrhotite oxidation are released in the water cover and this leads to decrease in pH and increase in electrical conductivity of the water cover.

4.3 Influence of Mixing

The primary oxidants in sulphide-mineral oxidation are oxygen and ferric iron. Mixing index, as defined in this study, represents the collective effect of concentration of resuspended tailings and degree of mixing in the water cover. An increase in oxygen flux from air to the water cover and in the amount of tailings resuspended in the water cover will lead to increased tailings oxidation and, potentially, greater release of metals to the water cover, over and above the case where tailings are at rest. This is because an increase in the concentration of resuspended tailings increases the exposure of tailings particles to the oxidant. The concentration of resuspended tailings is the same (27 mg/L) in columns C/45/200 and C/45/1 70, whose mixing index (1.78 and 1.5 1, respectively) is higher than those of the other columns (see Table 2 and Figure 3.46). The DO consumption in these columns is also similar (Figure 3.9). There is also adequate ferric iron in the water cover in both columns for tailings oxidation, as shown in Figure 4.1.

However, tailings in C/45/200 oxidize more than the tailings in C/45/170. In fact, the degree of oxidation, as measured by the thickness of tailings oxidized in each column during the experiments, is 20% greater in C/45/200 than in C/45/170. The different degree of mixing in the two columns would explain the difference in oxidation.

DO consumption in column C/80/200 is four times greater than the consumption in all other columns. This does not, however, result in greater oxidation of tailings and suggests that greater oxygen influx does not necessarily lead to increased oxidation, and that ferric iron plays a dominant role in tailings oxidation.

The predominant sulphide mineral present in the Strathcona Mine tailings used in the experiments is pyrrhotite (Fe_{1-x} S), where x = 0.125. When exposed to dissolved oxygen in the water cover, pyrrhotite will oxidize and the reaction may be typically described as (Janzen et al., 1997):

$$Fe_{1-x}S + (2-x/2)O_2 + xH_2O = (1-x)Fe^{2+} + SO_4^{2-} + 2xH^+ \qquad [3]$$

Equation [3] indicates that dissolved Fe^{2+}, SO_4^{2-}, and H^+ represent an increase in total dissolved solids and acidity of the water cover and the tailings pore water. The electrical conductivity represents the charged component of the total dissolved solids. The above oxidation reaction would explain the increase in sulphate (SO_4^{-2}) concentrations and electrical conductivity and the decreasing pH values of the water covers in all the columns. The higher the mixing index the greater the sulphate concentration and electrical conductivity. This trend is observed in all the columns.

The Fe^{2+} released in Equation [3] is relatively mobile under low pH to neutral pH conditions such as would exist in the tailings at the early stages of the experiments. When the pH decreases to 3.5 or lower and oxygen is readily available, subsequent oxidation of Fe^{2+} will occur as follows:

$$Fe^{2+}(aq) + \tfrac{1}{4}O_2 + H^+ \rightarrow Fe^{3+}(aq) + \tfrac{1}{2}H_2O \qquad [4]$$

Singer and Stumm (1969 and 1970) report that this reaction is rate limiting and very slow under sterile conditions. But bacteria are capable of catalyzing this iron oxidation.

Figure 4.2 shows a plot of the ferrous to ferric iron ratio with time. Clearly, the amount of ferrous iron present in the columns is quite small and this reaction may not be rate limiting. Bacteria may be present as a catalyst, but mixing could also play a major role in accelerating the above reaction.

The ferric iron released as in Equation [4] can act as an oxidant and react with pyrrhotite present in the tailings to produce ferrous iron:

$$Fe_{1-x}S + (8-2x)Fe^{3+} + 4H_2O = (9-3x)Fe^{2+} + SO_4^{-2} + 8H^+ \qquad [5]$$

This reaction commonly occurs in tailings below the water table, or in areas where oxygen is depleted. Oxygen is the major oxidant in the early stages of sulphide oxidation and is responsible for the initial decrease in pH to acidic levels. At pH 3.5 and lower, ferric iron is more soluble it becomes a major oxidant, as in Equation [5]. The reaction in Equation [5] is probably accelerated by the degree of mixing. Thus, as the mixing index increases, pyrrhotite oxidation also increases. This trend is been observed in all the columns.

The Strathcona Mine tailings also contain minor amounts of chalcopyrite ($CuFeS_2$), sphalerite (ZnS), and nickel sulphide. The oxidation of these sulphide minerals by ferric iron could release copper, zinc, and nickel into the overlying water cover. Direct oxidation of pyrrhotite could also release zinc and copper into solution as pyrrhotite can strongly bind heavy metals during its formation.

The cumulative release of zinc, copper, and nickel presented in this study may be explained by ferric iron release. When the pH of water cover is below 3.5, further oxidation of ferrous (Fe^{2+}) to ferric (Fe^{3+}) iron would proceed at rates possibly controlled by the degree of mixing. Ferric iron would leach zinc, copper and nickel through further oxidation, which may be illustrated by the following reaction:

$$8Fe^{3+} + CuS + 4H_2O \rightarrow 8Fe^{2+} + Cu^{2+} + SO_4^{2-} + 8H^+ \qquad [6]$$

A similar reaction could be written for sphalerite (ZnS) and nickel sulphide by substituting for CuS in Equation [6]. Mixing is also accelerated the rate of these

reactions. Thus, as mixing index increases greater concentrations of metals are leached; this would explain the trend observed in all the stirred columns.

Calcium released in the water cover is most likely derived from the original lime added to the tailings in the mill, while aluminosilicate minerals (chlorite and muscovite) would contribute aluminium, magnesium and potassium. These minerals would tend to dissolve and neutralize the acid formed as a result of sulphide mineral oxidation.

The results of the present experiments are similar to those of Morse (1994) who found that about 20 to 50% of the pyrite in sediments from Galveston Bay, Texas, oxidized in one day when resuspended. Calmano et al (1994) also found that resuspension of river sediments at a pH of 7.5 rapidly oxidized constituent pyrite and other metal sulphides and resulted in the release of zinc, copper lead and cadmium. The sulphate and metal concentrations versus time obtained in this study are similar to those of Calmano et al (1994).

4.4 Secondary Mineral Precipitation

The least amount of oxidized tailings is found in column C/80/140, with a mixing index of 0.70. If one takes the total metals released in this column as a reference, and calculates the total metal release in the other columns on a pro-rata basis, one should obtain the expected total metal release into the water cover in all the other columns. Figure 4.3 presents the actual and expected total release of nickel as a function of mixing index. The figure suggests that nickel is being precipitated and/or adsorbed, since the actual nickel release is much lower than the expected nickel release. As the mixing index increases, nickel precipitation and/or adsorption also increases. Nickel may also be adsorbed by the iron oxyhydroxides since freshly precipitated iron oxyhydroxides are known to scavenge trace metals. Calmano et al (1994) report adsorption of released cadmium, zinc and copper on iron hydroxide and manganese oxide in laboratory resuspension experiments. Leckie et al (1980) show that adsorption and/or coprecipitation with iron hydroxide can be used to remove copper, zinc and other trace metals from wastewater streams.

Nickel precipitation as sulphide is possible if, as a result of sulphate reduction, enough sulphide is produced to satisfy thermodynamic and geochemical requirements. In

an iron-rich system as in the experiments, the use of ferric-ferrous ratio to estimate the redox is probably reasonable. The ferric-ferrous iron redox couple (25°C and 1 atmosphere) may be represented as follows:

$$Fe^{++} = Fe^{3+} + e \qquad [7]$$

$$Eh = E^0 + 0.059 \log(Fe^{3+}/ Fe^{2+}) \qquad [8]$$

where Eh is the redox potential and E^0 is the half cell potential of 0.771 volt.

The (Fe^{3+}/Fe^{2+}) in the laboratory columns is approximately 10 (Figure 4.2). Calculating the redox potential using Equation [8] gives Eh = 0.771 volt. At this redox and the measured pH values (2.6 to 7.6), it is not likely that there is significant sulphate reduction to produce hydrogen sulphide. Thus it seems that nickel is probably adsorbed by iron oxyhydroxide and the higher the mixing index the greater the adsorption. Similar trend was obtained for other elements (Figures 4.4 to 4.6).

4.5 Shear Stress in Generated Stirred Columns

The stirring action in the columns can be modelled to obtain the shear stress generated at the bottom of the water cover using a computational fluid dynamic (CFD) program, CFX-Tascflow (Advanced Scientific Computing Ltd, 1997). The column is discretized into small control volumes of regular size by selecting 30,000 nodes. The walls of each column are modelled as a stationary rough wall and the stirrer as a steady rotating rough wall. The nodes are distributed closer to the boundary walls so as to pick up the boundary layer. Fluid flow is assumed to be turbulent and a k-s model is used, where k is the turbulent kinetic energy and ε is the rate of energy dissipation. The convergence criterion for mass and momentum balance is chosen to be 1×10^{-4}. For all cases modelled in the present study, the convergence criterion is satisfied, and the flow is found to be turbulent at 99.9% of the nodes.

A typical flow pattern along a vertical section passing through the centre of column C/80/200 is shown in Figure 4.7. The centrifugal force created by the action of the stirrer

carries and throws the adjacent water layer outward. At the walls of the column, however, the flow is directed downward. This is compensated by particles that flow in the upward direction towards the stirrer and are then carried and ejected centrifugally. Schlichting (1968) observed a similar flow pattern adjacent to a disk rotating in a fluid at rest.

The calculated average bottom shear stresses in the water covers are given in Table 9. It can be seen that an increase in stirrer speed leads to only a marginal increase in bottom shear stress and the shallower the water cover, the higher the bottom shear stress appears to be at any given stirrer speed. In fact, a comparison of means using the data in Table 9 shows that, at the 5% level of significance, there is no statistical difference between the average bottom shear stresses generated in the 80 and 60 cm water covers and in the 60 and 45 cm water covers. On the other hand, average bottom shear stresses generated in the 80 and 45 cm water covers are found to differ by 0.17 N/m^2 at the 5% level of significance. The lowest shear stress (0.14 N/m^2) in Table 9 is similar to the critical shear stress of 0.12-0.17 N/m^2 measured experimentally on similar tailings using a rotating flume. The bulk of the tailings started to erode at the high shear stress (Krishnappan, 1993; Yanful and Verma, 1998). The data in Table 9 show the critical shear stress for bed erosion was exceeded at the stirrer speeds used in the present study.

Table 9: Bottom shear stresses generated in water cover

Column	Mixing Index	Shear stress (N/m^2)
C/80/200	1.0	0.18
C/80/170	0.85	0.15
C/80/140	0.7	0.14
C/60/200	1.33	0.25
C/60/170	1.13	0.21
C/60/140	0.93	0.16
C/45/200	1.78	0.42
c/45/1 70	1.51	0.30
c/45/1 40	1.24	0.26

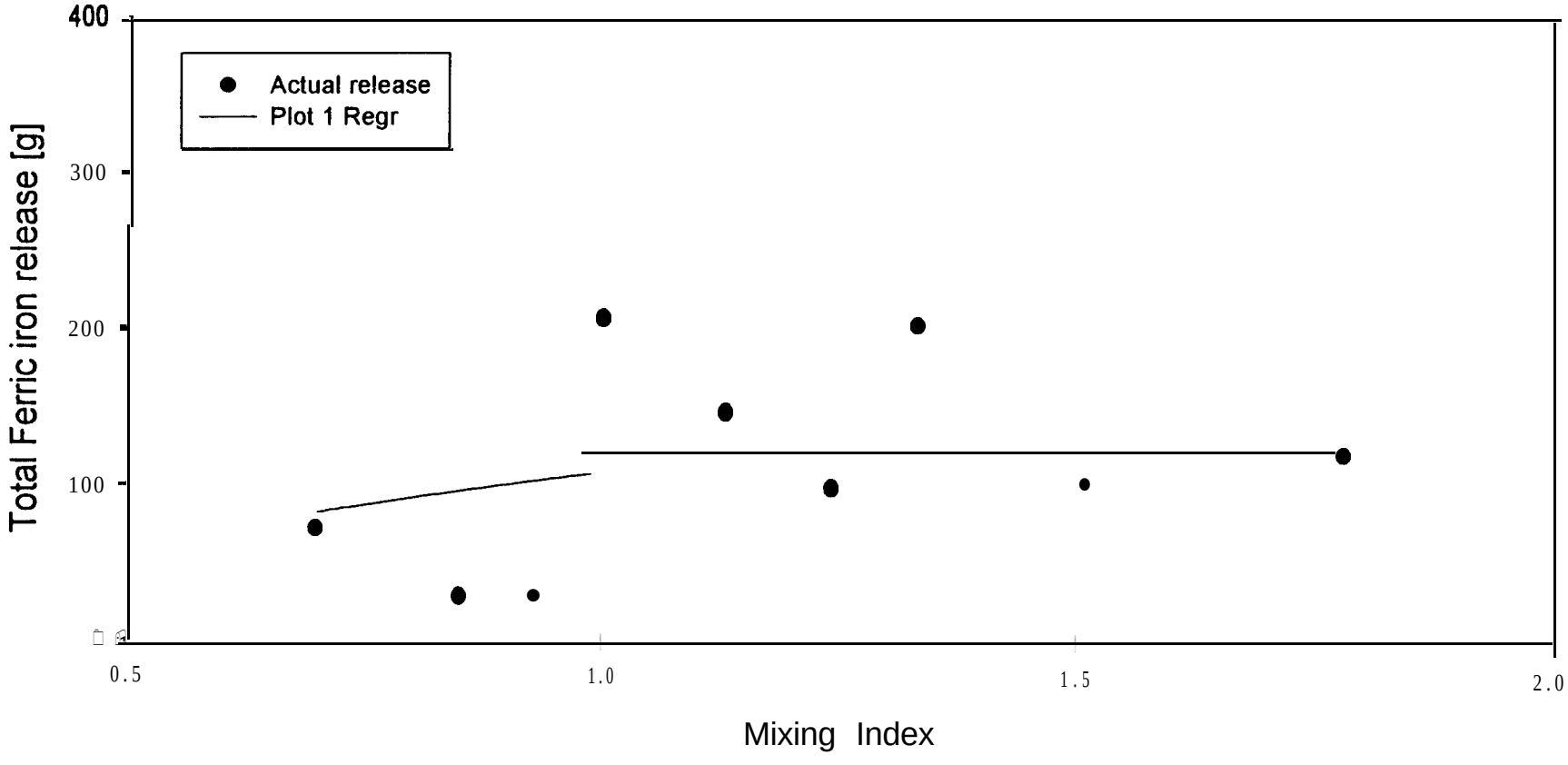

Figure 4.1 Variation of ferric iron release with mixing index

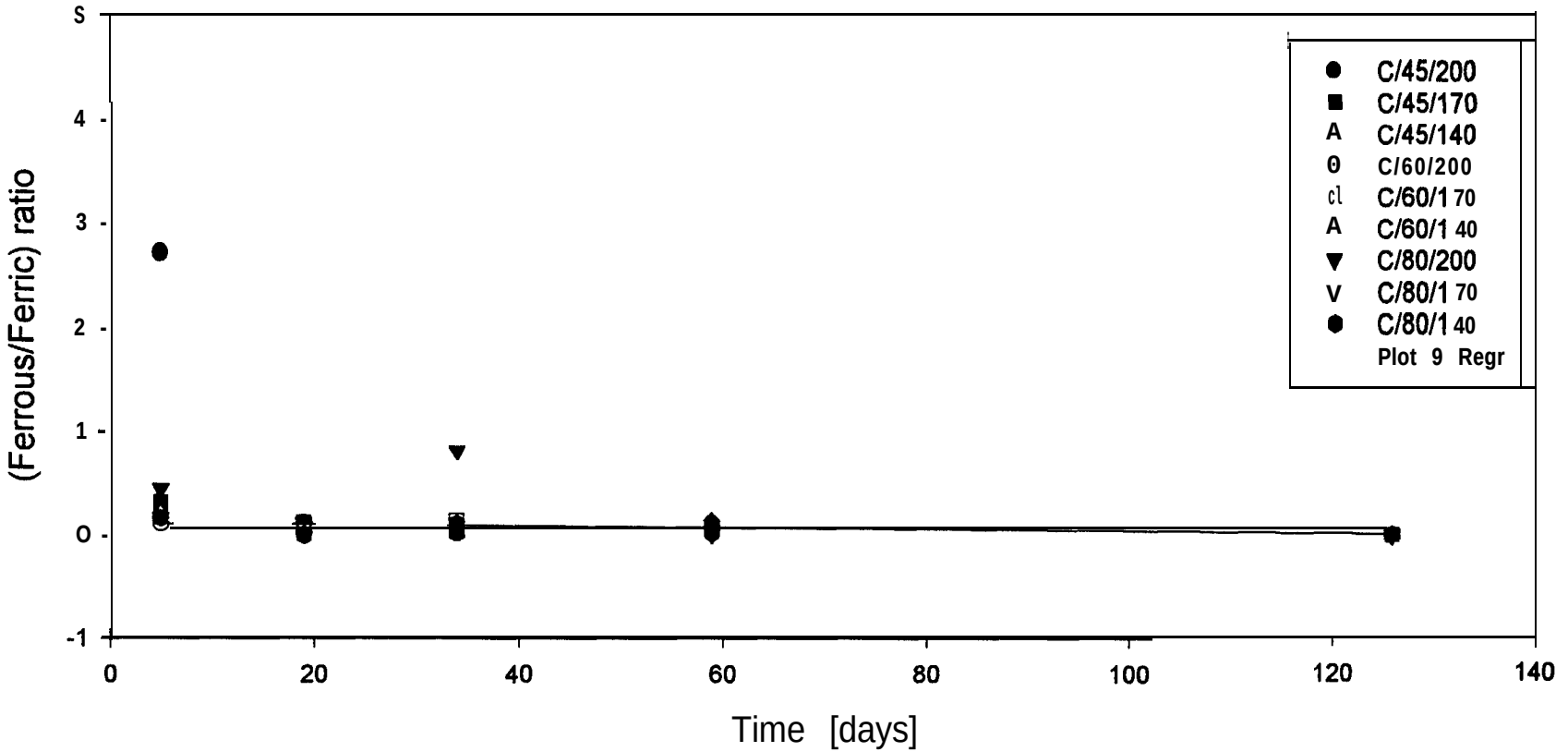

Figure 4.2 Variation of ferrous to ferric iron ratio with time in stirred columns

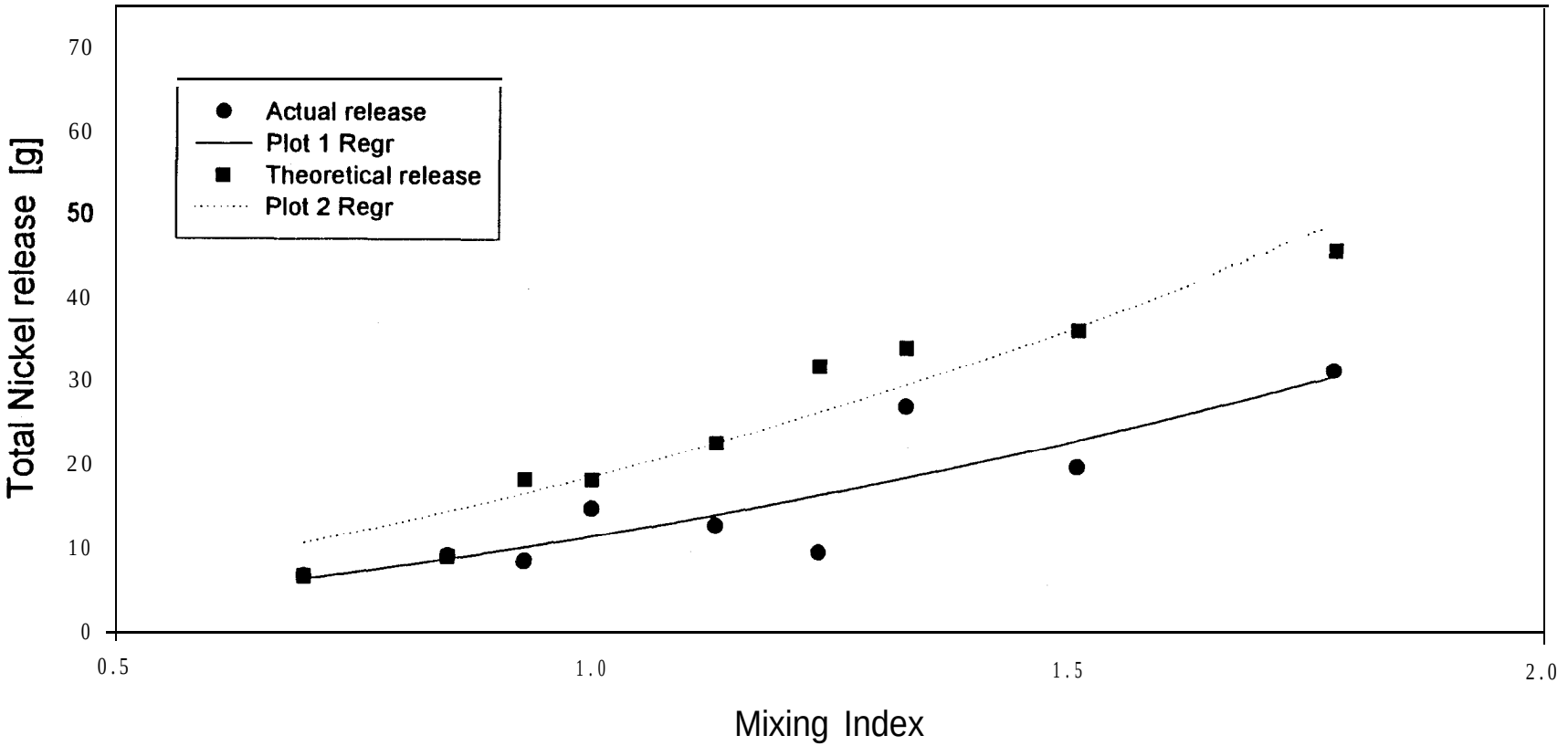

Figure 4.3 Variation of actual versus expected nickel release with mixing index

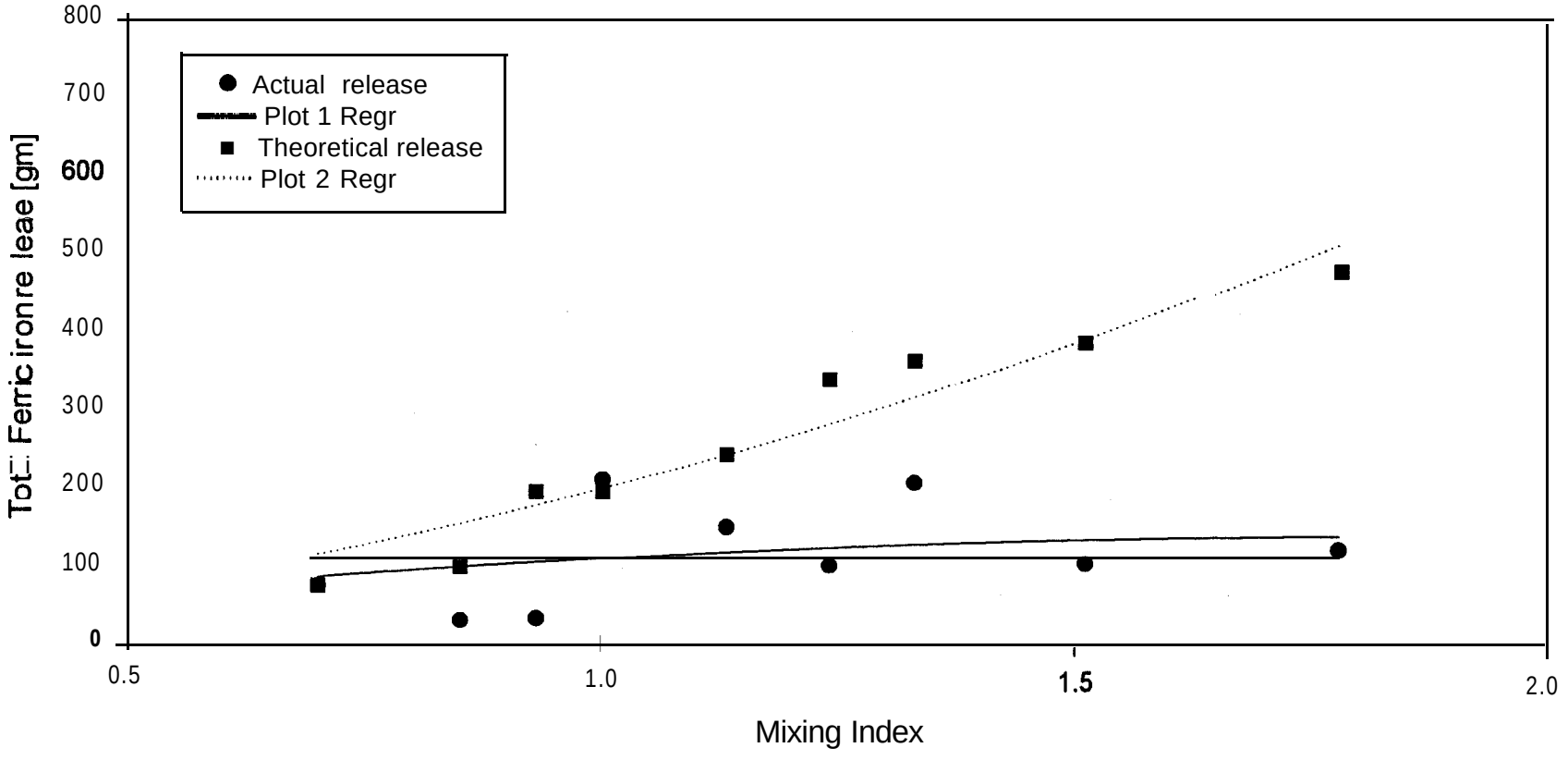

Figure 4.4 Variation of actual versus expected ferric iron release with mixing index

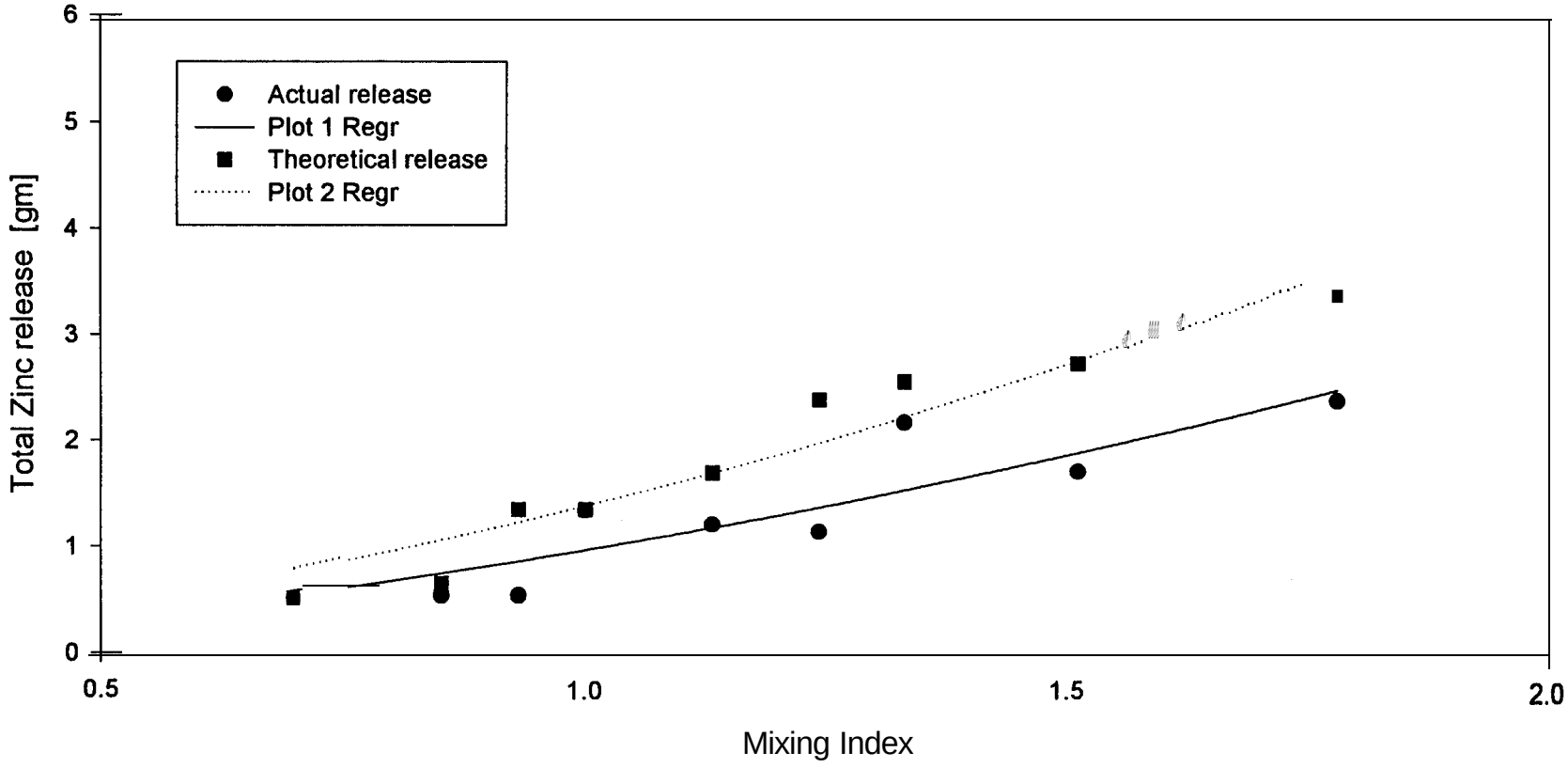

Figure 4.5 Variation of actual versus expected zinc release with mixing index

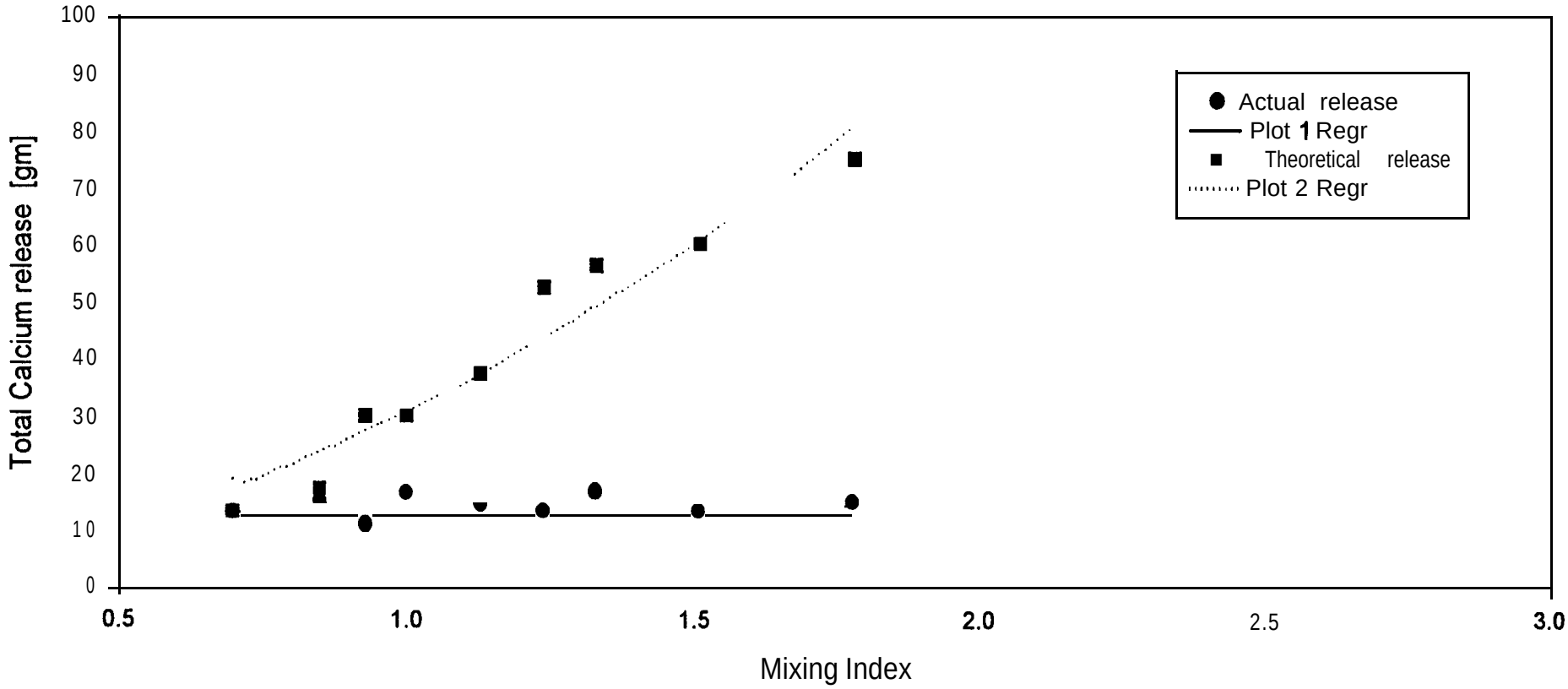

Figure 4.6 Variation of actual versus expected calcium release with mixing index

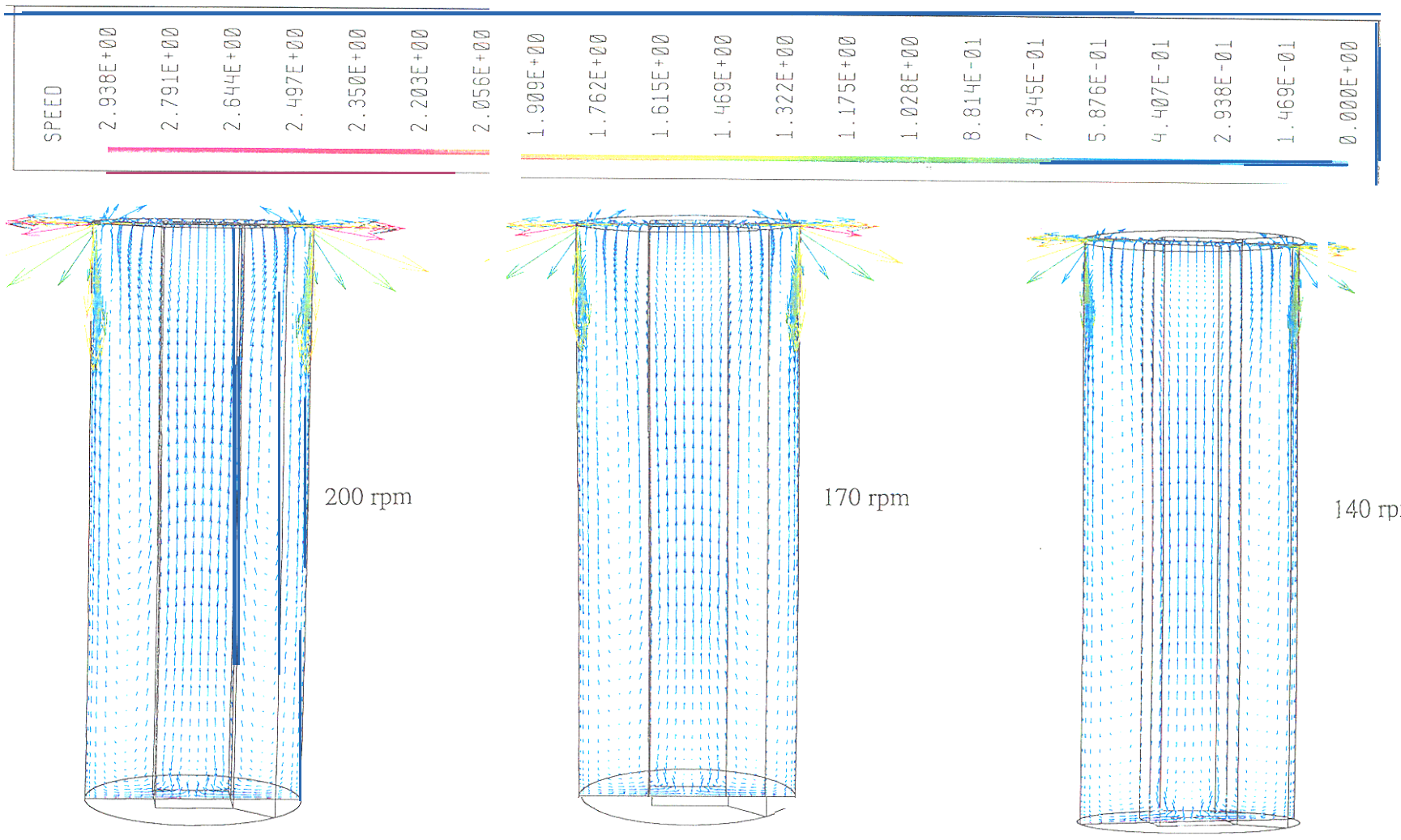

Figure 4.7 Flow of fluid particles in 80 cm water covers stirred at 200, 170 and 140 rpm

5. CONCLUSIONS

Laboratory experiments have been performed to assess the contribution of resuspension to the oxidation of pyrrhotite mine tailings covered with a varying shallow water cover. Resuspension was initiated by stirring the water cover above the tailings at selected speeds. Based on the results, the following is concluded:

1. In very shallow water covers with significant tailings resuspension, dissolved oxygen may not be saturated, as commonly believed. Resuspended tailings will continually consume oxygen at all depths in the water cover and produce a uniform oxygen concentration profile with values below the saturation limit. Hence the mass transfer of oxygen across the air-water interface in a shallow water cover may be a very important factor in the selection of water cover depth;

2. Resuspension significantly increases the rate of tailings oxidation, and may be accompanied by significant acidification and metal metals. The rate increases with mixing index. Hence the more intense the wind and wave activity in a tailings pond, for example, the greater the total amount of tailings oxidized;

3. An increase in stirrer speed for a given depth of water cover results in an increase in the rate of oxidation of resuspended pyrrhotite tailings;

4. There exists a unique maximum concentration of resuspended tailings that can be accommodated by a water cover for a given mixing index. This possibly depends on the nature of tailings;

5. The concentration resuspended tailings increases with the degree of mixing;

6. The degree of mixing may significantly increase the rate of reactions occurring in the water cover;

7. At pH values below 3.5, dissolved ferric iron plays a major role in tailings oxidation;

8. Resuspended tailings particles use up oxygen and lower the DO concentrations in the water cover. This helps in lowering the oxidation rate of the deeper,

undisturbed. In fact, the oxidation rate of the undisturbed tailings may be lower or equal to that of the tailings below the static water cover;

9. When tailings are resuspended the metals from the water cover do not infiltrate into the pore water of the tailings. This occurs as long as the surface of tailings is not severely disturbed;

10. Precipitation or adsorption of metals increases with mixing index. Iron oxyhydroxides are precipitated. These minerals tend to have a large surface area when freshly precipitated and can adsorb or scavenge trace metals released during the primary oxidation reactions.

ACKNOWLEDGEMENTS

This work is part of an ongoing research on water cover technology at the Geotechnical Research Centre, The University of Western Ontario. The work was done on behalf of MEND and sponsored by Battle Mountain Canada Ltd., Falconbridge Limited, Inco Limited, Noranda Mining and Mineral Exploration, Teck Corporation, the Ontario Ministry of Northern Development and Mines, and the Canada Centre for Mineral and Energy Technology (CANMET) through the CANADA/Northern Ontario Development Agreement (NODA).

REFERENCES

Advanced Scientific Computing Ltd. 1997. CFX-TASCflow 3-D Version 2.7.2-39.

Aubé, B.C., St-Arnaud, L.C., Payant, SC., and Yanful, E.K. 1995. Laboratory evaluation of the effectiveness of water covers for the prevention of acid generation from pyritic rock. Sudbury '95, Conference on Mining and the Environment, Sudbury, Ontario. May 28 – June 1, Vol. 2, pp. 495- 504.

Calmano, W., Förstner, U., and Hong, J. 1994. Mobilization and scavenging of heavy metals following resuspension of anoxic sediments from the Elbe River. In: *ACS Symposium Series 550. Environmental Geochemistry of Sufide Oxidation.* Editors: C.N. Alpers and D.W Blowes. American Chemical Society, Washington D.C., August 23-28, pp. 298-321.

Dave, N.K. 1992. Water cover on acid generating mine/mill wastes: A Technical Review. Division Report, Mineral Sciences Laboratories, MSL 92-38(CR), Project 30.14.99, Prepared for Noranda Technology Centre, Pointe-Claire, Quebec, Canada.

Dave, N.K., and Vivyurka, A.J. 1994. Water cover on acid generating uranium tailings-Laboratory and field studies. Proceedings of the International Land Reclamation and Mine Drainage Conference and 3rd International Conference on Abatement of Acid Mine Drainage, Pittsburgh, Pennsylvania, USA, April 25-29, pp. 297-306.

Dave, N.K, Lim, T.P., Home, D., Boucher, Y., and Stuparyk, R. 1997. Water cover on reactive tailings and wasterock: Laboratory studies of oxidation and metal release characteristics. Proceedings of the Fourth International Conference on Acid Rock Drainage, Vancouver,B.C., Canada, May 3 1 -June 6, Volume II, pp. 779-794.

Deer, Howie, and Zussman, 1966. An Introduction to the rock forming minerals. Longman.

Hurlbut Jr., C.S., and Klein C. 1977. Manual of Mineralogy, 19th Edition, John Wiley & Sons, New York.

Janzen, M.P., Nicholson, R.V., and Scharer, J.M. 1997. The role of enhanced particle surface area, crystal structure and trace metal content on pyrrhotite oxidation rates in tailings. Fourth International Conference on Acid Rock Drainage, Vancouver, B.C., Canada, May 31-June 6, Vol. 1, pp. 499-415.

Krishnappan, B.G. 1993. Rotating circular flume. ASCE Journal of Hydraulic Engineering, Vol. 119, No. 6, pp. 758-767.

Morse, J.W. 1994. Release of toxic metals via oxidation of authigenic pyrite in resuspended sediments. In: *ACS* Symposium Series *550*. Environmental Geochemistry of *Sufide* ***Oxidation.*** Editors: C.N. Alpers and D.W Blowes. American Chemical Society, Washington D.C., August 23-28, pp. 290-297.

Schlichting, H. 1968. Boundary-Layer Theory, 6th Edition, Chapter V, pp. 93-99. McGraw-Hill Book Company.

Shields, A. (1936) "Application of Similarity Principles and Turbulence Research to Bed-Load Movement," (in German but translated in English).

Singer, P.C., and Stumm, W. (1969). The rate determining step in the production of acidic mine waters. American Chemical Society, Div. Fuel Chem. 13:80-87.

Singer, P.C., and Sturnm, W. (1970). Acidic mine drainage: the rate determining step. Science, 67:1121-l 123.

Standard Methods for examination of water and wastewater, (1980), 1 5th edition, APHA-AWWA-WPCF.

Truesdale, G.A., Downing, A.L., and Lowden, G.F. 1955. The solubility of oxygen in pure water and sea-water. Journal of Applied Chemistry 5:53-62.

Yanful, E.K., and Sinnns, P.H. 1997. Review of water cover sites and research projects. Final Report to the Mine Environment Neutral Drainage (MEND) program. MEND Report 2.18.1. Geotechnical Research Centre, The University of Western Ontario, December, 110 p.

Yanful, E.K., and Verma, A. 1998. Predicting resuspension in flooded mine tailings. Proceedings of the 5 1st Canadian Geotechnical Conference, Edmonton, Alberta, Canada. October 4-7, 1998, Vol. I, pp. 113-l 19.